ESA Climate Change Initiative “Plus” (CCI+)

Product Validation and Intercomparison Report (PVIR) version 2

for the Essential Climate Variable (ECV)

Greenhouse Gases (GHG):

XCO_2 and/or XCH_4 from OCO-2, TanSat, Sentinel-5-Precursor and GOSAT-2

Written by:

GHG-CCI+ project team

Lead author: Michael Buchwitz, Institute of Environmental Physics (IUP), University of Bremen, Germany

Co-authors:

Bart Dils (BIRA-IASB, Belgium, Brussels)

Maximilian Reuter, Oliver Schneising (IUP, Univ. Bremen, Germany)

Simon Preval, Hartmut Boesch (Univ. Leicester, UK)

Trismono Candra Krisna, Ilse Aben (SRON, Utrecht, The Netherlands)

Change log:

Version Nr.	Date	Status	Reason for change
Version 1.1	13-Mar-2020	Approved	New document for CRDP5
Version 2.0	10-Feb-2021	Submitted	Update for CRDP6
Version 2.1	19-Mar-2020	Submitted	Content for Sect. 4.2.2 added on request of ESA.

Table of Contents

1 Executive Summary

This document is the Product Validation and Intercomparison Report (PVIR) version 2.0 (v2.0), which is a deliverable of the ESA project GHG-CCI+ (https://climate.esa.int/en/projects/ghgs/). The GHG-CCI+ project, which started in March 2019, is carrying out the research and development (R&D) needed to generate new Greenhouse Gas (GHG) Essential Climate Variable (ECV) satellite-derived CO_2 and CH_4 data products. These products are column-averaged dry-air mole fractions of carbon dioxide (CO_2), denoted XCO_2, and methane (CH_4), denoted XCH_4, from these satellites / satellite sensors using European scientific retrieval algorithms:

- XCO_2 from OCO-2 using the University of Bremen FOCAL algorithm (product **CO2_OC2_FOCA**),
- XCH_4 from Sentinel-5 Precursor (S5P) using University of Bremen's WFM-DOAS (or WFMD) algorithm (product **CH4_S5P_WFMD**),
- XCO_2 from TanSat using University of Leicester UoL-FP (or OCFP) algorithm (product **CO2_TAN_OCFP**), and
- XCO_2 and XCH_4 from GOSAT-2 using SRON's RemoTeC algorithm (products **CO2_GO2_SRFP, CH4_GO2_SRFP, CH4_GO2_SRPR**)

This project aims to generate GHG ECV data products in-line with GCOS (Global Climate Observing System) requirements. GCOS defines the ECV GHG as follows: "Retrievals of greenhouse gases, such as CO_2 and CH_4, of sufficient quality to estimate regional sources and sinks". Within the GHG-CCI+ project satellite-derived XCO_2 (in ppm) and XCH_4 (in ppb) data products are retrieved from satellite radiance observations in the Short-Wave-Infra-Red (SWIR) spectral region. These instruments are used because their measurements are sensitive also to the lowest atmospheric layer and therefore provide information on the regional surface sources and sinks of CO_2 and CH_4. All products are generated with independent retrieval algorithms developed to convert GOSAT-2, OCO-2, TanSat and/or TROPOMI/S5P radiance spectra into Level 2 (L2) XCO_2 and/or XCH_4 data products.

In this document validation and intercomparison results are presented. The validation is based on comparisons with TCCON (Total Carbon Column Observation Network) ground-based XCO_2 and XCH_4 retrievals. The validation has been carried out by the GHG-CCI+ independent Validation Team (VALT) and by the data provider (DP) of a given product.

For each data product and each assessment method the following validation summary "figures of merit" have been determined and are reported in this document: (i) Single measurement precision, (ii) mean bias (global offset), (iii) relative systematic error (or relative accuracy), (iv) stability (linear bias drift or trend). Furthermore, also the reported XCO_2 and XCH_4 uncertainties have been validated by computing a quantity called "Uncertainty ratio", which is the ratio of the (mean value of the) reported uncertainty and the standard deviation of satellite minus TCCON differences. The results are summarized in **Table 1-1** for the XCO_2 products and **Table 1-2** for the XCH_4 product.

Table 1-1: *Summary of the validation of XCO_2 products CO2_OC2_FOCA and CO2_TAN_OCFP of data set Climate Research Data Package No. 6 (CRDP#6, to be released in March 2021) via comparison with TCCON ground-based XCO_2 retrievals (using version GGG2014). VALT refers to the assessment results of the GHG-CCI+ independent validation team and DP refers to the assessment results of the data provider. (*) Excluding a possible global offset, which is reported separately in this document.*

Summary validation results GHG-CCI+ CRDP#6 XCO_2 products by comparisons with TCCON (GGG2014)			
Product CO2_OC2_FOCA (v09, global, 1.2015 – 5.2020)			
Parameter	**Achieved**	**Required**	**Comments**
Random error (single obs., 1σ) [ppm]	VALT: 1.39 DP: 1.48	T:<8; B:<3; G:<1	T=threshold; B=breakthrough; G=goal
Systematic error [ppm]	VALT: 0.41 / 0.73 DP: 0.57 / 0.68	< 0.5	"Relative accuracy" (*) Spatial / spatio-temp.
Stability: Linear bias trend [ppm/year]	VALT: 0.04 [-0.10, 0.09] DP: 0.03 ± 0.26	< 0.5	1σ uncertainty

Product CO2_TAN_OCFP (v1, global, 3.2017 – 5.2018)			
Parameter	**Achieved**	**Required**	**Comments**
Random error (single obs., 1σ) [ppm]	VALT: 1.46 DP: 1.78	T:<8; B:<3; G:<1	T=threshold; B=breakthrough; G=goal
Systematic error [ppm]	VALT: 0.70 / 0.99 DP: 0.84 / n.a.	< 0.5	"Relative accuracy" (*) Spatial / spatio-temp.
Stability: Linear bias trend [ppm/year]	VALT: n.a. DP: n.a.	< 0.5	1σ uncertainty Only short time period

Table is continued on the following page …

Table 1-1: *Continued from previous page.*

Product CO2_GO2_SRFP (v01.0.0, global, 2.2019 – 11.2019)			
Parameter	**Achieved**	**Required**	**Comments**
Random error (single obs., 1σ) [ppm]	VALT: 2.04 DP: 2.10	T:<8; B:<3; G:<1	T=threshold; B=breakthrough; G=goal
Systematic error [ppm]	VALT: 1.07 / 0.96 DP: 0.90 / n.a.	< 0.5	“Relative accuracy” (*) Spatial / spatio-temp.
Stability: Linear bias trend [ppm/year]	VALT: n.a. DP: n.a.	< 0.5	1σ uncertainty Only short time period

Table 1-2: *Summary of the validation of XCH_4 products CH4_S5P_WFMD of data set Climate Research Data Package No. 6 (CRDP#6, to be released in March 2021) via comparison with TCCON ground-based XCH_4 retrievals (using version GGG2014). VALT refers to the assessment results of the GHG-CCI+ independent validation team and DP refers to the assessment results of the data provider. (*) Excluding a possible global offset, which is reported separately in this document.*

Summary validation results GHG-CCI+ CRDP#6 XCH_4 products by comparisons with TCCON (GGG2014)			
Product CH4_S5P_WFMD (v1.2, global, 11.2017– 4.2020)			
Parameter	**Achieved**	**Required**	**Comments**
Random error (single obs., 1σ) [ppb]	VALT: 15.1 DP: 14.3	T:<34; B:<17; G:<9	T=threshold; B=breakthrough; G=goal
Systematic error [ppb]	VALT: 5.0 / 5.3 DP: 4.4 / 4.5	< 10	"Relative accuracy" (*) Spatial / spatio-temp.
Stability: Linear bias trend [ppb/year]	VALT: 1.7 [-1.7, 4.9] DP: 0.01	< 3	1σ uncertainty Only short time period

Product CH4_GO2_SRFP (v01.0.0, global, 2.2019– 10.2019)			
Parameter	**Achieved**	**Required**	**Comments**
Random error (single obs., 1σ) [ppb]	VALT: 14.9 DP: 14.4	T:<34; B:<17; G:<9	T=threshold; B=breakthrough; G=goal
Systematic error [ppb]	VALT: 6.4 / 7.1 DP: 2.4 / n.a.	< 10	"Relative accuracy" (*) Spatial / spatio-temp.
Stability: Linear bias trend [ppb/year]	VALT: n.a. DP: n.a.	< 3	1σ uncertainty Only short time period

Table is continued on the following page …

Table 1-2: *Continued from previous page.*

Product CH4_GO2_SRPR (v01.0.0, global, 2.2019– 10.2019)			
Parameter	**Achieved**	**Required**	**Comments**
Random error (single obs., 1σ) [ppb]	VALT: 15.8 DP: 15.5	T:<34; B:<17; G:<9	T=threshold; B=breakthrough; G=goal
Systematic error [ppb]	VALT: 7.1 / 9.1 DP: 4.2 / n.a.	< 10	“Relative accuracy” (*) Spatial / spatio-temp.
Stability: Linear bias trend [ppb/year]	VALT: n.a. DP: n.a.	< 3	1σ uncertainty Only short time period

2 Introduction

This document is the Product Validation and Intercomparison Report (PVIR) version 2.0 (v2.0), which is a deliverable of the ESA project GHG-CCI+ (https://climate.esa.int/en/projects/ghgs/).

The GHG-CCI+ project, which started in March 2019, is carrying out the R&D needed to generate new Greenhouse Gas (GHG) Essential Climate Variable (ECV) satellite-derived CO_2 and CH_4 data products.

These products are column-averaged dry-air mole fractions of carbon dioxide (CO_2), denoted XCO_2, and methane (CH_4), denoted XCH_4, from these satellites / satellite sensors using European scientific retrieval algorithms:

- XCO_2 from OCO-2 and TANSAT,
- XCO_2 and XCH_4 from GOSAT-2 and
- XCH_4 from S5P

This project aims to generate GHG ECV data products in-line with GCOS (Global Climate Observing System) requirements **/GCOS-154/ /GCOS-195/ /GCOS-200/**. GCOS defines the ECV GHG as follows: "Retrievals of greenhouse gases, such as CO_2 and CH_4, of sufficient quality to estimate regional sources and sinks".

Once the products are of sufficient quality for a climate service and cover a long enough time period, it is expected that the data will become part of the Copernicus Climate Change Service (C3S, https://climate.copernicus.eu/).

Within GHG-CCI+ satellite-derived XCO_2 (in ppm) and XCH_4 (in ppb) data products are retrieved from satellite radiance observations in the Short-Wave-Infra-Red (SWIR) spectral region. These instruments are used because their measurements are sensitive also to the lowest atmospheric layer and therefore provide information on the regional surface sources and sinks of CO_2 and CH_4.

This document provides validation and intercomparison results for the XCO_2 and XCH_4 datasets as listed in **Table 2-1** for XCO_2 and **Table 2-2** for XCH_4.

All products are generated with independent retrieval algorithms developed to convert GOSAT-2, OCO-2, TANSAT and/or TROPOMI/S5P radiance spectra into Level 2 (L2) XCO_2 and/or XCH_4 data products.

For more information on these products see also **Table 2-3**.

Table 2-1: *Overview GHG-CCI+ algorithms for XCO_2 retrieval.*

XCO_2 Product Identifier	Algorithm (version)	Institute	Technique	Reference
CO2_OC2_FOCA	FOCAL (v09)	IUP, Univ. Bremen, Germany	Optimal Estimation; approximation for an optically thin Lambertian scattering layer	Reuter et al., 2017a, b
CO2_TAN_OCFP	UoL-FP (v1)	Univ. Leicester (UoL), United Kingdom	Optimal Estimation	Boesch et al., 2011
CO2_GO2_SRFP	SRFP or RemoTeC (v1)	SRON, Netherlands	Phillips-Tikhonov regularization	Butz et al., 2009, 2010

Table 2-2: *Overview GHG-CCI+ algorithms for XCH_4 retrieval.*

XCH_4 Product Identifier	Algorithm (version)	Institute	Technique	Reference
CH4_S5P_WFMD	WFM-DOAS (v1.2)	IUP, Univ. Bremen, Germany	Weighted least squares	Schneising et al., 2019
CH4_GO2_SRPR	SRPR or RemoTeC (v1)	SRON, Netherlands	Proxy (PR) retrieval method	Frankenberg et al., 2005
CH4_GO2_SRFP	SRFP or RemoTeC (v1)	SRON, Netherlands	Phillips-Tikhonov regularization; Full Physics (FP) method	Butz et al., 2009, 2010

Table 2-3: *Overview of (other) GHG-CCI+ product related documents. ATBD = Algorithm Theoretical Basis Document, PUG = Product User Guide, E3UB = End-to-End ECV Uncertainty Budget document.*

Product ID	Document	Link
CO2_OC2_FOCA	ATBD	Available from https://www.iup.uni-bremen.de/carbon_ghg/cg_data.html#GHG-CCI
-“-	PUG	- “ -
-“-	E3UB	- “ -
CH4_S5P_WFMD	ATBD	- “ -
-“-	PUG	- “ -
-“-	E3UB	- “ -
CO2_TAN_OCFP	ATBD	- “ -
-“-	PUG	- “ -
-“-	E3UB	- “ -
CO2_GO2_SRFP	ATBD	- “ -
-“-	PUG	- “ -
-“-	E3UB	- “ -
CH4_GO2_SRFP	ATBD	- “ -
-“-	PUG	- “ -
-“-	E3UB	- “ -
CH4_GO2_SRPR	ATBD	- “ -
-“-	PUG	- “ -
-“-	E3UB	- “ -

3 General description of the processing system

A schematic overview of the GHG-CCI+ processing system is given in **Figure 3-1**.

The processing system consists of the different algorithms (see **Tables 2-1 and 2-2**), running at the different responsible institutes.

The different institutes have their own access to the required input data (satellite data, ECMWF meteo data, model data for priors, spectroscopic databases, etc.), and their own computational facilities in the form of multi CPU Unix/Linux systems.

The Level-2 (L2) output data (XCO_2 and XCH_4) generated by the algorithms at the different institutes are available via the CCI Open Data Portal (*https://climate.esa.int/en/odp/#/dashboard*) and additional information is given at the GHG-CCI+ website (https://climate.esa.int/en/projects/ghgs/).

The different parts of the GHG-CCI+ processing systems running at the different institutes are described in more detail in the System Specification Document (SSD) document **/Aben et al., 2019/**.

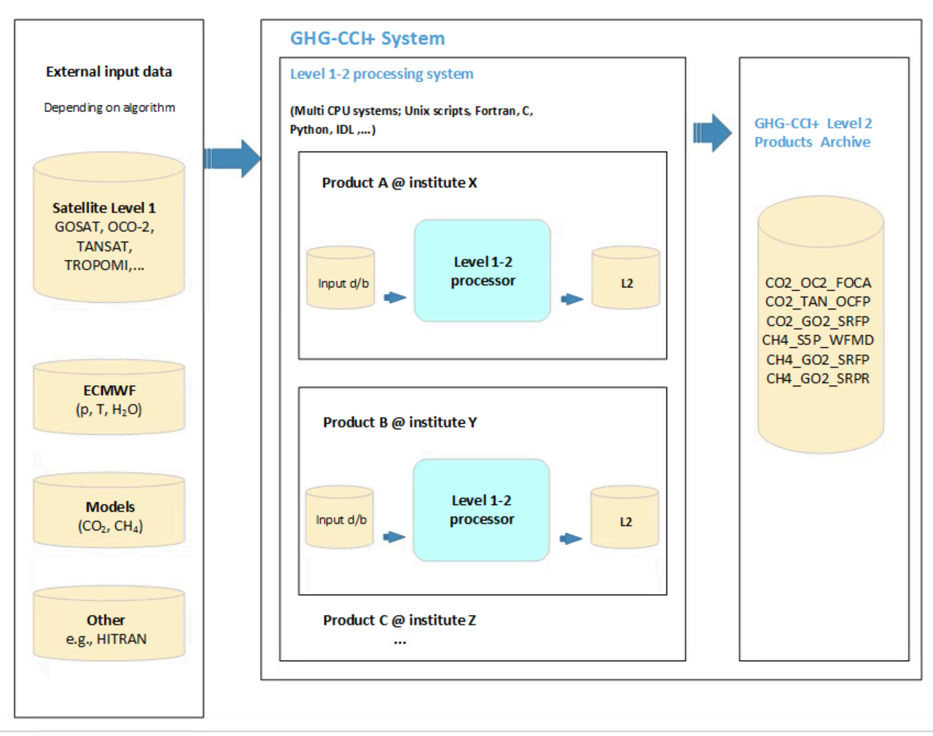

Figure 3-1: *Overview of the GHG-CCI+ processing system. Note that the GHG-CCI+ Level 2 product data archive is the CCI Open Data Portal (https://climate.esa.int/en/odp/#/dashboard).*

4 Independent validation by validation team

This chapter deals with the validation of the GHG-CCI+ retrieval products using ground-based FTIR remote sensing measurements from the Total Carbon Column Observing Network (TCCON) **/Wunch et al.2011/**. The key concept behind this validation is to apply an as uniform as possible validation strategy for all the involved algorithms. With respect to the last PVIR (see **/PVIR GHG-CCI+ v1.1, 2020**/ for details) analysis, several changes have been implemented. These changes concern the actual collocation method as well as taking into account the differences in *a priori* and vertical sensitivity of the measurements. Additionally, several methodologies concerning the calculation of certain quality indicators (the so-called Figures of Merit) have been altered.

As always, choosing collocation criteria is a balance between minimizing the potential collocation error and still retaining a large enough sample so as to be able to derive adequate statistics. Also of note is that some of the current available algorithms have processed data for a limited time span only, which hampers certain aspects of the analysis.

Concerning the Figures of Merit (FoM), we did not employ any pre-analysis averaging and looked at individual satellite-TCCON pairs. This was done mainly to have statistical parameters that relate to the quality of the original data. Users of the data however should keep in mind that some algorithms opt to have a high density dataset with a larger random error component versus a much stricter quality-flagged low density dataset with a smaller random error component. After averaging (in space or time) the first might outperform the latter.

4.1 Validation method

Each individual satellite measurement is paired, if the criteria are met, with an individual TCCON measurement. This particular TCCON measurement needs to be taken within 2 hours and within 500 km of the TCCON measurement. Only for CH4_S5P_WFMD is the collocation criteria tightened to within 100 km and within 1 hour due to its high data density. If more than one TCCON measurement fits the above criteria, the TCCON measurement that has been measured closest (in time) to the satellite coordinates will be the one paired with said satellite measurement. This creates a collocated dataset with unique individual satellite-TCCON pairs.

Prior to the FoM analysis we try to limit the impact of differences in *a priori* and vertical sensitivity between TCCON and the satellite product (**/Rodgers, 2000/**). To limit the impact of the former we adjust the satellite dry air mole fraction using the TCCON *a priori* as in

$$\hat{c}_{S,adj} = \hat{c}_S + \sum_l pw_l\,(1 - A_l)(x^l_{T,a} - x^l_{S,a})$$

where, $\hat{c}_S$ represents the originally retrieved satellite column-averaged dry air mole fraction, l is the index of the vertical layer, A_l the corresponding column averaging kernel of the satellite algorithm, $\boldsymbol{x}_{S,a}$ and $\boldsymbol{x}_{T,a}$ are the satellite and TCCON *a priori* dry air mole fraction profiles respectively. pw_l is the pressure weight associated with level or layer l.

Likewise, to address the latter we apply the satellite averaging kernel onto the TCCON data. Given that TCCON provides total column dry air mole fractions only, we apply this smoothing onto the scaled TCCON *a priori* ($x_{T,r}$), where the scaling factor takes into account the actual retrieval (which is based on a scaling an *a priori* profile) as well as the post retrieval correction to bring TCCON in line with in situ measurements. Thus the scaled TCCON profile ($x_{T,r}$) corresponds with

$$x_{T,r} = x_{T,a} \times \hat{c}_{T,r}/\hat{c}_{T,a}$$

where $x_{T,a}$ is the TCCON *a priori* profile. $\hat{c}_{T,r}$ *and* $\hat{c}_{T,a}$ are the TCCON retrieved and *a priori* column-averaged dry air mole fractions. The adjusted TCCON dry air mole fraction then corresponds with

$$\hat{c}_{T,adj} = \sum_{l} pw_l \left(x_{T,a}^{l} + (x_{T,r}^{l} - x_{T,a}^{l})A_l\right)$$

where, pw_l again represents the pressure weight associated with the level or vertical layer with index l and A_l the corresponding column averaging kernel of the satellite algorithm. $\boldsymbol{x}_{T,a}$ and $\boldsymbol{x}_{T,r}$ are the TCCON *a priori* and scaled dry air mole fraction profiles respectively.

Prior to these adjustments, the TCCON *a priori* needs to be interpolated onto the satellite product vertical grid. This is done using a regridding method that preserves mass (**/Langerock et al., 2015/**) and in case the satellite pixel surface altitude is below that of the TCCON site, the regridded TCCON profile is extrapolated using the satellite's *a priori* profile.

This approach should minimize the differences between satellite and ground-based retrievals, regardless of the algorithm and target species involved. For XCO_2, where the column averaging kernel approximates 1, the impact is expected to be negligible.

To assess the impact of these smoothing steps we also performed an as-is comparison (without *a priori* correction and smoothing) for all products. The sole correction applied to this control run is a height adjustment onto the satellite data where the satellite's dry air mole fraction ($\hat{c}_S$) is scaled by the ratio between the satellite *a priori* partial column associated with the vertical range covered by the TCCON station ($\hat{c}_{S,ap,part}$)and the total *a priori* column ($\hat{c}_{S,ap}$).

$$(\hat{c}_{S,adj}) = \hat{c}_S \left(\frac{\hat{c}_{S,ap,part}}{\hat{c}_{S,ap}}\right)$$

It is on these paired adjusted satellite ($\hat{c}_{S,adj}$) and TCCON ($\hat{c}_{T,adj}$) measurements that we perform our validation analysis and derive our so-called Figures of Merit (FoM).

We have used all public TCCON GGG2014 data as available on the TCCON Data Archive (https://tccondata.org/) on the 1st of January 2021 in our initial analysis. For the determination of the statistical parameters we did remove the high altitude sites Zugspitze and Izaña from the roster.

The bias is defined as the median difference between the individual satellite and TCCON pairs

$$\tilde{X}_{bias} = median(\hat{c}_{S,adj} - \hat{c}_{T,adj})$$

This is done for each station after which the overall Bias FoM is defined as the median of all calculated station biases. One could also group all individual measurements, regardless of station, into one sample onto which we calculate the bias, but this would increase the impact of stations where the data density is high. Since having a high data density, does not necessarily correspond with the highest quality data, we deem our median of station biases approach more accurate.

The scatter at each station corresponds with the median absolute deviation (mad) scaled by 1.4826 which is a statistically more robust proxy for the standard deviation (std) of said difference as in:

$$scatter = 1.4826 \times median(|X_{bias} - \tilde{X}_{bias}|)$$

where

$$X_{bias} = \hat{c}_{S,adj} - \hat{c}_{T,adj}$$

Again for the overall assessment of the scatter we take the median of all individual station scatter values.

Both parameters, bias and scatter, are presented with their 95% confidence interval in the validation summary tables (see **Tables 4-2, 4-4, 4-6, 4-8, 4-10**). These confidence bands have been determined using a bootstrap methodology (**/Lunneborg, 2020/**), where the 95% confidence limits around the median $\tilde{X}$ corresponds with

[$\tilde{X}$ - *(97.5%tile -* $\tilde{X}$*),* $\tilde{X}$ + *(*$\tilde{X}$*- 0.25%tile*)]

Using medians and scaled median absolute deviations instead of means and standard deviations makes for a more robust assessment as it is far less impacted by outliers. These outliers could be haphazard single outliers (in the satellite data as well as TCCON, due to cloud interference etc.) when calculation the station bias and scatter values, but also caused by far from ideal collocation circumstances, limited data, etc. at various TCCON sites when calculating the overall FoMs.

Other FoM are the Relative Accuracy (RA) and Seasonal Relative Accuracy (SRA), which give an indication of the spatial and spatio-temporal accuracy of the algorithm. We define RA as the scaled median absolute deviation on the overall median biases (derived from individual data) obtained at each station. The "Seasonal Relative Accuracy" (SRA), differs from the relative accuracy in that it uses the seasonal bias medians at each station, instead of the overall biases obtained at each station, it is thus the scaled median absolute deviation over all station seasonal median bias results. The seasonal bias results are constructed, for each TCCON station, from all data pairs which fall within the months of January till March (JFM), April till June (AMJ), July till September (JAS) or October till December (OND), regardless of the year the measurements are taken. Some stations feature only limited data during certain seasons, which sometimes results in erratic (seasonal) bias results. To avoid the inclusion of these results into the RA and SRA calculation, we do not include those results which are derived from less than 4 individual SAT-TCCON pairs. This may seem as a low threshold, but combined with the fact that we draw upon median values, we deem this sufficient.

To verify the stability of the algorithm over time we fit a linear trend and seasonal cycle through the bias timeseries:

$$X = i + s.t + A.\sin(2\pi.(t + ph))$$

Here, *X* represents the satellite minus TCCON difference, *i* the intercept, *s* the slope which corresponds with the linear drift, *A* the amplitude of the seasonal cycle and *ph* the phase shift. While the slope yields information on any potential drift, the amplitude in the above fit results gives us information on the potential mismatch between Satellite and TCCON seasonal cycles. Ideally there should be no difference between these cycles which would yield a slope and amplitude=0 in the bias timeseries. This is done for all stations provided that the overlapping station satellite timeseries covers a timespan of at least 2 years. The overall long term stabilty then corresponds with the median slope over all these stations as we expect the linear drift to be consistent for the entire dataset.

Another Figure of Merit is the so-called Uncertainty Ratio, which is defined as the ratio between the algorithm's reported uncertainty and the above mentioned scatter. If the reported uncertainty is correctly assessed, the uncertainty ratio should approach unity. However, this baseline number ignores any aspect of temporal, spatial or TCCON variability embedded in the scatter.

We therefore also calculate an improved Uncertainty Ratio, which is the ratio between the reported uncertainty and the uncertainty on the Satellite (σ_{SAT}) as determined from the scatter using the method outlined below. Both are reported in the summary tables of each algorithm (see **Tables 4-2, 4-4, 4-6, 4-8, 4-10**), where the improved uncertainty ratio is marked by an *.

Taking into account the variability of the TCCON reference data and the collocation error, when assuming independence, the scatter can be written down as:

$$\text{scatter}=\sqrt{(\sigma_{SAT}^2 + \sigma_{TCCON}^2 + \sigma_{Collocation}^2)}$$

where σ_{SAT} is the standard deviation due to variability of the satellite product, σ_{TCCON} due to variability within TCCON and $\sigma_{Collocation}$ due to variability in time and space.
σ_{SAT} as derived from our comparison between the satellite and TCCON measurements is thus:

$$\sigma_{SAT} = \sqrt{(scatter^2 - \sigma_{TCCON}^2 - \sigma_{Collocation}^2)}$$

The standard deviation on the TCCON measurements can be readily calculated from the average variability of the FTIR measurements within the collocation timeframe (4 hours).

The Collocation uncertainty is harder to define and consists of a spatial and temporal component. The latter can be ignored since it is already embedded in our calculation of the TCCON uncertainty (which is based on the actual variability of the TCCON measurements in time and thus also contains the temporal natural variability).

Unfortunately we have no solid information on the spatial collocation uncertainty. Our best, but flawed, estimate of this factor can be derived from fitting a linear equation through the sat-TCCON residuals as a function of distance between the TCCON site and the satellite pixel center points (we do this for all satellite TCCON pairs drawn from all stations, see **Figure 4-2**). From the obtained slope a, we can then estimate the uncerainty associated with the collocation by simply taking the standard deviation of points along the slope (a×dist(i)), where dist(i) is the distance between the TCCON station and satellite centre point for a given sat-TCCON pair with index i. Note that we here use the normal standard deviation as, by default, there are no outliers in the points that constitute the slope.

As already mentioned, this is a mere estimate as station to station bias results can differ profoundly. Most noticeable is to look at bias value differences between sites where the collocation areas overlap to a large degree, such as Paris and Orleans, and Pasadena and Edwards (see **Figure 4-1 and Tables 4-1, 4-3, 4-5, 4-7**).

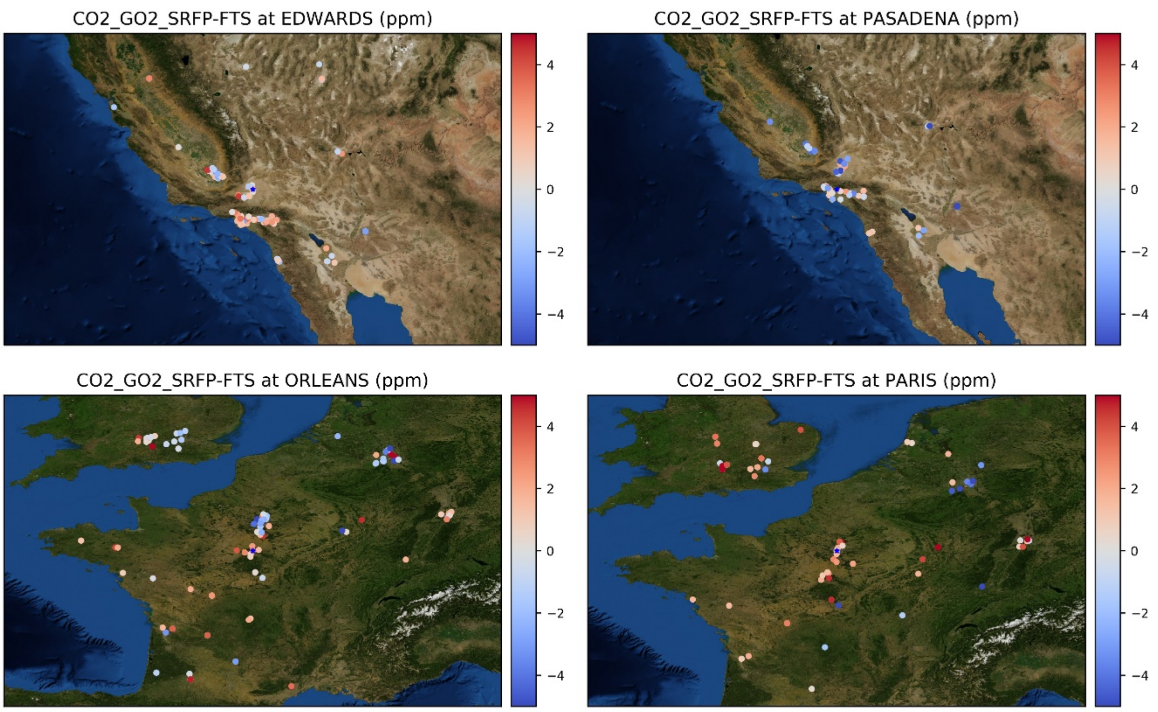

Figure 4-1: Example plot of collocated data (in this case SRFP XCO_2) at Orleans and Paris (top) and Pasadena and Edwards (bottom).

As can be seen in **Figure 4-2**, which shows all the 'bias as a function of distance' plots, the effect is fairly limited. For XCO_2, values range between -0.01 and 0.05 ppm/100 km, for XCH_4 we see values between -0.03 and -0.35 ppb/100km. This does not mean that there is no such thing as a bias due to collocation issues, but rather that it does not present itself as a general feature over the entire dataset. If we look at the slopes on a per station basis for the two algorithms with the highest datadensity, we find that for CO2_OC2_FOCA these range between -0.39 (Hefei) and 0.56 ppm/100 km (Paris). For CH4_S5P_WFMD the slopes ranged between -15.4 and +15.2 ppb/100 km (for Nicosia and Edwards respectively)

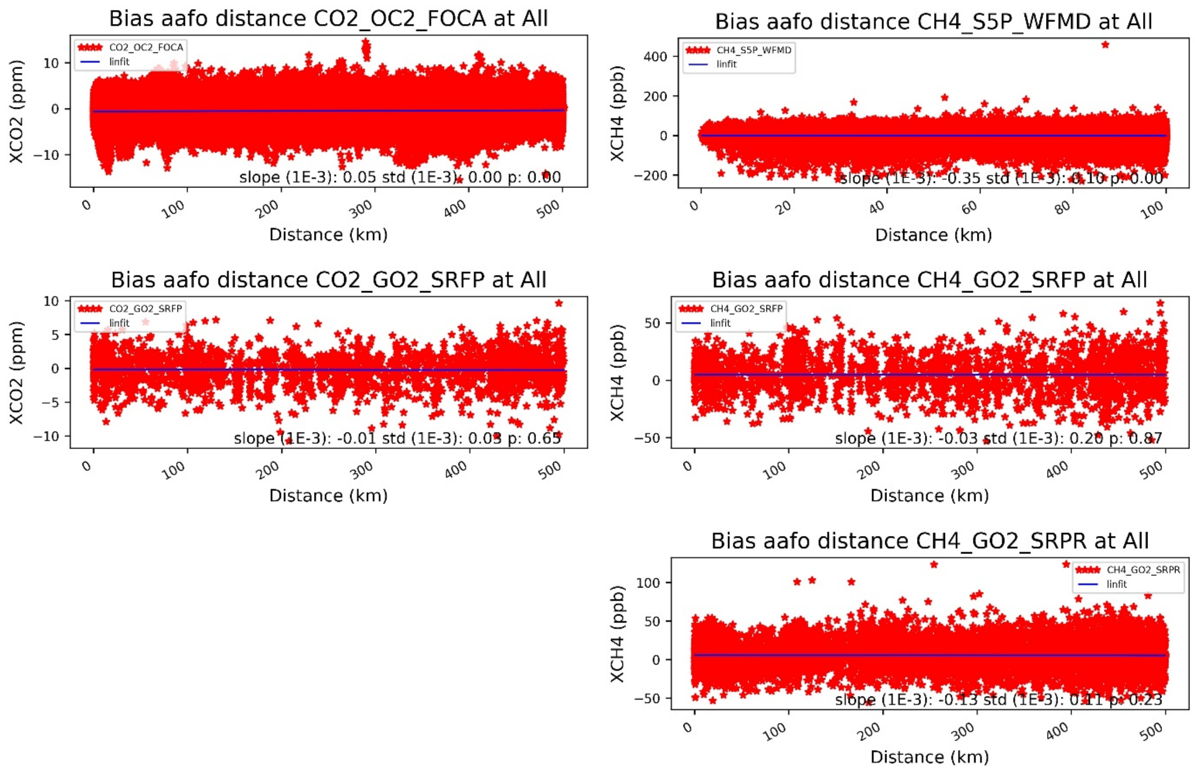

Figure 4-2: Satellite-TCCON bias as a function of (aafo) distance between the satellite and TCCON sampling point, for all algorithms in this study. Slope in ppm/100 km for XCO_2 and ppb/100 km for XCH_4.

4.2 Validation results

This section lists all validation results for the algorithms presently available in this study. First we show, for each algorithm, a general overview of the collocated data.

This comprises of a Taylor plot and a mosaic overview of the obtained timeseries.

The Taylor plot shows the correlation between the various TCCON sites and the retrieval algorithm (straight lines), the standard deviation of the TCCON data at each site, relative to the standard deviation of the satellite (normalized to 1) (light grey arches) and the root mean square error of the sat-fts difference (dark grey arches).

After this we discuss the different statistical parameters as obtained on a per station level.

Then the temporal variability is discussed, showing all the station timeseries as well as a more broad 'latitudinal band' based discussion on the long term trend (if any) and seasonality.

After this we discuss the overall FoM, obtained from the analysis of individual data, and their statistical reliability.

Thus in each section we show:

1) A Taylor and Mosaic overview plot.
2) A table listing all Bias, Scatter, correlation (R), number of collocated data pairs (N) for all stations, and, if the timeseries allows, the slopes and amplitudes of the trend fits.
3) Example timeseries of individual data.
4) Monthly averaged timeseries and seasonal plots for broader latitude bands.
5) A Summary table of the Figures of Merit drawn from the values, drawn from individual measurements, at all stations, excluding Izaña and Zugspitze.

4.2.1 Validation results for product CO2_OC2_FOCA

Below we show the validation results of the XCO_2 concentrations as derived by the CO2_OC2_FOCA algorithm using OCO-2 spectra. Data was available from January 2015 up to and including May 2020. The FOCAL algorithm provides *a priori* and column averaging kernel data on a 5 layer profile. The difference between the smoothed and unsmoothed data is minimal, as expected for XCO_2. (an 0.1 ppm improvement in the median bias and a 0.01 ppm reduction in the scatter). All results shown pertain to the smoothed dataset.

4.2.1.1 Detailed results

The Taylor diagram below in **Figure 4-3** yields a concise overview of the capabilities of the CO2_OC2_FOCA algorithm. Most TCCON sites cluster around the 0.9 correlation line. Also, the normalized standard deviation of most sites is close to 1, indicating that the variability of both datasets (due to natural variability and random error) is comparable. The normalized standard deviation of the bias (std(sat-fts)/std(sat)) sits (for most sites) around 0.4, which is very encouraging as it indicates that a large fraction of the variability (we can only assume it is the natural variability part) within the TCCON timeseries is also captured by the satellite.

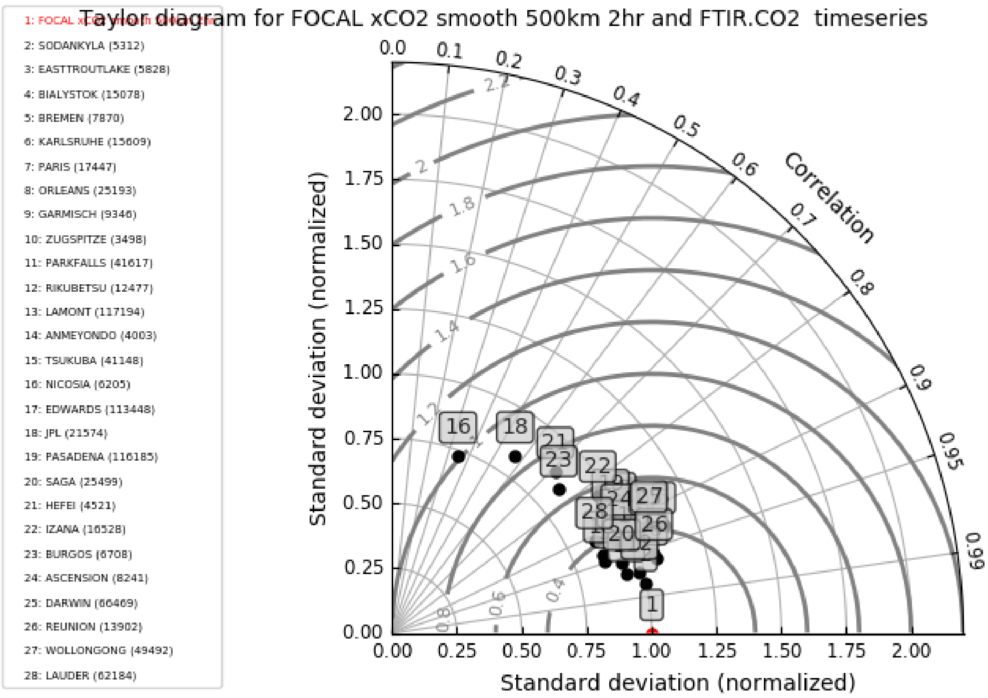

Figure 4-3: Tayor plot of XCO_2 TCCON values relative to CO2_OC2_FOCA. Straight lines correspond with the correlation, light grey lines yield the variability of the TCCON data relative to the satellite variability and the dark grey lines correspond with the variability of the Satellite -TCCON bias relative to the satellite variability.

Notable outliers are Nicosia, Hefei and JPL with lower correlations and higher standard deviations on the bias, but all of them showing more limited (in time) overlapping datasets.

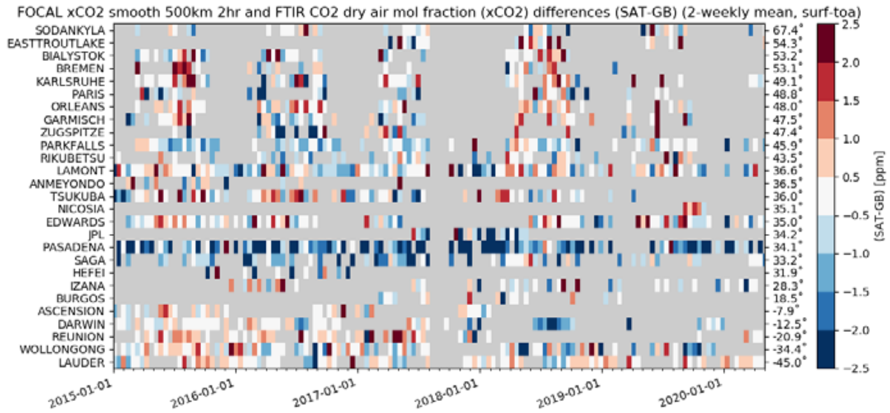

Figure 4-4: Mosaic plot of bi-weekly mean CO2_OC2_FOCA-TCCON XCO_2 biases as a function of time and TCCON station.

It is hard to discern a pattern in the above mosaic plot (**Figure 4-4**), which shows the mean bi-weekly bias between the satellite and TCCON measurement pairs. One can see the seasonal unavailability of data during winter (not visible for the Southern hemisphere as Lauder (New Zealand) still sits at a modest 45°S. Pasadena has outspoken and consistent negative biases (see also **Table 4-1**). This is not surprizing as it is located within the Los Angeles basin and typically measures larger concentrations than what is present outside the basin. The nearby Edwards site which to a large degree has an overlapping collocation area (see **Figure 4-1**) features much different bias values (-0.07 ppm compared to -1.84 ppm at Pasadena). The algorithm produces on average ~15800 data pairs per station. Which roughly corresponds with around 800 data pairs per station per year. Of the stations, only 6 out of 25 have a correlation coefficient under 0.90 and 2 of those still have a correlation of 0.89. The correlation of all data (regardless of station) equals 0.93. The bias ranges between -1.84 ppm (Pasadena) and 1.01 ppm (Nicosia) and the scatter between 2.52 ppm (JPL) and 0.89 ppm (Reunion). Long term trends on the bias (the so-called drift) range between -0.28 ppm/year (Anmeyondo) and 0.32 ppm/year (Tsukuba). Note that we only calculated long-term trends for stations whose collocated dataset spans at least 2 years. The amplitude on the other hand ranges between 1.39 ppm at Karlsruhe and 0.15 ppm at Ascension, Darwin and Wollongong.

Table 4-1: Number of collocated data pairs (N), Correlation (R), Bias, Scatter, long term trend difference (ltt) and uncertainty thereon (ltt_err), seasonal amplitude difference (A) and uncertainty thereon (A_err) as well as the latitude of the TCCON station. The last row lists the median values over all stations. Product: CO2_OC2_FOCA.

STATION	N	R	Bias	Scat	ltt	ltt_err	A	A_err	lat
SODANKYLA	5312	0.98	-0.18	1.08	0.22	0.09	0.96	0.5	67.4
EASTTROUTLAKE	6615	0.95	0.03	1.37	0.28	0.17	1.23	1.29	54.3
BIALYSTOK	15078	0.92	-0.03	1.37	0.01	0.17	0.29	0.25	53.2
BREMEN	7870	0.93	0.07	1.97	0.19	0.14	0.75	0.54	53.1
KARLSRUHE	15821	0.96	0.08	1.6	-0.11	0.13	1.39	0.53	49.1
PARIS	17447	0.89	-1.07	1.64	-0.01	0.13	0.89	0.52	48.8
ORLEANS	25193	0.93	0.45	1.16	0.02	0.1	0.87	0.34	48
GARMISCH	9346	0.91	-0.05	1.8	-0.04	0.19	0.45	0.24	47.5
PARKFALLS	42866	0.97	-0.4	1.2	-0.16	0.07	0.41	0.17	45.9
RIKUBETSU	12477	0.97	-0.28	1.24	-0.12	0.13	0.33	0.25	43.5
LAMONT	118074	0.92	-0.3	1.62	0.02	0.09	0.63	0.15	36.6
ANMEYONDO	4003	0.92	0.2	1.57	-0.28	0.25	0.69	0.57	36.5
TSUKUBA	41148	0.93	-0.44	1.74	0.32	0.15	0.31	0.21	36
NICOSIA	6205	0.35	1.01	1.28	-	-	-	-	35.1
EDWARDS	115880	0.94	-0.07	1.54	0.04	0.06	0.55	0.16	35
JPL	21574	0.57	-0.81	2.51	-	-	-	-	34.2
PASADENA	117926	0.89	-1.84	1.78	0.28	0.1	0.57	0.17	34.1
SAGA	25739	0.96	-1.08	1.27	-0.05	0.11	0.3	0.23	33.2
HEFEI	4521	0.71	-1.6	2.43	-	-	-	-	31.9
BURGOS	6708	0.76	-0.13	1.1	-	-	-	-	18.5
ASCENSION	8241	0.91	0.09	1.22	0.07	0.19	0.15	0.28	-7.9
DARWIN	66469	0.92	-0.35	1.47	0.23	0.11	0.15	0.14	-12.5
REUNION	13902	0.96	0.63	0.89	0.14	0.09	0.44	0.2	-20.9
WOLLONGONG	49492	0.92	-0.48	1.39	0.2	0.07	0.15	0.16	-34.4
LAUDER	62505	0.91	0.18	1.24	0.04	0.05	0.38	0.13	-45
MEDIAN	**15821**	**0.92**	**-0.13**	**1.39**	**0.04**	**0.11**	**0.45**	**0.24**	**36**

The timeseries below in **Figure 4-5** show individual satellite and ground-based fts measurements. Capture of the seasonal cycle, stability and uncertainty is similar to that of TCCON, even exhibiting far less outlier values at certain stations.

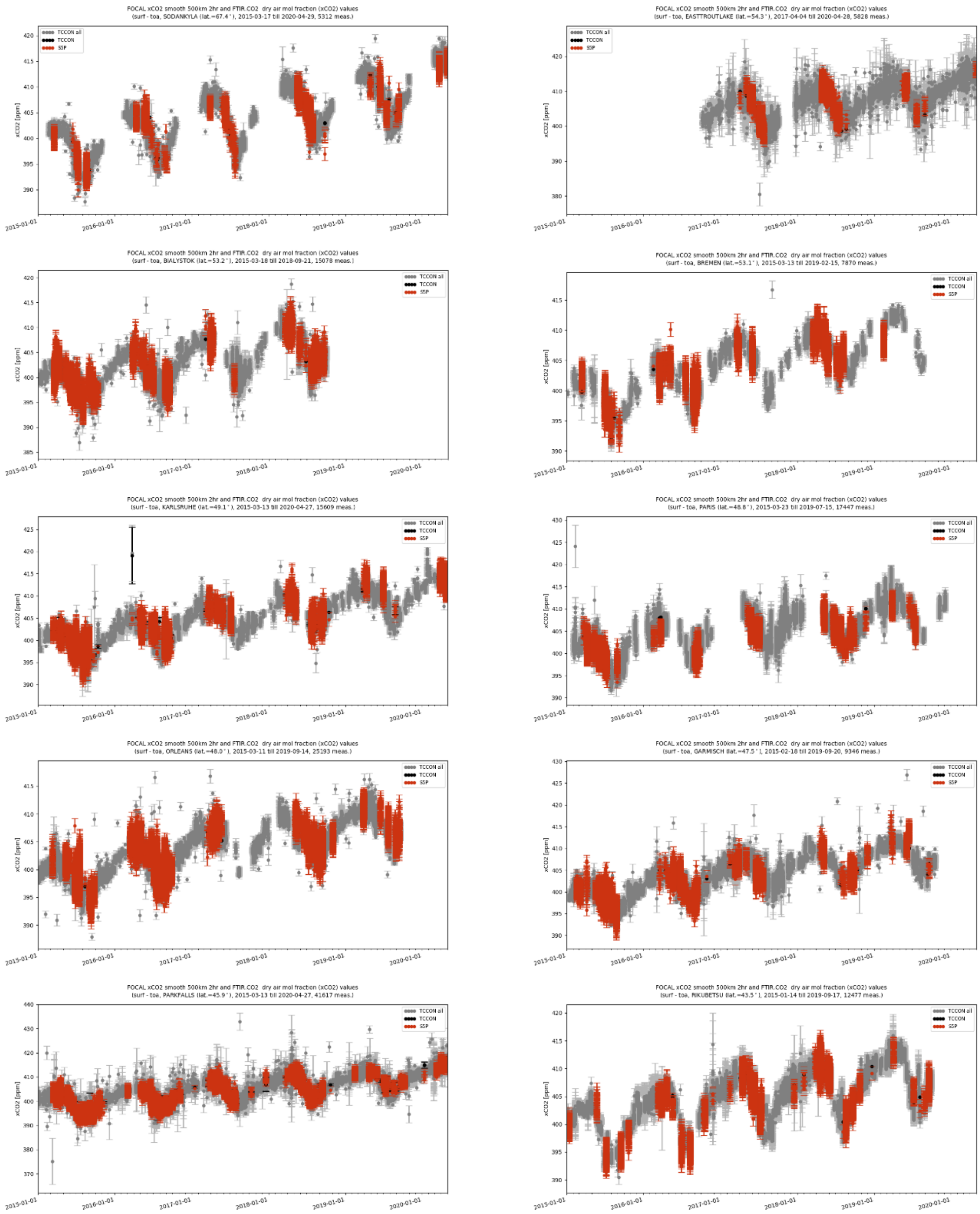

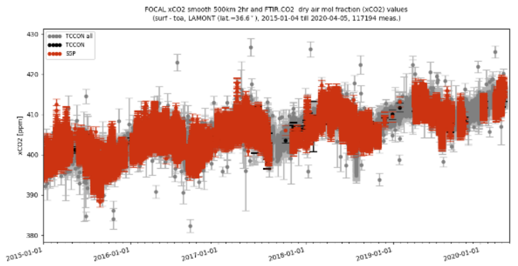

FOCAL xCO2 smooth 500km 2hr and FTIR.CO2 dry air mol fraction (xCO2) values
(surf - toa, LAMONT (lat.=36.6 °), 2015-01-04 till 2020-04-05, 117194 meas.)
TCCON all
TCCON
SSP
xCO2 [ppm]

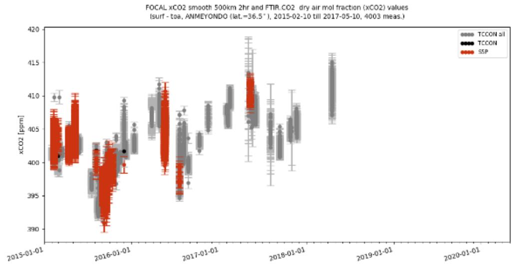

FOCAL xCO2 smooth 500km 2hr and FTIR.CO2 dry air mol fraction (xCO2) values
(surf - toa, ANMEYONDO (lat.=36.5 °), 2015-02-10 till 2017-05-10, 4003 meas.)
TCCON all
TCCON
SSP
xCO2 [ppm]

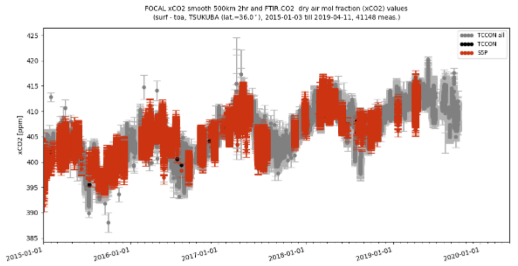

FOCAL xCO2 smooth 500km 2hr and FTIR.CO2 dry air mol fraction (xCO2) values
(surf - toa, TSUKUBA (lat.=36.0 °), 2015-01-03 till 2019-04-11, 41148 meas.)
TCCON all
TCCON
SSP
xCO2 [ppm]

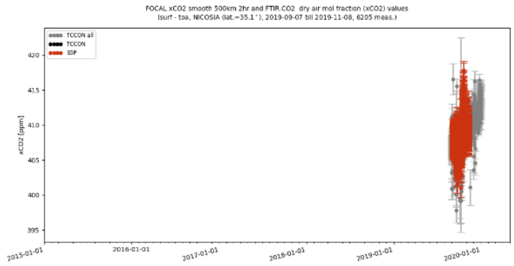

FOCAL xCO2 smooth 500km 2hr and FTIR.CO2 dry air mol fraction (xCO2) values
(surf - toa, NICOSIA (lat.=35.1 °), 2019-09-07 till 2019-11-08, 6205 meas.)
TCCON all
TCCON
SSP
xCO2 [ppm]

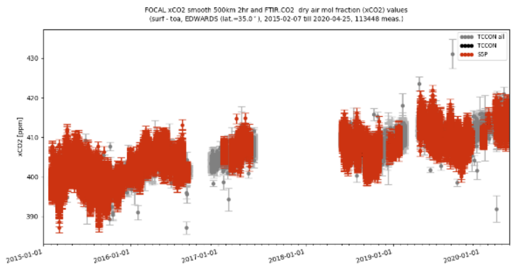

FOCAL xCO2 smooth 500km 2hr and FTIR.CO2 dry air mol fraction (xCO2) values
(surf - toa, EDWARDS (lat.=35.0 °), 2015-02-07 till 2020-04-25, 113448 meas.)
TCCON all
TCCON
SSP
xCO2 [ppm]

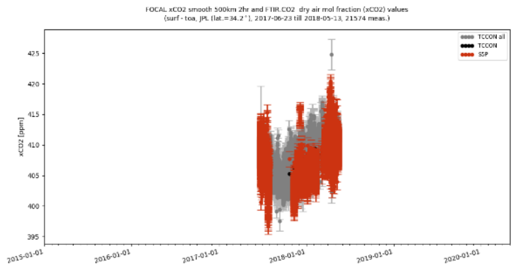

FOCAL xCO2 smooth 500km 2hr and FTIR.CO2 dry air mol fraction (xCO2) values
(surf - toa, JPL (lat.=34.2 °), 2017-06-23 till 2018-05-13, 21574 meas.)
TCCON all
TCCON
SSP
xCO2 [ppm]

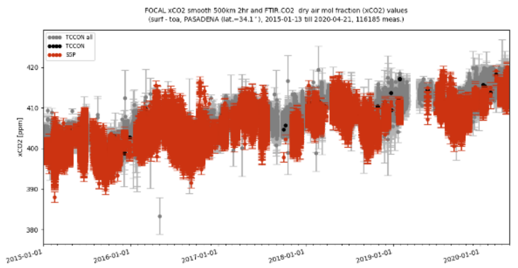

FOCAL xCO2 smooth 500km 2hr and FTIR.CO2 dry air mol fraction (xCO2) values
(surf - toa, PASADENA (lat.=34.1 °), 2015-01-13 till 2020-04-21, 116185 meas.)
TCCON all
TCCON
SSP
xCO2 [ppm]

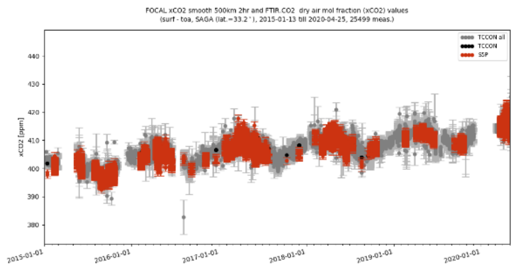

FOCAL xCO2 smooth 500km 2hr and FTIR.CO2 dry air mol fraction (xCO2) values
(surf - toa, SAGA (lat.=33.2 °), 2015-01-13 till 2020-04-25, 25499 meas.)
TCCON all
TCCON
SSP
xCO2 [ppm]

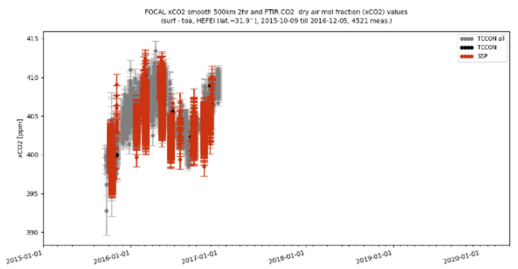

FOCAL xCO2 smooth 500km 2hr and FTIR.CO2 dry air mol fraction (xCO2) values
(surf - toa, HEFEI (lat.=31.9 °), 2015-10-09 till 2016-12-05, 4521 meas.)
TCCON all
TCCON
SSP
xCO2 [ppm]

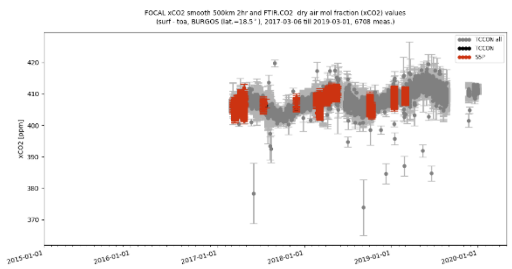

FOCAL xCO2 smooth 500km 2hr and FTIR.CO2 dry air mol fraction (xCO2) values
(surf - toa, BURGOS (lat.=18.5 °), 2017-03-06 till 2019-03-01, 6708 meas.)
TCCON all
TCCON
SSP
xCO2 [ppm]

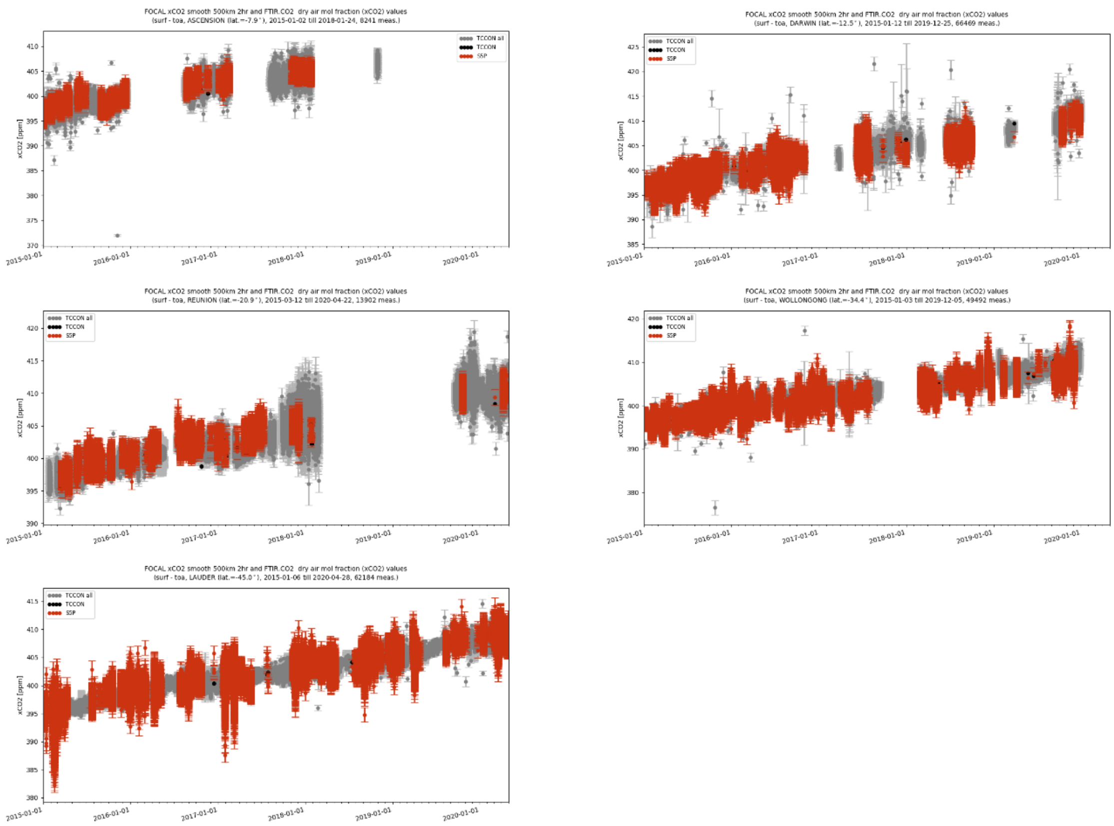

Figure 4-5: XCO_2 timeseries at all TCCON sites (red= CO2_OC2_FOCA data, black is collocated TCCON data and grey are the uncollocated TCCON data).

Figure 4-6 shows monthly median timeseries for TCCON and FOCAL XCO_2 for all data that fall within certain latitude bands, namely all sites north of 40°N latitude (top), all sites between 40°N and the equator (mid) and all sites in the Southern hemisphere (bottom). As can be seen, for all bands, the TCCON and FOCAL data feature the exact same long term trend. On the right hand side of each figure is the detrended monthly median values as a function of month. Again this clearly shows that FOCAL accurately captures the seasonal cycle. The median amplitude derived from seasonal fits through the individual bias data at each station amounts to 0.45 [0.21,0.56] ppm.

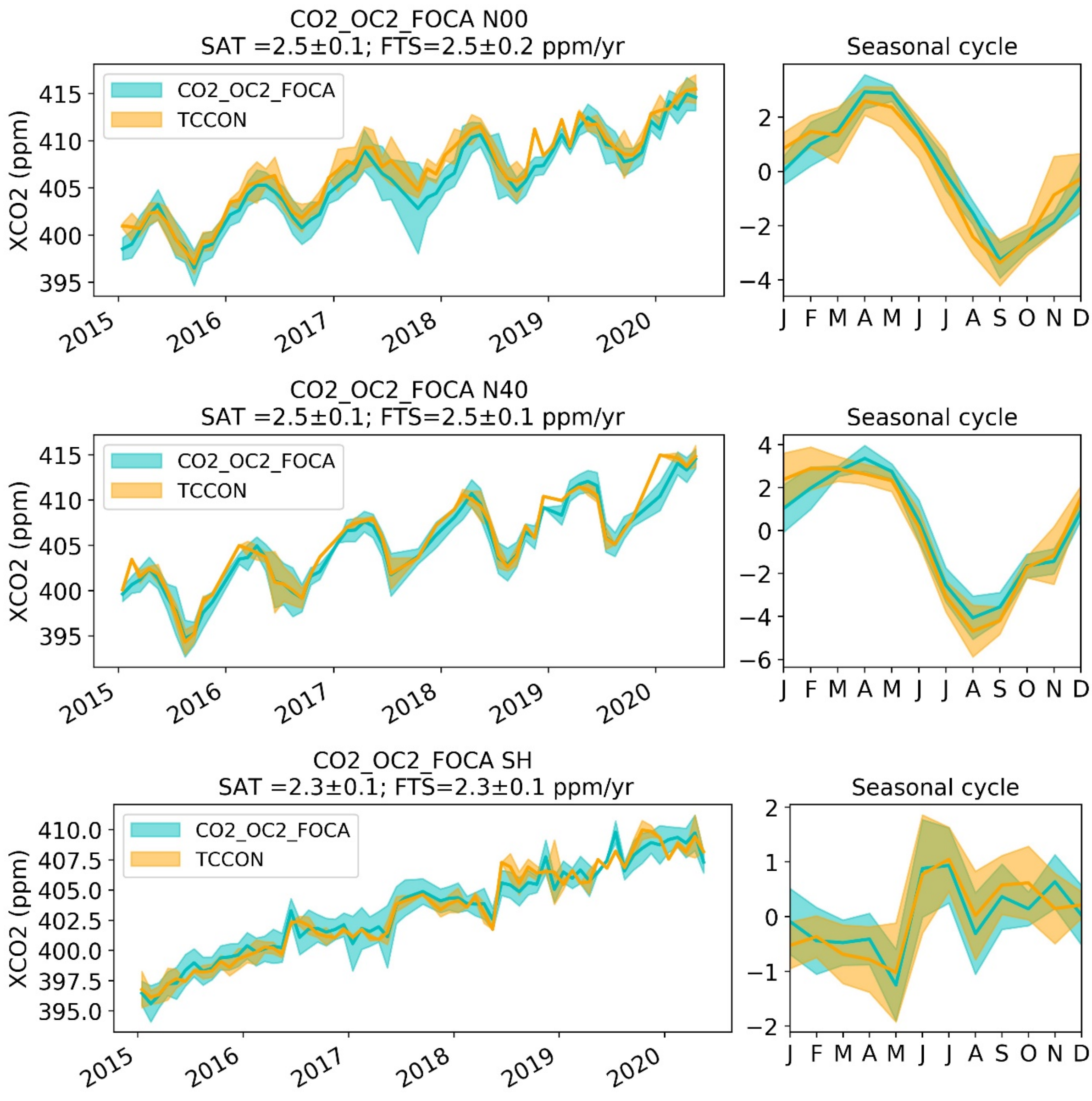

Figure 4-6: Monthly median collocated Sat and TCCON XCO_2 concentrations as a function of time and the detrended monthly medians as a function of season. The shaded areas correspond with the scaled median absolute deviation.

4.2.1.2 Summary

Listed in the table below (**Table 4-2**) are the Figure of Merit parameters as derived from the individual data pairs at the different TCCON stations. Values in square brackets [ ] correspond with the upper and lower 95% confidence bound on the parameter. The uncertainty ratio features 2 numbers as outlined in the validation method

Also important to note is that the results not only pertain to the actual data quality but also contain a collocation error component. For instance, the difference in the observed bias at the relatively close by Pasadena and Edwards stations is 1.77 ppm. The same holds true for Paris and Orleans (1.52 ppm difference).

Overall the CO2_OC2_FOCA product delivers data that matches very well with that of TCCON. This is apparent in the Taylor diagram time series plots as well as the Figures of Merit.

Given that the accuracy requirements of < 0.5 ppm, assumes the abolishment of any collocation influence, nor any station-to-station differences within the TCCON network (its network accuracy is estimated to be within 0.4 ppm), it is impressive that the determined Relative Accuracy (0.41) is lower than this target. Even the Seasonal Relative Accuracy (SRA at 0.73) is close and has itself confidence bands that overlap with the target. Therefore, at this stage we certainly cannot claim that the algorithms has not met this accuracy target.

The reported uncertainty is, when compared to the scatter, slightly underestimated, but that said the scatter itself (1.39 ppm) has reached the so-called breakthrough levels (< 3 ppm) and is edging towards the goal target (<1 ppm). From the timeseries plots and Taylor diagram we in fact see that the variability closely matches this of TCCON. The overall bias is slightly negative but with confidence bounds that overlap with 0.

And finally the dataset shows no significant long term drift.

Table 4-2: presents an overview of the estimated data quality of CO2_OC2_FOCA, as obtained by the VALT team, from comparisons with TCCON ground-based reference observations. Values in square brackets [ ] correspond with the upper and lower 95% confidence bound on the parameter. The uncertainty ratio features 2 numbers as outlined in the validation method.

Product Quality Summary Table for Product: CO2_OC2_FOCA Level: 2, Version: v09, Time period covered: 1.2015 – 5.2020 Assessment: Validation Team (VALT)			
Parameter [unit]	**Achieved performance**	**Requirement**	**Comments**
Single measurement precision (1-sigma) in [ppm]	1.39 [1.15,1.54]	< 8 (T) < 3 (B) < 1 (G)	Computed as the median over all station scaled median absolute differences to TCCON
Uncertainty ratio [-]: Ratio reported uncertainty to standard deviation of satellite-TCCON difference	0.74, 0.79*	-	No requirement but value close to unity expected for a high quality data product with reliable reported uncertainty.
Median bias (global offset) [ppm]	-0.13 [-0.32,0.15]	-	No requirement but value close to zero expected for a high quality data product.
Accuracy: Relative systematic error [ppm]	Spatial: 0.41 [0.05,0.61] Spatio-temporal: 0.73 [0.47,0.90]	< 0.5	Spatial: Computed as standard deviation of the biases at the various TCCON sites. Spatio-temporal: As "Spatial" but also considering seasonal biases.
Stability: Drift [ppm/year]	0.04 [-0.10,0.09]	< 0.5	Linear drift

4.2.2 Validation results for product CO2_TAN_OCFP

Here we present the VALT validation results for the CO2_TAN_OCFP product. Note that the actual product did not change with respect to our previous validation effort, (**/PVIR GHG-CCI+ v1.1, 2020/),** but a revaluation was nevertheless performed as our comparison methodology has changed considerably. Data was available from March 2017 up to and including May 2018. The OCFP algorithm provides *a priori* and column averaging kernel information on a 20 level profile. Given the very limited time period that is covered by this product, these validation results will be rather preliminary in nature, nor can we make useful statements about long term. The difference between the smoothed and unsmoothed data is noticeable (a 1 ppm improvement in the median bias and a 0.1 ppm reduction in the scatter) and far more significant than for instance for the FOCAL product. All results shown pertain to the smoothed dataset.

4.2.2.1 Detailed results

The Taylor diagram below in **Figure 4-7** shows a short overview of the capabilities of the CO2_TAN_OCFP product. Most TCCON sites cluster around a 0.75 correlation value, but with negative correlation values for Darwin (no doubt a combination of the limited seasonal variability in the Southern hemisphere and the short time period covered). The normalized standard deviation of most sites is smaller than 1 (between 0.5 and 1), indicating that the variability of the TCCON data is smaller. The normalized standard deviation of the bias sits (for most sites) between 1 and 0.6. All this indicates that while OCFP data features a stronger variability (random error and/or seasonal variability) than the TCCON data, the biases still harbors less variability then either of them, an indication of OCFP capturing the natural variability.

There is no real discernible pattern in the mosaic plot (**Figure 4-8**), which shows the mean bi-weekly bias between the satellite and TCCON measurement pairs. However, the period covered by the plot is very limited.

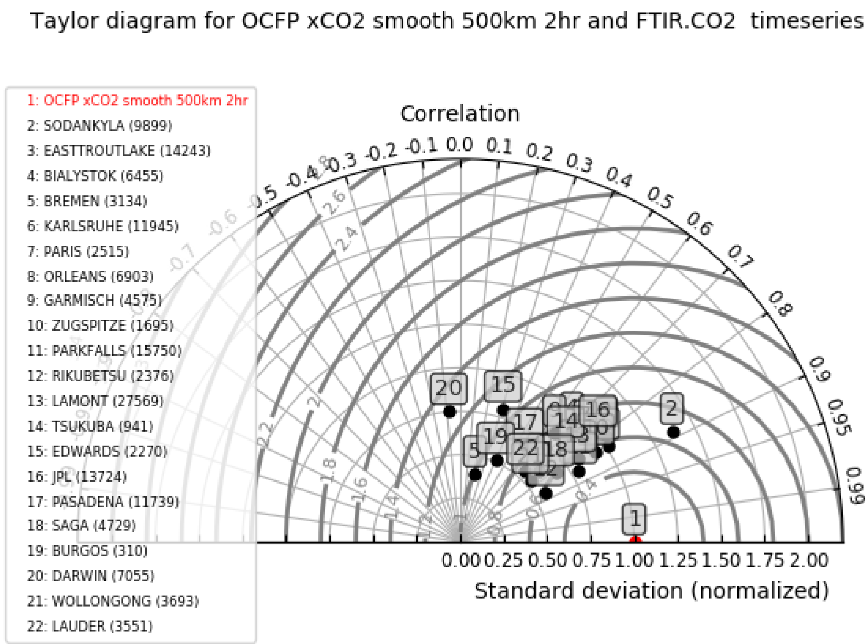

Figure 4-7: Taylor plot of daily averaged XCO_2 TCCON values relative to product CO2_TAN_OCFP. Straight lines correspond with the correlation, light grey lines yield the variability of the TCCON data relative to the satellite variability and the dark grey lines correspond with the variability of the Satellite -TCCON bias relative to the satellite variability.

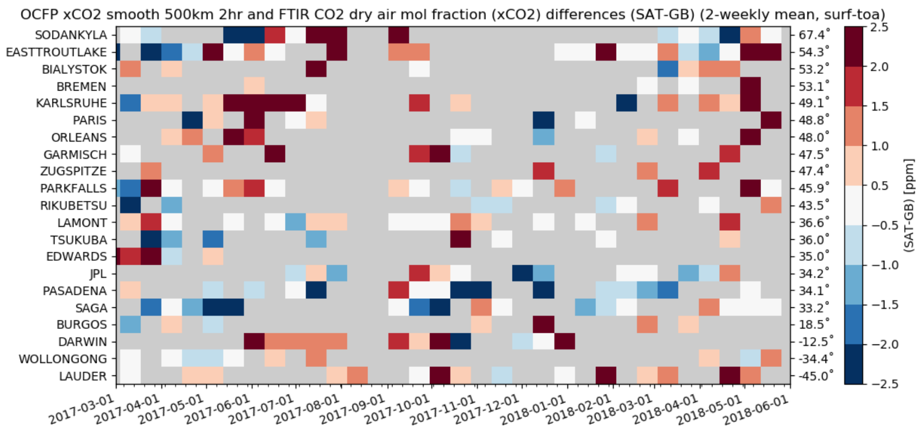

Figure 4-8: Mosaic plot of bi-weekly mean CO2_TAN_OCFP-TCCON XCO_2 biases as a function of time and TCCON station.

Table 4-3 lists all bias and scatter results derived from individual data pairs at all TCCON stations. The algorithm produces on average ~5600 data pairs per station which corresponds with ~4500 pairs per station per year. The observed median bias ranges between -1.21 (Pasadena) and 1.7 ppm(Edwards), while the scatter ranges between 3.34 ppm (Bremen) and 1.90 (JPL). Note that the extreme bias results are observed at stations that are quite close to one another. One in the Los Angeles basin (Pasadena) and the other just outside on the other side of the San Gabriel Mountain range (Edwards), that separates the basin from the Mojave Desert. Correlation values range between -0.09 (Darwin) and 0.89 (Sodankyla), with the median over all stations equal to 0.75. Given the limited timespan covered by the product, we did not calculate any long term trend. But as can be seen in **Figures 4-9 and 4-10** no clear-cut drift is observable.

Table 4-3: Number of collocated data pairs (N), Correlation (R), Bias, Scatter, long term trend difference (ltt) and uncertainty thereon (ltt_err), seasonal amplitude difference (A) and uncertainty thereon (A_err) as well as the latitude of the TCCON station. The last row lists the median values over all stations. Product: CO2_TAN_OCFP.

STATION	N	R	Bias	Scat	ltt	ltt_err	A	A_err	lat
WOLLONGONG	3693	0.75	0.03	1.35	-	-	-	-	-34.4
TSUKUBA	941	0.73	-0.54	1.89	-	-	-	-	36
SODANKYLA	9899	0.89	0.36	1.79	-	-	-	-	67.4
SAGA	4729	0.81	-0.34	1.80	-	-	-	-	33.2
RIKUBETSU	2376	0.87	-0.17	1.25	-	-	-	-	43.5
PASADENA	11739	0.56	-1.21	2.09	-	-	-	-	34.1
PARKFALLS	15750	0.86	0.46	1.68	-	-	-	-	45.9
PARIS	2515	0.77	0.42	1.27	-	-	-	-	48.8
ORLEANS	6903	0.75	0.71	0.98	-	-	-	-	48
LAUDER	3551	0.68	1.03	1.21	-	-	-	-	-45
LAMONT	27569	0.82	0.44	1.22	-	-	-	-	36.6
KARLSRUHE	11945	0.84	1.35	1.56	-	-	-	-	49.1
JPL	13724	0.79	-0.41	1.90	-	-	-	-	34.2
GARMISCH	4575	0.66	-0.11	1.61	-	-	-	-	47.5
EDWARDS	2270	0.31	1.70	1.33	-	-	-	-	35
EASTTROUTLAKE	14243	0.81	-0.05	1.24	-	-	-	-	54.3
DARWIN	7055	-0.09	1.04	1.60	-	-	-	-	-12.5
BURGOS	310	0.4	0.47	1.33	-	-	-	-	18.5
BREMEN	3134	0.21	0.35	1.03	-	-	-	-	53.1
BIALYSTOK	6455	0.71	0.47	1.72	-	-	-	-	53.2
MEDIAN	**5592**	**0.75**	**0.39**	**1.46**	**-**	**-**	**-**	**-**	**40.0**

The timeseries below in **Figure 4-9** show individual satellite and ground-based fts measurements. As can be seen, and was already apparent from the Taylor diagram, OCFP XCO_2 features a somewhat higher scatter than TCCON, but overall the seasonality is well captured. Some outliers are noticeable (both in the TCCON and OCFP dataset).

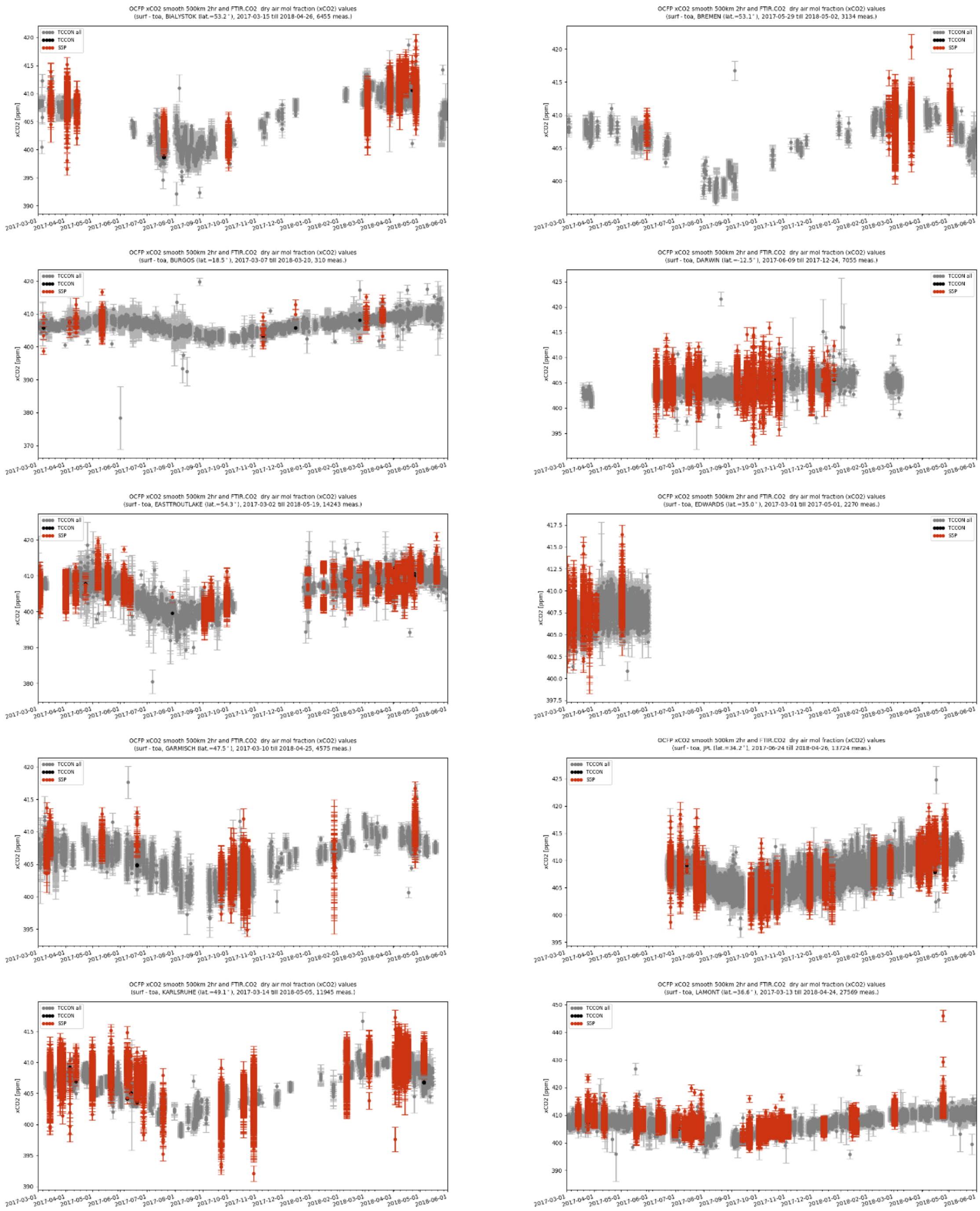

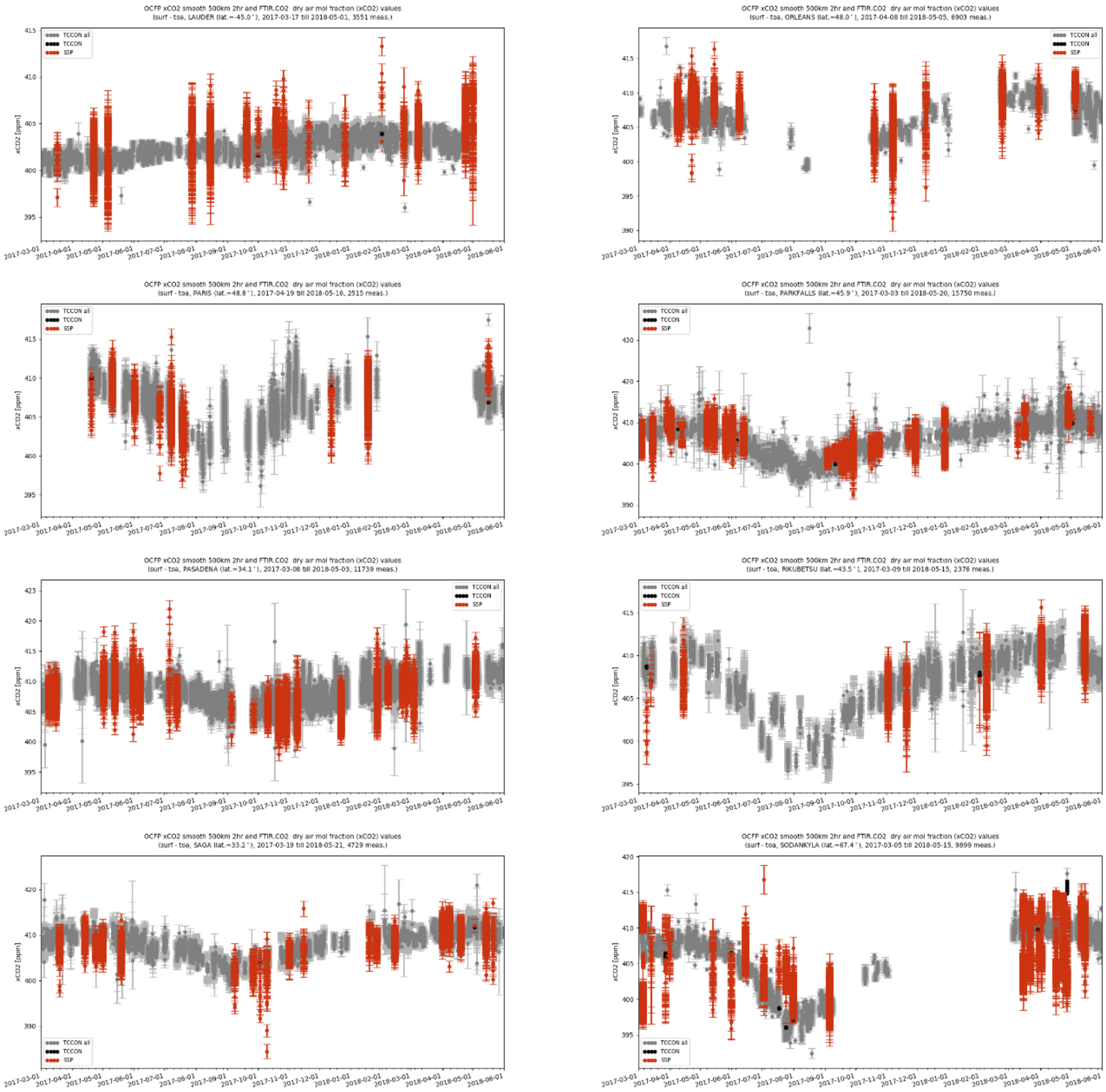
OCFP xCO2 smooth 500km 2hr and FTIR.CO2 dry air mol fraction (xCO2) values
(surf - toa, LAUDER (lat.=-45.0°), 2017-03-17 till 2018-05-01, 3551 meas.)
OCFP xCO2 smooth 500km 2hr and FTIR.CO2 dry air mol fraction (xCO2) values
(surf - toa, ORLEANS (lat.=48.0°), 2017-04-08 till 2018-05-05, 6903 meas.)
OCFP xCO2 smooth 500km 2hr and FTIR.CO2 dry air mol fraction (xCO2) values
(surf - toa, PARIS (lat.=48.8°), 2017-04-19 till 2018-05-16, 2515 meas.)
OCFP xCO2 smooth 500km 2hr and FTIR.CO2 dry air mol fraction (xCO2) values
(surf - toa, PARKFALLS (lat.=45.9°), 2017-03-03 till 2018-05-20, 15750 meas.)
OCFP xCO2 smooth 500km 2hr and FTIR.CO2 dry air mol fraction (xCO2) values
(surf - toa, PASADENA (lat.=34.1°), 2017-03-08 till 2018-05-03, 11739 meas.)
OCFP xCO2 smooth 500km 2hr and FTIR.CO2 dry air mol fraction (xCO2) values
(surf - toa, RIKUBETSU (lat.=43.5°), 2017-03-09 till 2018-05-15, 2376 meas.)
OCFP xCO2 smooth 500km 2hr and FTIR.CO2 dry air mol fraction (xCO2) values
(surf - toa, SAGA (lat.=33.2°), 2017-03-19 till 2018-05-21, 4729 meas.)
OCFP xCO2 smooth 500km 2hr and FTIR.CO2 dry air mol fraction (xCO2) values
(surf - toa, SODANKYLA (lat.=67.4°), 2017-03-05 till 2018-05-15, 9899 meas.)
TCCON all
TCCON
SSP
xCO2 [ppm]

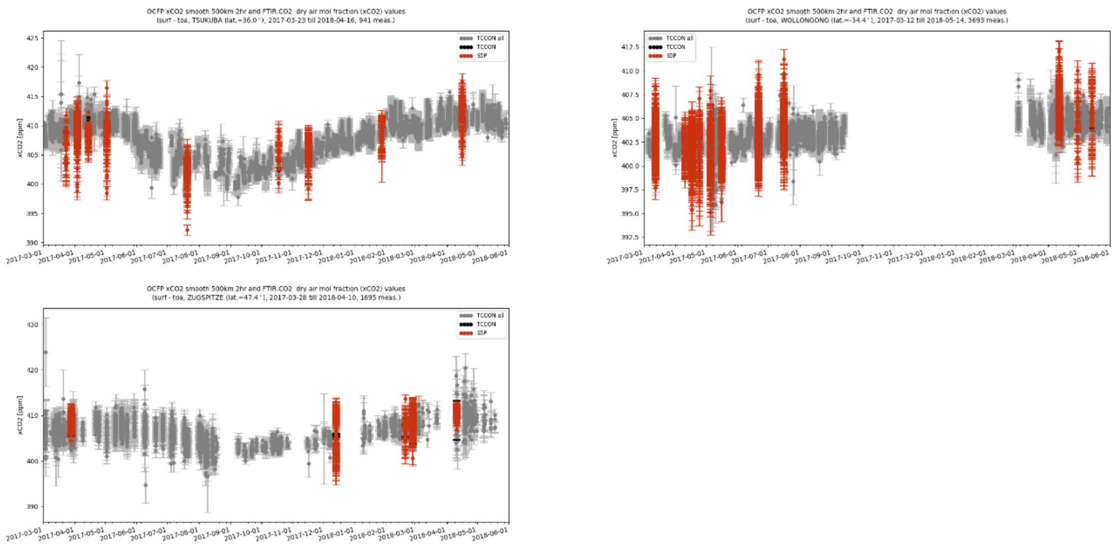

Figure 4-9: XCO_2 timeseries at all TCCON sites (red= CO2_TAN_OCFP data, black is collocated TCCON data and grey are the uncollocated TCCON data).

Figure 4-10 shows monthly median timeseries for TCCON and OCFP XCO_2 for all data that falls within certain latitude bands, namely all sites North of 40°N latitude (top), all sites between 40°N and the equator (mid) and all sites in the Southern hemisphere (bottom). It also features the values for a trend+seasonal fit through both datasets. The observed trend values are, given the short timeframe covered, not robust. That said all obtained long term trends have overlapping standard deviations. Both FTIR and OCFP XCO_2 seem to follow the same seasonal cycle

All in all, we can state that OCFP clearly captures the overall seasonality.

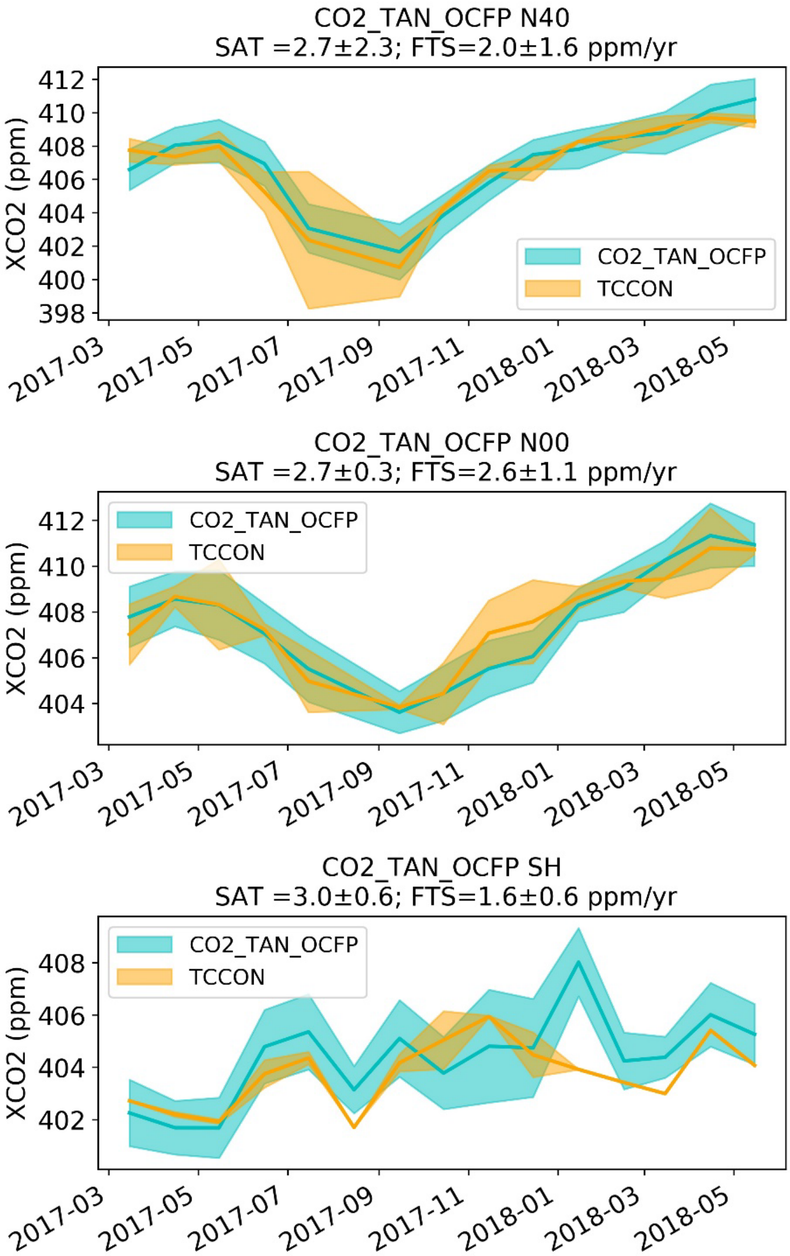

Figure 4-10: Monthly median collocated Sat and TCCON XCO_2 concentrations as a function of time. The shaded areas correspond with the scaled median absolute deviation.

4.2.2.2 Summary

Despite the limited amount of collocated data and the relatively small time period covered, we can already state that we see no obvious defects embedded within the CO2_TAN_OCFP product.

The OCFP reported uncertainty is underestimated by roughly 20% (Uncertainty ratio = 0.79) and the overall bias equals 0.39 ppm and the scatter equals 1.46 ppm. The spatial (RA) and spatio-temporal relative accuracy (SRA) have not met the stated goal requirement of (>0.5 ppm). For the RA however its 95% confidence bands do overlap with the stated 0.5 ppm goal. As already mentioned we did not calculate a Stability, due to the limited time period covered but nor did we see any apparent problems in this area.

Table 4-4 presents an overview of the estimated data quality of CO2_TAN_OCFP, as obtained by the VALT team, from comparisons with TCCON ground-based reference observations. Values in square brackets [ ] correspond with the upper and lower 95% confidence bound on the parameter. The uncertainty ratio features 2 numbers as outlined in the validation method.

Product Quality Summary Table for Product: CO2_TAN_OCFP Level: 2, Version: v01.0.0, Time period covered: 03.2017 – 05.2018 Assessment: Validation Team (VALT)			
Parameter [unit]	**Achieved performance**	**Requirement**	**Comments**
Single measurement precision (1-sigma) in [ppm]	1.46 [1.21,1.66]	< 8 (T) < 3 (B) < 1 (G)	Computed as the median over all station scaled median absolute differences to TCCON
Uncertainty ratio [-]: Ratio reported uncertainty to standard deviation of satellite-TCCON difference	0.73, 0.79*	-	No requirement but value close to unity expected for a high quality data product with reliable reported uncertainty.
Mean bias (global offset) [ppm]	0.39 [0.32,0.87]	-	No requirement but value close to zero expected for a high quality data product.
Accuracy: Relative systematic error [ppm]	Spatial: 0.70 [0.39,1.29] Spatio-temporal: 0.99 [0.74,1.37]	< 0.5	Spatial: Computed as standard deviation of the biases at the various TCCON sites. Spatio-temporal: As "Spatial" but also considering seasonal biases.
Stability: Drift [ppm/year]	-	< 0.5	Linear drift

4.2.3 Validation results for product CO2_GO2_SRFP

Below we show the validation results of the XCO_2 concentrations as derived by the CO2_GO2_SRFP algorithm using GOSAT-2 spectra. Data was available from February 2019 up to and including October 2019. The SRFP algorithm provides *a priori* and column averaging kernel information on a 12 layers profile. Given the very limited time period that is covered by this product, these validation results will be rather preliminary in nature, nor can we make useful statements about long term stability and even seasonality as it does not cover a full year of data. The smoothing process results in a small reduction in the bias (by 0.21 ppm and a small increase in the scatter (by 0.05 ppm). All results shown pertain to the smoothed dataset.

4.2.3.1 Detailed results

The Taylor diagram below in **Figure 4-11**shows a short overview of the capabilities of the CO2_GO2_SRFP product. Most TCCON sites cluster around the 0.6 correlation line, with Zugspitze, Reunion and Bremen, notable exceptions. However, Reunion and Zugspitze pose geographical challenges while there are only 7 data pairs for Bremen. Also the normalized standard deviation of most sites is smaller than 1 (between 0.5 and 0.75), indicating that the variability of the TCCON data is smaller. The normalized standard deviation of the bias sits (for most sites) around 0.8. Notable outliers are again Bremen and Zugspitze with much larger TCCON variability as with Paris and Rikubetsu (but less extreme). All this indicates that while SRFP data features a stronger variability (random error and/or seasonal variability) than the TCCON data, the biases still harbours less variability then either of them, an indication of SRFP capturing the natural variability.

There is no real discernible pattern in the mosaic plot (**Figure 4-12**), which shows the mean bi-weekly bias between the satellite and TCCON measurement pairs. However, the period covered by the above plot is very limited. One could point at an increase in the bias between 45 and 55° N latitude during the summer months and somewhat lower values from October onwards but with only one year of data this can hardly be substantiated.

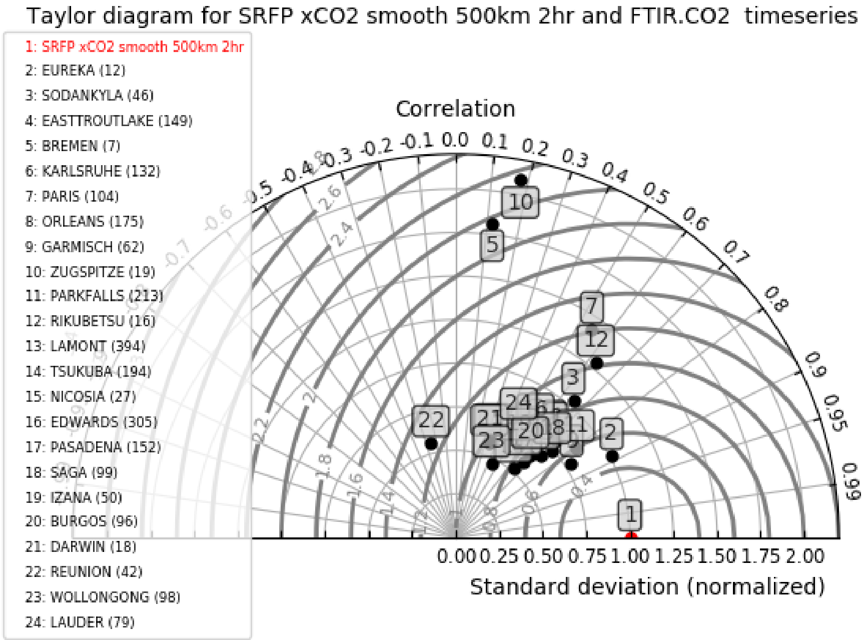

Figure 4-11: Tayor plot of daily averaged XCO_2 TCCON values relative to product CO2_GO2_SRFP. Straight lines correspond with the correlation, light grey lines yield the variability of the TCCON data relative to the satellite variability and the dark grey lines correspond with the variability of the Satellite -TCCON bias relative to the satellite variability.

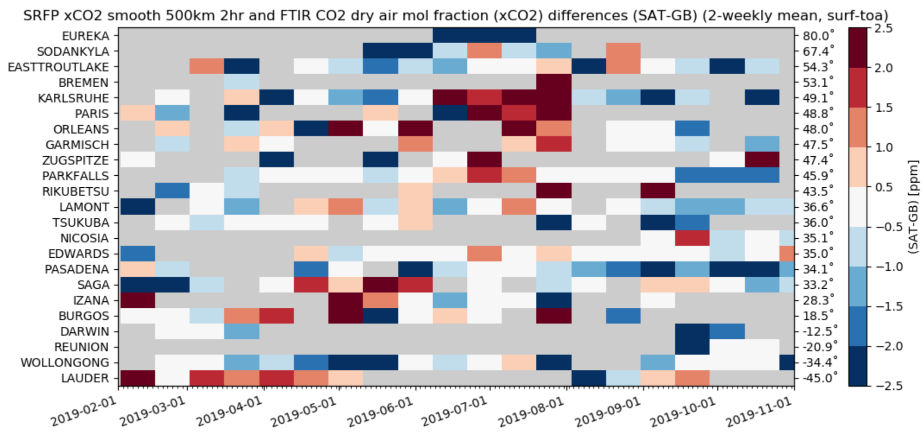

Figure 4-12: Mosaic plot of bi-weekly mean CO2_GO2_SRFP-TCCON XCO_2 biases as a function of time and TCCON station.

Table 4-5 lists all bias and scatter results derived from individual data pairs at all TCCON stations. The algorithm produces on average ~100 data pairs per station which corresponds with ~120 pairs per station per year. The observed median bias ranges between -3.99 ppm (Eureka) and 1.54 ppm(Paris), while the scatter ranges between 3.34 ppm (Bremen) and 0.93 (Eureka). Correlation values range between 0.89 (Eureka) and -0.25 (Reunion), with most correlation values sitting around 0.6. Of course the limited dataset hampers the correlation values at certain stations. The correlation using all data regardless of station equals 0.72. Given the limited timespan covered by the product, we did not calculate any long term trend. But as can be seen in **Figures 4-13 and 4-14** no clear-cut drift is observable.

Table 4-5: Number of collocated data pairs (N), Correlation (R), Bias, Scatter, long term trend difference (ltt) and uncertainty thereon (ltt_err), seasonal amplitude difference (A) and uncertainty thereon (A_err) as well as the latitude of the TCCON station. The last row lists the median values over all stations. Product: CO2_GO2_SRFP.

STATION	N	R	Bias	Scat	ltt	ltt_err	A	A_err	lat
EUREKA	12	0.89	-3.99	0.93	-	-	-	-	80
SODANKYLA	46	0.65	-1.65	2.57	-	-	-	-	67.4
EASTTROUTLAKE	149	0.71	-0.31	2.87	-	-	-	-	54.3
BREMEN	7	0.12	0.85	3.34	-	-	-	-	53.1
KARLSRUHE	132	0.61	0.71	2.44	-	-	-	-	49.1
PARIS	104	0.55	1.54	2.18	-	-	-	-	48.8
ORLEANS	175	0.72	0.25	2.18	-	-	-	-	48
GARMISCH	62	0.84	0.31	1.39	-	-	-	-	47.5
PARKFALLS	213	0.8	0.11	2.31	-	-	-	-	45.9
RIKUBETSU	16	0.63	1.09	1.77	-	-	-	-	43.5
LAMONT	394	0.72	-0.31	1.93	-	-	-	-	36.6
TSUKUBA	194	0.64	-0.38	1.95	-	-	-	-	36
NICOSIA	27	0.36	-0.01	1.83	-	-	-	-	35.1
EDWARDS	305	0.6	-0.12	2.04	-	-	-	-	35
PASADENA	152	0.66	-1.49	2.56	-	-	-	-	34.1
SAGA	99	0.74	0.11	2.1	-	-	-	-	33.2
BURGOS	96	0.67	0.68	1.45	-	-	-	-	18.5
DARWIN	18	0.33	-1.17	1.78	-	-	-	-	-12.5
REUNION	42	-0.25	-1.36	2.85	-	-	-	-	-20.9
WOLLONGONG	98	0.44	-0.88	2	-	-	-	-	-34.4
LAUDER	79	0.49	0.82	1.51	-	-	-	-	-45
MEDIAN	**98**	**0.64**	**-0.01**	**2.04**	**-**	**-**	**-**	**-**	**36.6**

The timeseries below in **Figure 4-13** show individual satellite and ground-based fts measurements. As can be seen, and was already apparent from the Taylor diagram, SRFP XCO_2 features a somewhat higher scatter than TCCON, but overall the seasonality is well captured.

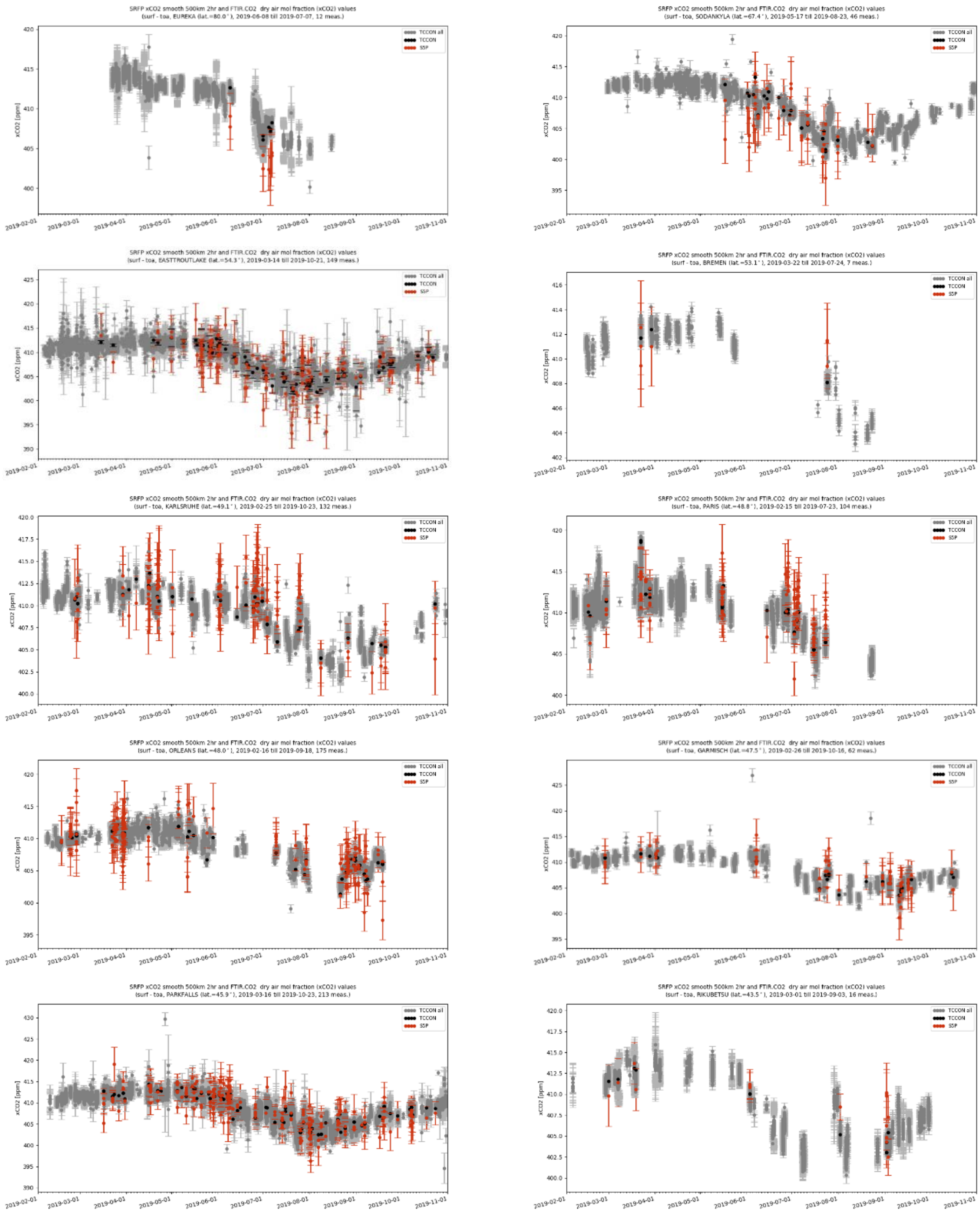

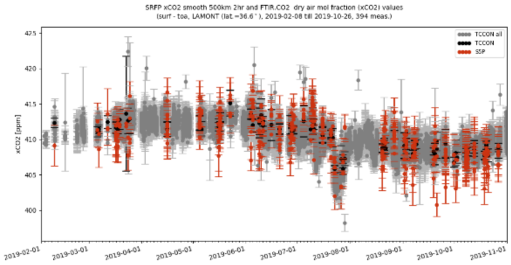
SRFP xCO2 smooth 500km 2hr and FTIR.CO2 dry air mol fraction (xCO2) values
(surf - toa, LAMONT (lat.=36.6°), 2019-02-08 till 2019-10-26, 394 meas.)
TCCON all
TCCON
SSP
xCO2 [ppm]

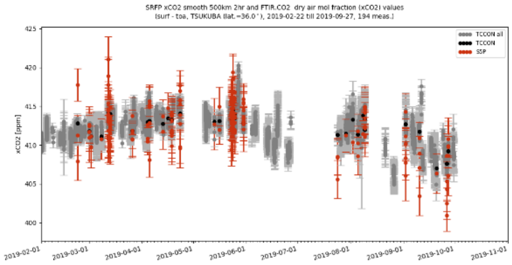
SRFP xCO2 smooth 500km 2hr and FTIR.CO2 dry air mol fraction (xCO2) values
(surf - toa, TSUKUBA (lat.=36.0°), 2019-02-22 till 2019-09-27, 194 meas.)
TCCON all
TCCON
SSP
xCO2 [ppm]

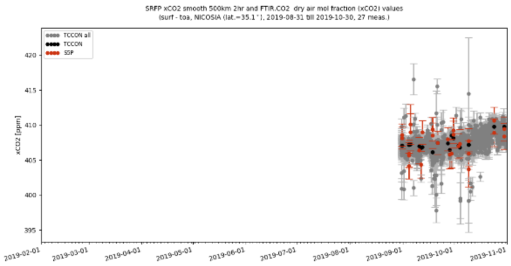
SRFP xCO2 smooth 500km 2hr and FTIR.CO2 dry air mol fraction (xCO2) values
(surf - toa, NICOSIA (lat.=35.1°), 2019-08-31 till 2019-10-30, 27 meas.)
TCCON all
TCCON
SSP
xCO2 [ppm]

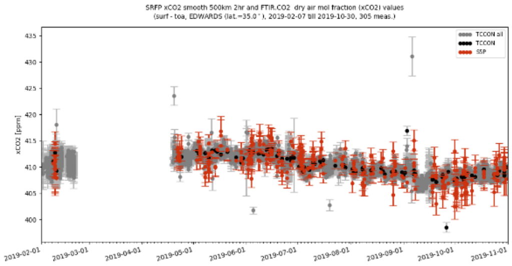
SRFP xCO2 smooth 500km 2hr and FTIR.CO2 dry air mol fraction (xCO2) values
(surf - toa, EDWARDS (lat.=35.0°), 2019-02-07 till 2019-10-30, 305 meas.)
TCCON all
TCCON
SSP
xCO2 [ppm]

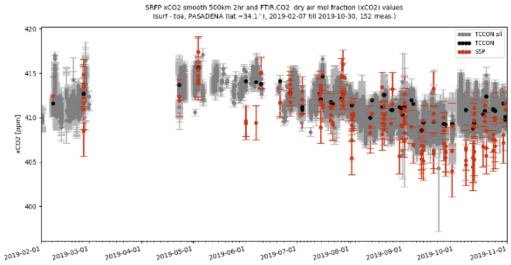
SRFP xCO2 smooth 500km 2hr and FTIR.CO2 dry air mol fraction (xCO2) values
(surf - toa, PASADENA (lat.=34.1°), 2019-02-07 till 2019-10-30, 152 meas.)
TCCON all
TCCON
SSP
xCO2 [ppm]

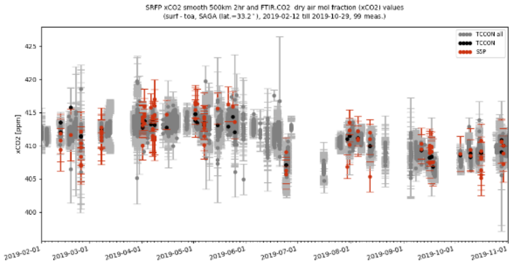
SRFP xCO2 smooth 500km 2hr and FTIR.CO2 dry air mol fraction (xCO2) values
(surf - toa, SAGA (lat.=33.2°), 2019-02-12 till 2019-10-29, 99 meas.)
TCCON all
TCCON
SSP
xCO2 [ppm]

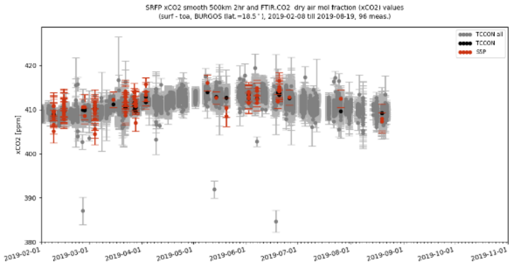
SRFP xCO2 smooth 500km 2hr and FTIR.CO2 dry air mol fraction (xCO2) values
(surf - toa, BURGOS (lat.=18.5°), 2019-02-08 till 2019-08-19, 96 meas.)
TCCON all
TCCON
SSP
xCO2 [ppm]

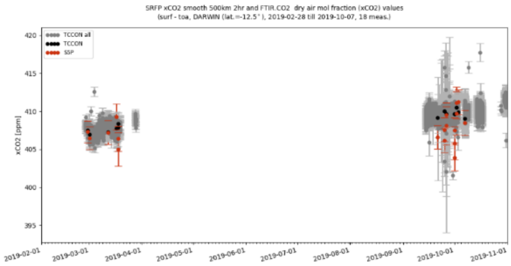
SRFP xCO2 smooth 500km 2hr and FTIR.CO2 dry air mol fraction (xCO2) values
(surf - toa, DARWIN (lat.=-12.5°), 2019-02-28 till 2019-10-07, 18 meas.)
TCCON all
TCCON
SSP
xCO2 [ppm]

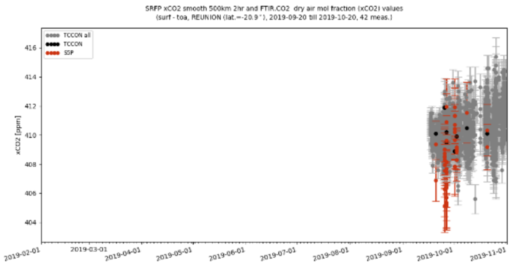
SRFP xCO2 smooth 500km 2hr and FTIR.CO2 dry air mol fraction (xCO2) values
(surf - toa, REUNION (lat.=-20.9°), 2019-09-20 till 2019-10-20, 42 meas.)
TCCON all
TCCON
SSP
xCO2 [ppm]

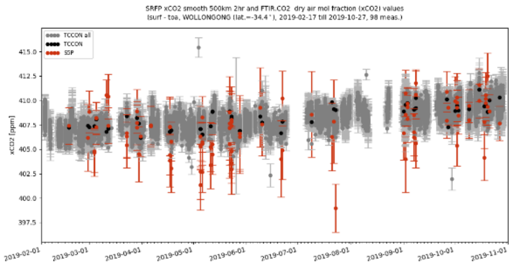
SRFP xCO2 smooth 500km 2hr and FTIR.CO2 dry air mol fraction (xCO2) values
(surf - toa, WOLLONGONG (lat.=-34.4°), 2019-02-17 till 2019-10-27, 98 meas.)
TCCON all
TCCON
SSP
xCO2 [ppm]

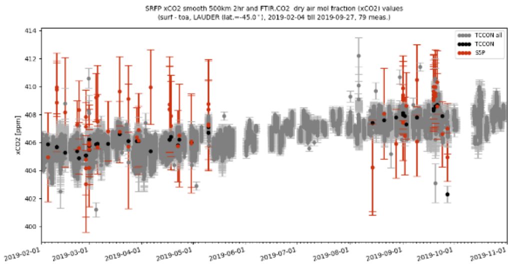

Figure 4-13: XCO_2 timeseries at all TCCON sites (red= CO2_GO2_SRFP data, black is collocated TCCON data and grey are the uncollocated TCCON data).

Figure 4-14 shows monthly median timeseries for TCCON and SRFP XCO_2 for all data that falls within certain latitude bands, namely all sites North of 40°N latitude (top), all sites between 40°N and the equator (mid) and all sites in the Southern hemisphere (bottom). It also features the values for a trend+seasonal fit through both datasets. For the Southern hemisphere and 0-40° North latitude band, the obtained long term trends are quasi identical with overlapping standard deviations. For the >40°N latitude band a clear difference does exist, but if we look at the actual data, both FTIR and SRFP XCO_2 seem to follow the same seasonal cycle apart from some deviation in October. Due to the short time series, the biases that present themselves at the end of the time series will heavily impact the obtained long term trend. It is for this very reason that we do not list the stability in the overview **Table 4-6**.

All in all, we can state that SRFP clearly captures the overall seasonality.

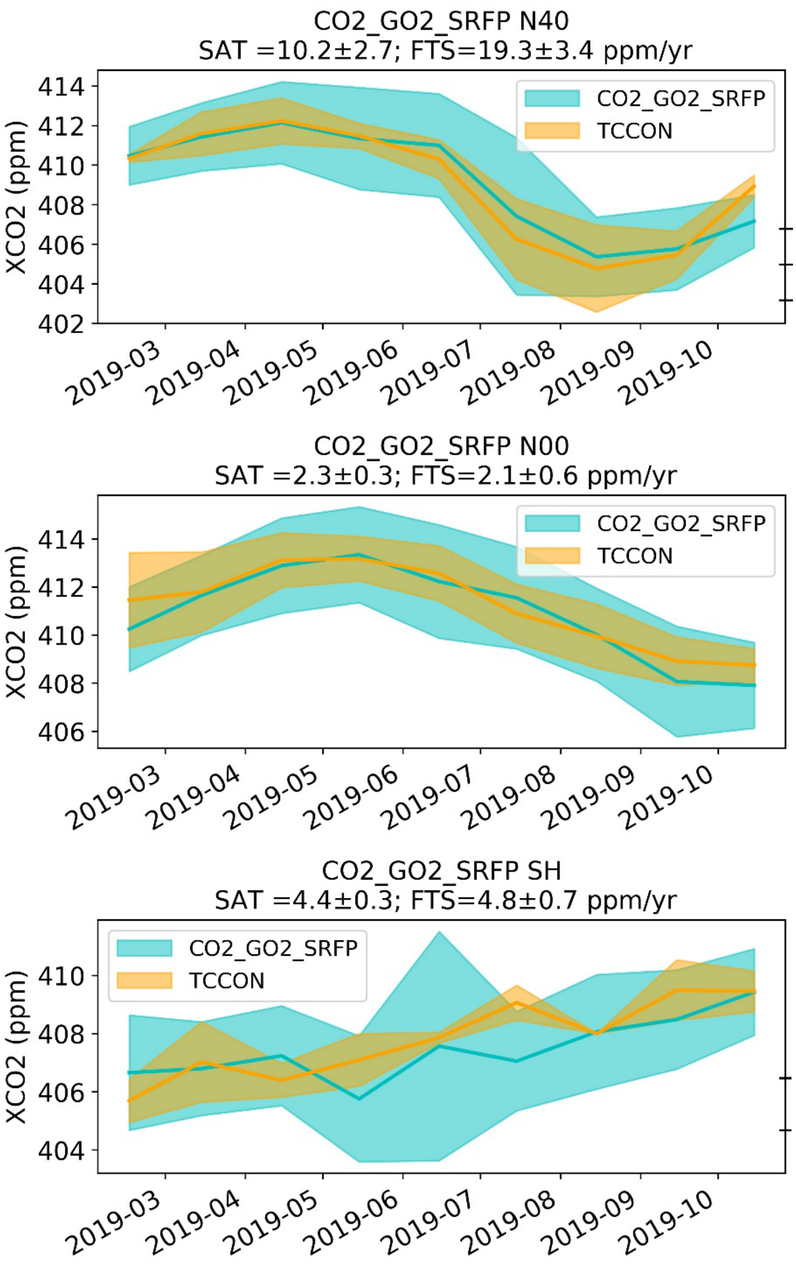

Figure 4-14: Monthly median collocated Sat and TCCON XCO_2 concentrations as a function of time. The shaded areas correspond with the scaled median absolute deviation.

4.2.3.2 Summary

Despite the limited amount of collocated data and the relatively small time period covered, we can already state that we see no obvious defects embedded within the CO2_GO2_SRFP product. The SRFP reported uncertainty corresponds closely with our analysis, or is even slightly overestimated (Uncertainty ratio = 1.06) and the overall bias approximates zero (-0.01 ppm). The spatial (RA) and spatio-temporal relative accuracy (SRA) have not met the stated goal requirement of (>0.5 ppm), nor do its confidence bands overlap with the target. Somewhat counterintuitive is the fact that the SRA is smaller than the RA, which is probably an indication that the data sample is, at this stage of development, too small. As already mentioned we did not calculate a Stability, due to the limited time period covered but nor did we see any apparent problems in this area.

Table 4-6 presents an overview of the estimated data quality of CO2_GO2_SRFP, as obtained by the VALT team, from comparisons with TCCON ground-based reference observations. Values in square brackets [ ] correspond with the upper and lower 95% confidence bound on the parameter. The uncertainty ratio features 2 numbers as outlined in the validation method.

Product Quality Summary Table for Product: CO2_GO2_SRFP Level: 2, Version: v01.0.0, Time period covered: 2.2019 – 11.2019 Assessment: Validation Team (VALT)			
Parameter [unit]	**Achieved performance**	**Requirement**	**Comments**
Single measurement precision (1-sigma) in [ppm]	2.04 [1.77,2.25]	< 8 (T) < 3 (B) < 1 (G)	Computed as the median over all station scaled median absolute differences to TCCON
Uncertainty ratio [-]: Ratio reported uncertainty to standard deviation of satellite-TCCON difference	1.03, 1.06*	-	No requirement but value close to unity expected for a high quality data product with reliable reported uncertainty.
Mean bias (global offset) [ppm]	-0.01 [-0.33,0.36]	-	No requirement but value close to zero expected for a high quality data product.
Accuracy: Relative systematic error [ppm]	Spatial: 1.07 [0.52,1.74] Spatio-temporal: 0.96 [0.59,1.28]	< 0.5	Spatial: Computed as standard deviation of the biases at the various TCCON sites. Spatio-temporal: As "Spatial" but also considering seasonal biases.
Stability: Drift [ppm/year]	-	< 0.5	Linear drift

4.2.4 Validation results for product CH4_S5P_WFMD

Below we show the validation results of the XCH_4 concentrations as derived by the CH4_S5P_WFMD algorithm using S5P spectra. Data was available from November 2017 up to and including May 2020. The WFMD algorithm provides *a priori* and column averaging kernel data on a 20 layers vertical profile. The difference between the smoothed and unsmoothed data is minimal (a 2.8 ppb shift in the median bias from -1.90 to 0.90 ppb and no noticeable difference in the scatter). All results shown pertain to the smoothed dataset. Note that instead of 'within 500 km and 2 hour' collocation criteria, we here have used 'within 100km and 1 hour'.

4.2.4.1 Detailed results

The Taylor plot for product CH4_S5P_WFMD is shown in **Figure 4-15**. Most FTIR sites are clustered around the 0.4 correlation line, with the standard deviation of the differences almost equal to the standard deviation of the satellite data itself. The variability on the TCCON data is consistently smaller than that of WFMD, with most sites sitting between 25 and 80%. No clear outliers are identified but some stations clearly have better statistics than others.

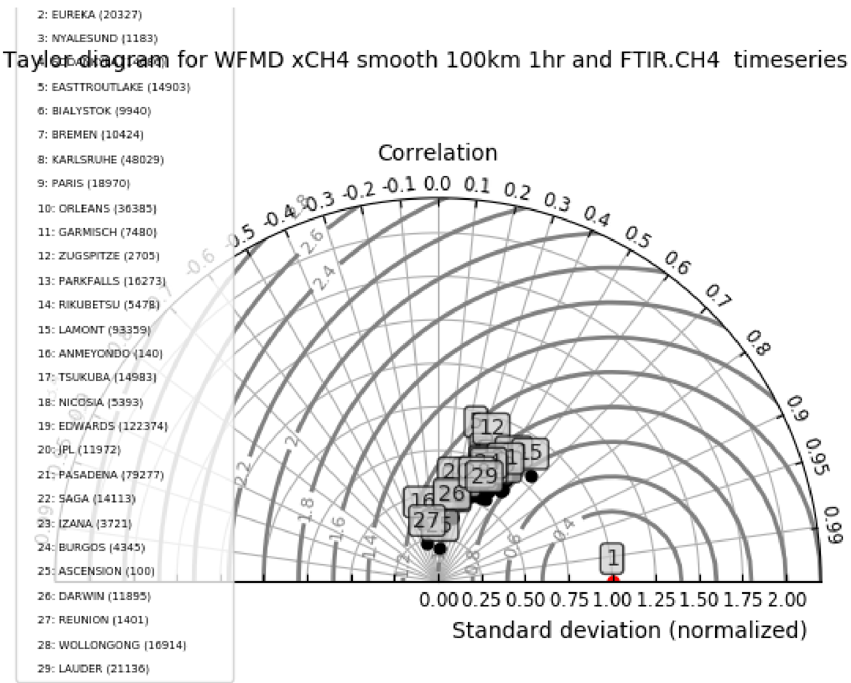

Figure 4-15: Tayor plot of daily averaged XCH_4 TCCON values relative to CH4_S5P_WFMD. Straight lines correspond with the correlation, light grey lines yield the variability of the TCCON data relative to the satellite variability and the dark grey lines correspond with the variability of the Satellite -TCCON bias relative to the satellite variability.

The mosaic overview of bi-weekly sat-TCCON biases (**Figure 4-16**) does not reveal any systematic trend over time, nor any as a function of latitude. There are some very pronounced biases (negative in Parkfalls and positive in Zugspitze and Izaña, the latter 2, being high altitude stations, have been withheld from our further analysis).

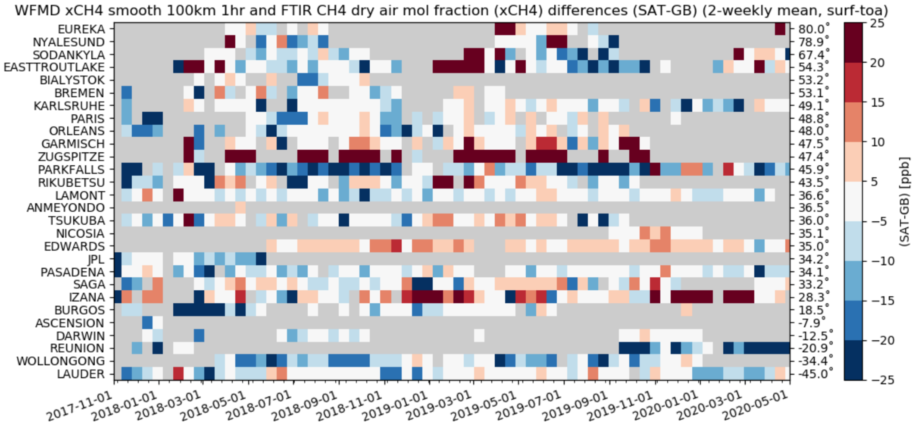

Figure 4-16: Mosaic plot of bi-weekly mean CH4_S5P_WFMD - TCCON XCH_4 biases as a function of time and TCCON station.

Table 4-7 lists all bias and scatter results derived from individual data pairs at all TCCON stations. The algorithm produces on average ~14400 data pairs per station which corresponds with ~5700 pairs per station per year. Also keep in mind that the collocation criteria are substantially stricter. The observed median bias ranges between -13.13 ppb (Parkfalls) and 9.29 ppb (Anmeyondo), while the scatter ranges between 7.62 ppb (Ascension) and 28.05 ppb (Reunion). Correlation values range between -0.27 (Reunion and Anmeyondo) and 0.66 (Lamont), with most correlation values sitting between 0.4 and 0.5. The correlation of all data, regardless of station, equals 0.78. The long term trend on the bias ranges between 13.32 ppb/year at Eureka and -4.8 ppb/year at Easttroutlake. Finally, the seasonal amplitude present in the sat-TCCON bias ranges between 63.87 ppb (Reunion) and 0.88 ppb (Lamont). The time series plots in **Figure 4-17** reveal that while the data at Reunion covers a 2 year timespan, it features a significant data gap which hampers an accurate determination of the seasonal amplitude.

Figure 4-17 shows all collocated WFMD and TCCON data time series. From these figures, it is clear that the variability of WFMD XCH_4 is substantially stronger. Also a fair amount of, particularly negative, outliers is present at many stations.

Table 4-7: Number of collocated data pairs (N), Correlation (R), Bias, Scatter, long term trend difference (ltt) and uncertainty thereon (ltt_err), seasonal amplitude difference (A) and uncertainty thereon (A_err) as well as the latitude of the TCCON station. The last row lists the median values over all stations. Product: CH4_S5P_WFMD.

STATION	N	R	Bias	Scat	ltt	ltt_err	A	A_err	lat
EUREKA	20327	0.48	7.68	18	13.32	5.97	28.59	8.13	80
NYALESUND	1183	0.45	-0.3	19.72	-	-	-	-	78.9
SODANKYLA	14686	0.58	-3.32	15.29	-4.63	2.99	13.97	2.22	67.4
EASTTROUTLAKE	14903	0.27	2.9	25.38	-4.8	2.92	11.27	1.68	54.3
BIALYSTOK	9940	0.37	1.14	13.21	-	-	-	-	53.2
BREMEN	10424	0.49	1.76	14.17	-	-	-	-	53.1
KARLSRUHE	48029	0.52	1.31	14.08	1.17	2.2	3.46	1.19	49.1
PARIS	18970	0.46	0.65	14.34	5.84	3.39	3.87	1.74	48.8
ORLEANS	36385	0.45	2.24	13.46	-	-	-	-	48
GARMISCH	7480	0.29	7.14	16.94	-	-	-	-	47.5
PARKFALLS	16273	0.45	-13.13	15.39	-0.21	1.74	12.08	1.62	45.9
RIKUBETSU	5478	0.58	3.55	16.02	-	-	-	-	43.5
LAMONT	93359	0.66	-2.32	13.77	-1.38	1.24	0.88	0.92	36.6
ANMEYONDO	140	-0.27	9.29	10.6	-	-	-	-	36.5
TSUKUBA	14983	0.48	4.34	15.86	-	-	-	-	36
NICOSIA	5393	0.37	6.74	13.59	-	-	-	-	35.1
EDWARDS	122374	0.58	6.18	14.94	-	-	-	-	35
JPL	11972	0.2	-7.31	19.29	-	-	-	-	34.2
PASADENA	79277	0.56	-2.42	16.62	1.75	1.04	3.55	0.85	34.1
SAGA	14113	0.49	5.65	18.61	1.73	2.35	5.06	1.86	33.2
BURGOS	4345	0.47	0.29	13.19	13.2	3.21	3.3	2.24	18.5
ASCENSION	100	0.06	-0.94	7.62	-	-	-	-	-7.9
DARWIN	11895	0.21	-0.88	12.32	5.12	2.27	2.37	2.03	-12.5
REUNION	1401	-0.27	-10.05	28.05	-2	10.02	63.87	12.21	-20.9
WOLLONGONG	16914	0.41	-6.88	18.58	-	-	-	-	-34.4
LAUDER	21136	0.49	-3.1	14.72	2.21	1.1	3.29	0.92	-45
MEDIAN	**14400**	**0.46**	**0.90**	**15.12**	**1.73**	**2.35**	**3.87**	**1.74**	**36.6**

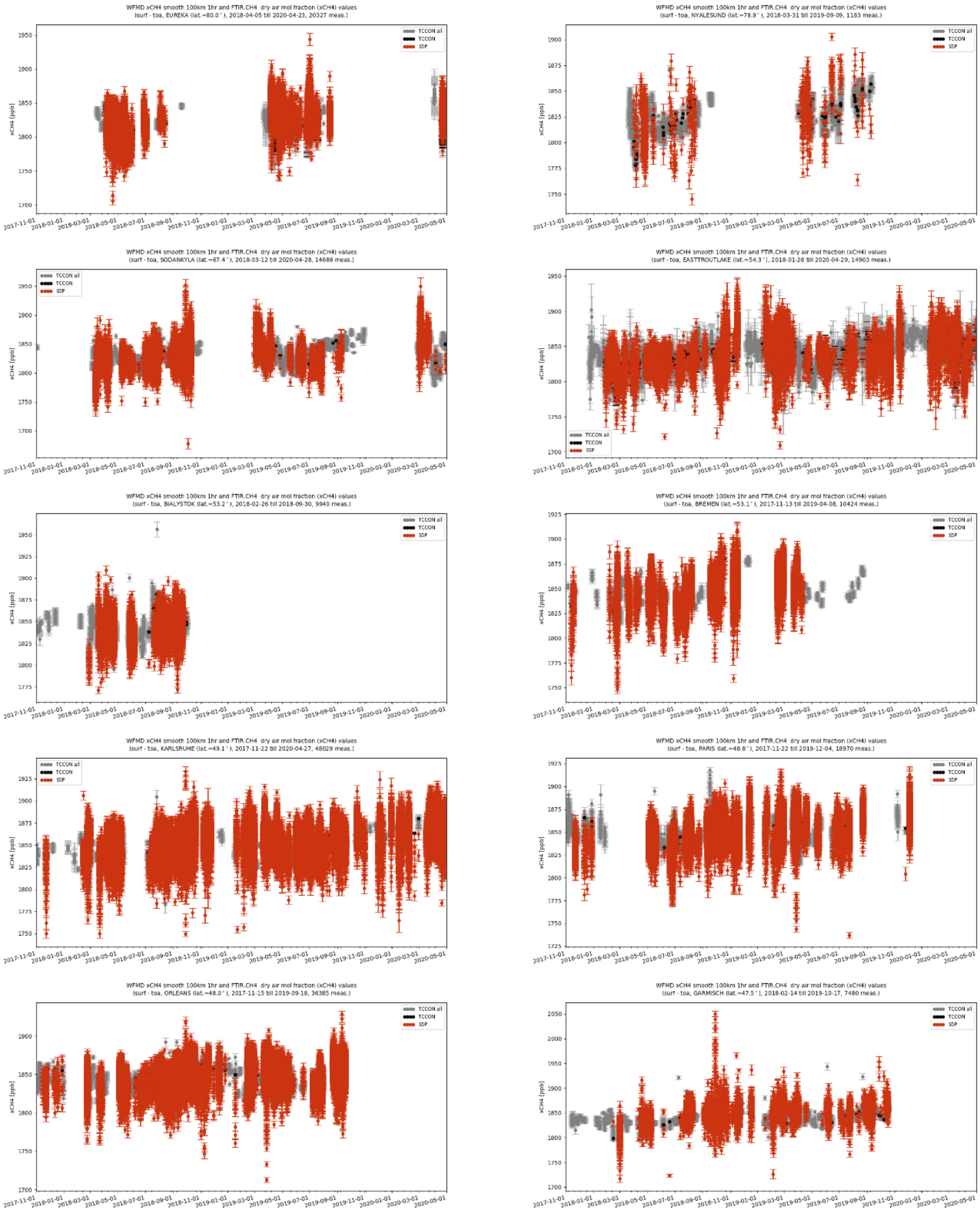

WFMD xCH4 smooth 100km 1hr and FTIR.CH4 dry air mol fraction (xCH4) values
(surf - toa, EUREKA (lat.=80.0 °), 2018-04-05 till 2020-04-23, 20327 meas.)
WFMD xCH4 smooth 100km 1hr and FTIR.CH4 dry air mol fraction (xCH4) values
(surf - toa, NYALESUND (lat.=78.9 °), 2018-03-31 till 2019-09-09, 1183 meas.)
WFMD xCH4 smooth 100km 1hr and FTIR.CH4 dry air mol fraction (xCH4) values
(surf - toa, SODANKYLA (lat.=67.4 °), 2018-03-12 till 2020-04-28, 14686 meas.)
WFMD xCH4 smooth 100km 1hr and FTIR.CH4 dry air mol fraction (xCH4) values
(surf - toa, EASTTROUTLAKE (lat.=54.3 °), 2018-01-28 till 2020-04-29, 14903 meas.)
WFMD xCH4 smooth 100km 1hr and FTIR.CH4 dry air mol fraction (xCH4) values
(surf - toa, BIALYSTOK (lat.=53.2 °), 2018-02-26 till 2018-09-30, 9940 meas.)
WFMD xCH4 smooth 100km 1hr and FTIR.CH4 dry air mol fraction (xCH4) values
(surf - toa, BREMEN (lat.=53.1 °), 2017-11-13 till 2019-04-08, 10424 meas.)
WFMD xCH4 smooth 100km 1hr and FTIR.CH4 dry air mol fraction (xCH4) values
(surf - toa, KARLSRUHE (lat.=49.1 °), 2017-11-22 till 2020-04-27, 48029 meas.)
WFMD xCH4 smooth 100km 1hr and FTIR.CH4 dry air mol fraction (xCH4) values
(surf - toa, PARIS (lat.=48.8 °), 2017-11-22 till 2019-12-04, 18970 meas.)
WFMD xCH4 smooth 100km 1hr and FTIR.CH4 dry air mol fraction (xCH4) values
(surf - toa, ORLEANS (lat.=48.0 °), 2017-11-15 till 2019-09-18, 36385 meas.)
WFMD xCH4 smooth 100km 1hr and FTIR.CH4 dry air mol fraction (xCH4) values
(surf - toa, GARMISCH (lat.=47.5 °), 2018-02-14 till 2019-10-17, 7480 meas.)
TCCON all
TCCON
S5P

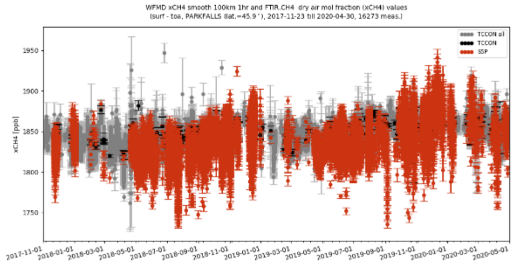

WFMD xCH4 smooth 100km 1hr and FTIR.CH4 dry air mol fraction (xCH4) values
(surf - toa, PARKFALLS (lat.=45.9°), 2017-11-23 till 2020-04-30, 16273 meas.)
TCCON all
TCCON
SSP
xCH4 [ppb]

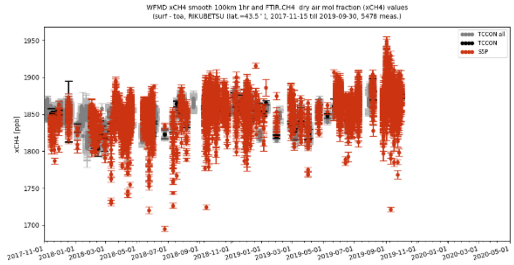

WFMD xCH4 smooth 100km 1hr and FTIR.CH4 dry air mol fraction (xCH4) values
(surf - toa, RIKUBETSU (lat.=43.5°), 2017-11-15 till 2019-09-30, 5478 meas.)
TCCON all
TCCON
SSP
xCH4 [ppb]

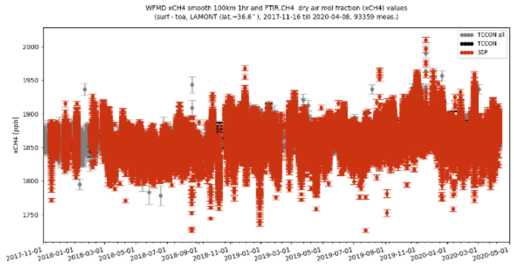

WFMD xCH4 smooth 100km 1hr and FTIR.CH4 dry air mol fraction (xCH4) values
(surf - toa, LAMONT (lat.=36.6°), 2017-11-16 till 2020-04-08, 93359 meas.)
TCCON all
TCCON
SSP
xCH4 [ppb]

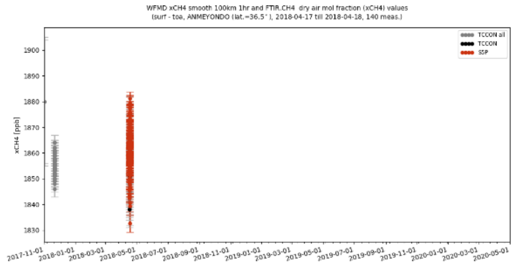

WFMD xCH4 smooth 100km 1hr and FTIR.CH4 dry air mol fraction (xCH4) values
(surf - toa, ANMEYONDO (lat.=36.5°), 2018-04-17 till 2018-04-18, 140 meas.)
TCCON all
TCCON
SSP
xCH4 [ppb]

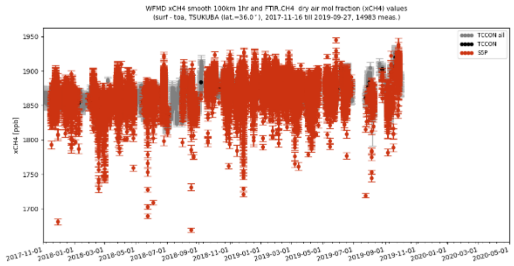

WFMD xCH4 smooth 100km 1hr and FTIR.CH4 dry air mol fraction (xCH4) values
(surf - toa, TSUKUBA (lat.=36.0°), 2017-11-16 till 2019-09-27, 14983 meas.)
TCCON all
TCCON
SSP
xCH4 [ppb]

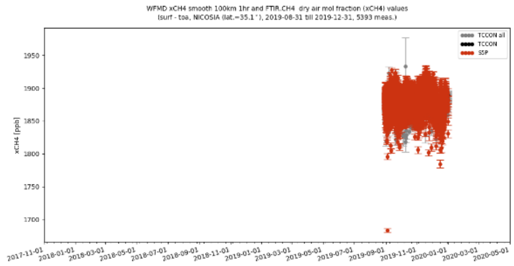

WFMD xCH4 smooth 100km 1hr and FTIR.CH4 dry air mol fraction (xCH4) values
(surf - toa, NICOSIA (lat.=35.1°), 2019-08-31 till 2019-12-31, 5393 meas.)
TCCON all
TCCON
SSP
xCH4 [ppb]

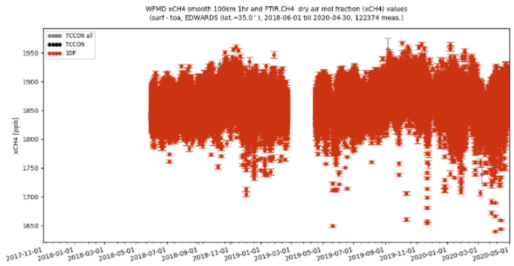

WFMD xCH4 smooth 100km 1hr and FTIR.CH4 dry air mol fraction (xCH4) values
(surf - toa, EDWARDS (lat.=35.0°), 2018-06-01 till 2020-04-30, 122374 meas.)
TCCON all
TCCON
SSP
xCH4 [ppb]

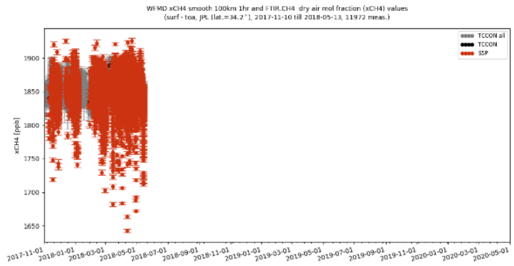

WFMD xCH4 smooth 100km 1hr and FTIR.CH4 dry air mol fraction (xCH4) values
(surf - toa, JPL (lat.=34.2°), 2017-11-10 till 2018-05-13, 11972 meas.)
TCCON all
TCCON
SSP
xCH4 [ppb]

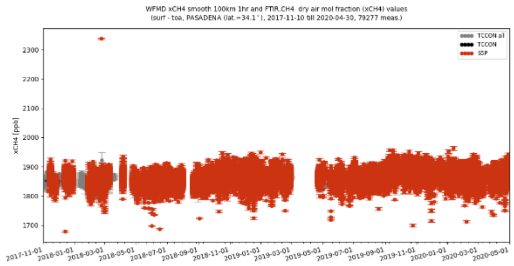

WFMD xCH4 smooth 100km 1hr and FTIR.CH4 dry air mol fraction (xCH4) values
(surf - toa, PASADENA (lat.=34.1°), 2017-11-10 till 2020-04-30, 79277 meas.)
TCCON all
TCCON
SSP
xCH4 [ppb]

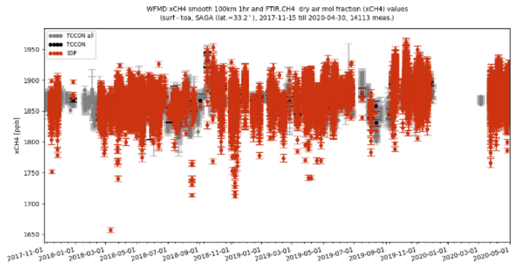

WFMD xCH4 smooth 100km 1hr and FTIR.CH4 dry air mol fraction (xCH4) values
(surf - toa, SAGA (lat.=33.2°), 2017-11-15 till 2020-04-30, 14113 meas.)
TCCON all
TCCON
SSP
xCH4 [ppb]

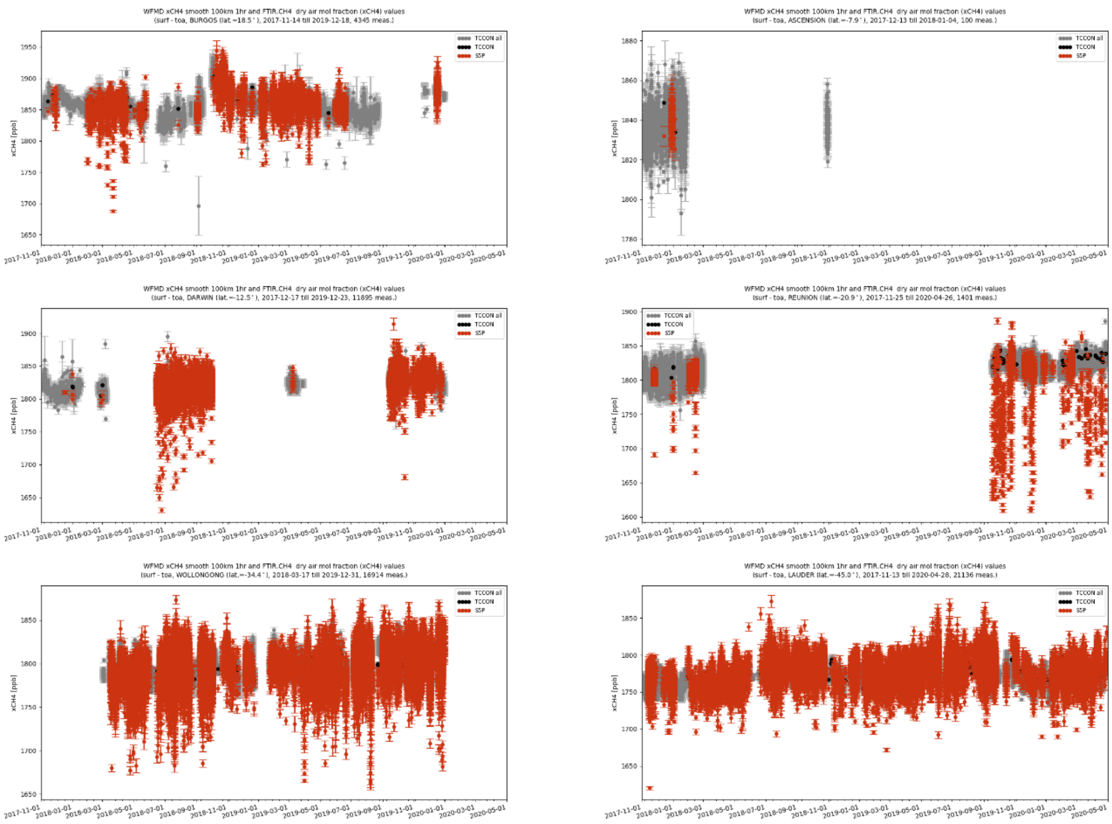

Figure 4-17: Timeseries of XCH_4 TCCON (collocated=black, all=grey) and CH4_S5P_WFMD (red) data at selected TCCON sites.

Figure 4-18 shows monthly median timeseries for TCCON and WFMD XCH_4 for all data that fall within certain latitude bands, namely all sites North of 40°N latitude (top), all sites between 40°N and the equator (mid) and all sites in the Southern hemisphere (bottom). As with SRFP XCO_2, the strongest difference in long-term trends is at the North of 40°N latitude band. But, again as with SRFP XCO_2, this is mainly due to biases that feature at the tail ends of the time series (this time the beginning). Around April 2018, this bias disappears and from thereon further the TCCON and WFMD time series evolve in sync as it does at the other latitude bands. The figures clearly show that WFMD is capable of capturing the larger scale temporal evolution of XCH_4.

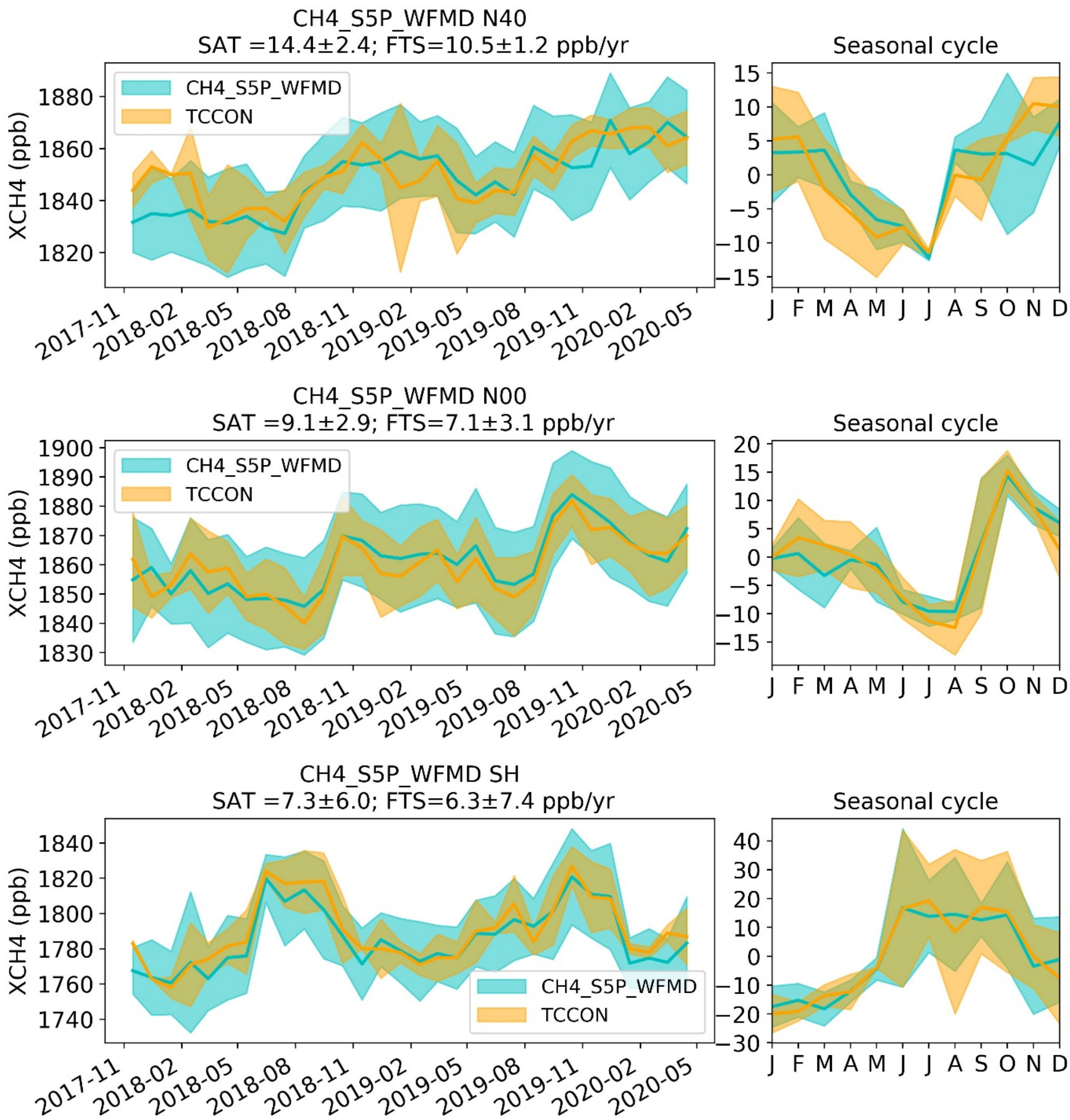

Figure 4-18: Monthly median collocated Sat and TCCON XCH_4 concentrations as a function of time and the detrended monthly medians as a function of season. The shaded areas correspond with the scaled median absolute deviation.

4.2.4.2 Summary

The CH4_S5P_WFMD data contains, unfortunately, a substantial amount of outliers (most of them negative) which might affect the numbers to some degree even though using medians limits their impact on the FoMs. That said, the seasonal cycles and long term trends seem well captured. The obtained Stability equals 1.7 ppb/year but the confidence interval is quite wide and encompasses 0 [-1.7,4.9]. The single measurement precision equals 15.1 ppb, thus reaching the breakthrough < 17 ppb target value. The reported uncertainty however is only a quarter of what we find in our analysis. The overall bias, as with the drift has confidence intervals that overlap with 0 [-1.1, 3.4], the median standing at 0.9 ppb.

The Relative and Seasonal relative accuracies equal 5.0 and 5.3 ppb respectively, thus reaching the <10 ppb target.

Table 4-8 presents an overview of the estimated data quality of CH4_S5P_WFMD, as obtained by the VALT team, from comparisons with TCCON ground-based reference observations. Values in square brackets [ ] correspond with the upper and lower 95% confidence bound on the parameter. The uncertainty ratio features 2 numbers as outlined in the validation method.

Product Quality Summary Table for Product: CH4_S5P_WFMD Level: 2, Version: v1.2, Time period covered: 11.2017 – 12.2018 Assessment: Validation Team (VALT)			
Parameter [unit]	**Achieved performance**	**Requirement**	**Comments**
Single measurement precision (1-sigma) in [ppb]	15.1 [13.6,16.3]	< 34 (T) < 17 (B) < 9 (G)	Computed as the median over all station scaled median absolute differences to TCCON
Uncertainty ratio [-]: Ratio reported uncertainty to standard deviation of satellite-TCCON difference	0.25, 0.26*	-	No requirement but value close to unity expected for a high quality data product with reliable reported uncertainty.
Mean bias (global offset) [ppb]	0.9 [-1.1, 3.4]	-	No requirement but value close to zero expected for a high quality data product.
Accuracy: Relative systematic error [ppb]	Spatial: 5.0 [1.8,7.3] Spatio-temporal: 5.3 [3.9,6.7]	< 10	Spatial: Computed as standard deviation of the biases at the various TCCON sites. Spatio-temporal: As "Spatial" but also considering seasonal biases.
Stability: Drift [ppb/year]	1.7 [-1.7,4.9]	< 3	Linear drift

4.2.5 Validation results for product CH4_GO2_SRFP

Below we show the validation results of the XCH_4 concentrations as derived by the CH4_GO2_SRFP algorithm using GOSAT-2 spectra, FP standing for the Full Physics version of the algorithm developed at SRON. Data was available from February 2019 up to and including October 2019. The SRFP algorithm provides *a priori* and column averaging kernel information on a 12 layer profile. Given the very limited time period that is covered by this product, these validation results will be rather preliminary in nature, nor can we make useful statements about long term stability and even seasonality as it does not cover a full year of data.

Here the smoothing had a more profound impact. We observe an almost 10 ppb upward shift in the bias and a slight 0.6 ppb improvement in the scatter. The shift in the bias is almost entirely due to the difference between the SRFP and TCCON XCH_4 *a priori* profiles, particularly in the Upper Troposphere-Lower Stratosphere. As always, the data discussed in this analysis has undergone the smoothing steps as discussed in the methodology.

4.2.5.1 Detailed results

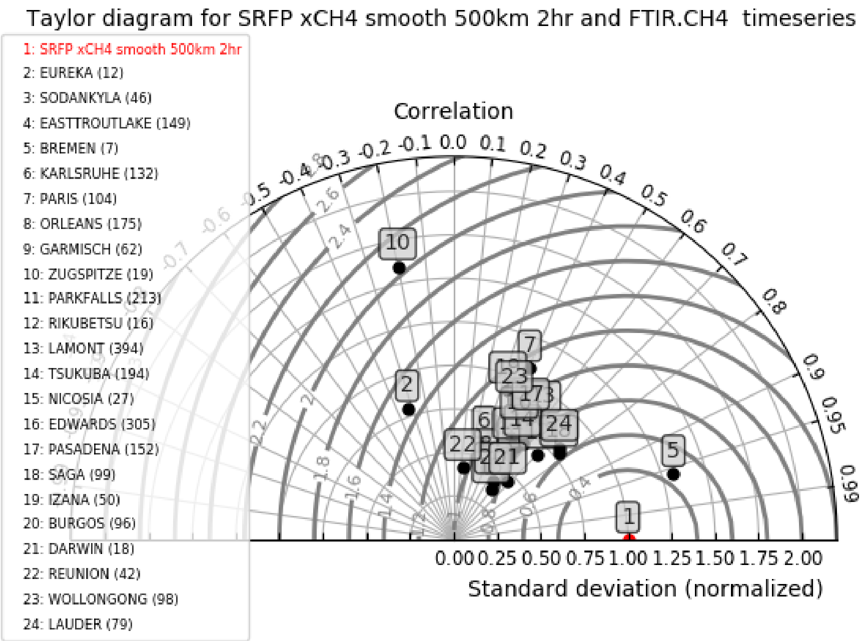

Figure 4-19: Tayor plot of XCH_4 TCCON values relative to CH4_GO2_SRFP. Straight lines correspond with the correlation, light grey lines yield the variability of the TCCON data relative to the satellite variability and the dark grey lines correspond with the variability of the Satellite -TCCON bias relative to the satellite variability.

The Taylor diagram above in **Figure 4-19** yields a concise overview of the capabilities of the CH4_GO2_SRFP algorithm. Most TCCON sites cluster around the 0.5 correlation line, with some noticeable outliers. Bremen reaches a 0.95 correlation but only features 7 collocation pairs. Likewise Eureka also features a limited dataset but this time it results in a correlation of -0.3. The correlation for all data (regardless of station) equals 0.80. As with WFMD, the TCCON scatter is smaller than that of SRFP while the variability of the bias roughly ranges between 0.8 and 1, relative to the SRFP variability. Particularly the correlation values should improve as the timeseries gets expanded and with it the range of natural variability.

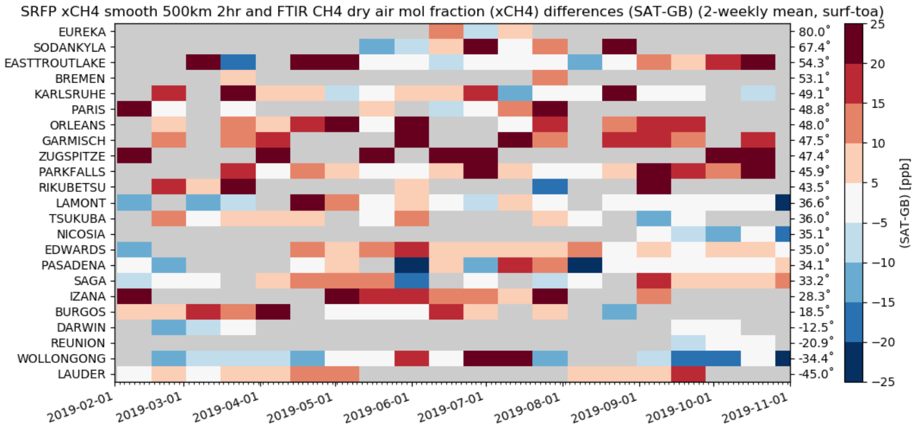

Figure 4-20. Mosaic plot of bi-weekly mean CH4_GO2_SRFP - TCCON XCH_4 biases as a function of time and TCCON station.

Again, it is hard to discern a pattern in the above mosaic plot (**Figure 4-20**), which shows the mean bi-weekly bias between the satellite and TCCON measurement pairs. Apart from the high altitude sites, no station clearly stands out. High bias values do seem to be more prominent in the 40 to 50°N latitude band.

Table 4-9 lists all bias and scatter results derived from individual data pairs at all TCCON stations. As with its XCO_2 counterpart, the algorithm produces on average ~100 data pairs per station, which corresponds with ~120 pairs per station per year. Several stations however have far less collocated measurements hampering an accurate assessment of the data quality at these sites. The observed median bias ranges between -4.79 ppb (Darwin) and 18.02 ppb (Rikubetsu), while the scatter ranges between 3.47 ppb (Bremen) and 18.46 ppb (Pasadena). Due to the limited dataset we did not determine long term bias drift numbers. While expanding the timeseries in the future will certainly mitigate some of the low data issues, for some stations the number of collocated measurements will most likely remain low. This can somewhat be countered by relaxing the collocation criteria, however the current criteria are already fairly relaxed as they are.

The timeseries below in **Figure 4-21** show individual satellite and ground-based TCCON measurements. While the scatter is somewhat higher for SRFP XCH_4, it is relatively free of outliers. It is also clear that the algorithm manages to capture the natural variability of XCH_4. A good example of this is the Tsukuba data, where blocks of reduced XCH_4 concentrations in August and September have been well captured by the satellite.

Table 4-9: Number of collocated data pairs (N), Correlation (R), Bias, Scatter, long term trend difference (ltt) and uncertainty thereon (ltt_err), seasonal amplitude difference (A) and uncertainty thereon (A_err) as well as the latitude of the TCCON station. The last row lists the median values over all stations. Product: CH4_GO2_SRFP.

STATION	N	R	Bias	Scat	ltt	ltt_err	A	A_err	lat
EUREKA	12	-0.33	-4.47	17.1	-	-	-	-	80
SODANKYLA	46	0.55	8.53	16.33	-	-	-	-	67.4
EASTTROUTLAKE	149	0.55	1.95	17.93	-	-	-	-	54.3
BREMEN	7	0.96	6.27	3.47	-	-	-	-	53.1
KARLSRUHE	132	0.31	9.43	15.51	-	-	-	-	49.1
PARIS	104	0.41	7.71	15.55	-	-	-	-	48.8
ORLEANS	175	0.41	11.79	14.2	-	-	-	-	48
GARMISCH	62	0.47	16.5	13.27	-	-	-	-	47.5
PARKFALLS	213	0.52	9.44	15.94	-	-	-	-	45.9
RIKUBETSU	16	0.7	18.02	13.24	-	-	-	-	43.5
LAMONT	394	0.59	-0.33	15.89	-	-	-	-	36.6
TSUKUBA	194	0.58	2.25	15.46	-	-	-	-	36
NICOSIA	27	0.6	-6.9	9.38	-	-	-	-	35.1
EDWARDS	305	0.5	6.3	17.92	-	-	-	-	35
PASADENA	152	0.53	1.13	18.46	-	-	-	-	34.1
SAGA	99	0.77	7.75	12.08	-	-	-	-	33.2
BURGOS	96	0.55	10.58	14.55	-	-	-	-	18.5
DARWIN	18	0.68	-4.79	8.63	-	-	-	-	-12.5
REUNION	42	0.12	-2.67	11.57	-	-	-	-	-20.9
WOLLONGONG	98	0.4	-2.98	14.92	-	-	-	-	-34.4
LAUDER	79	0.75	6.33	10.72	-	-	-	-	-45
MEDIAN	**98**	**0.55**	**6.3**	**14.92**	**-**	**-**	**-**	**-**	**36.6**

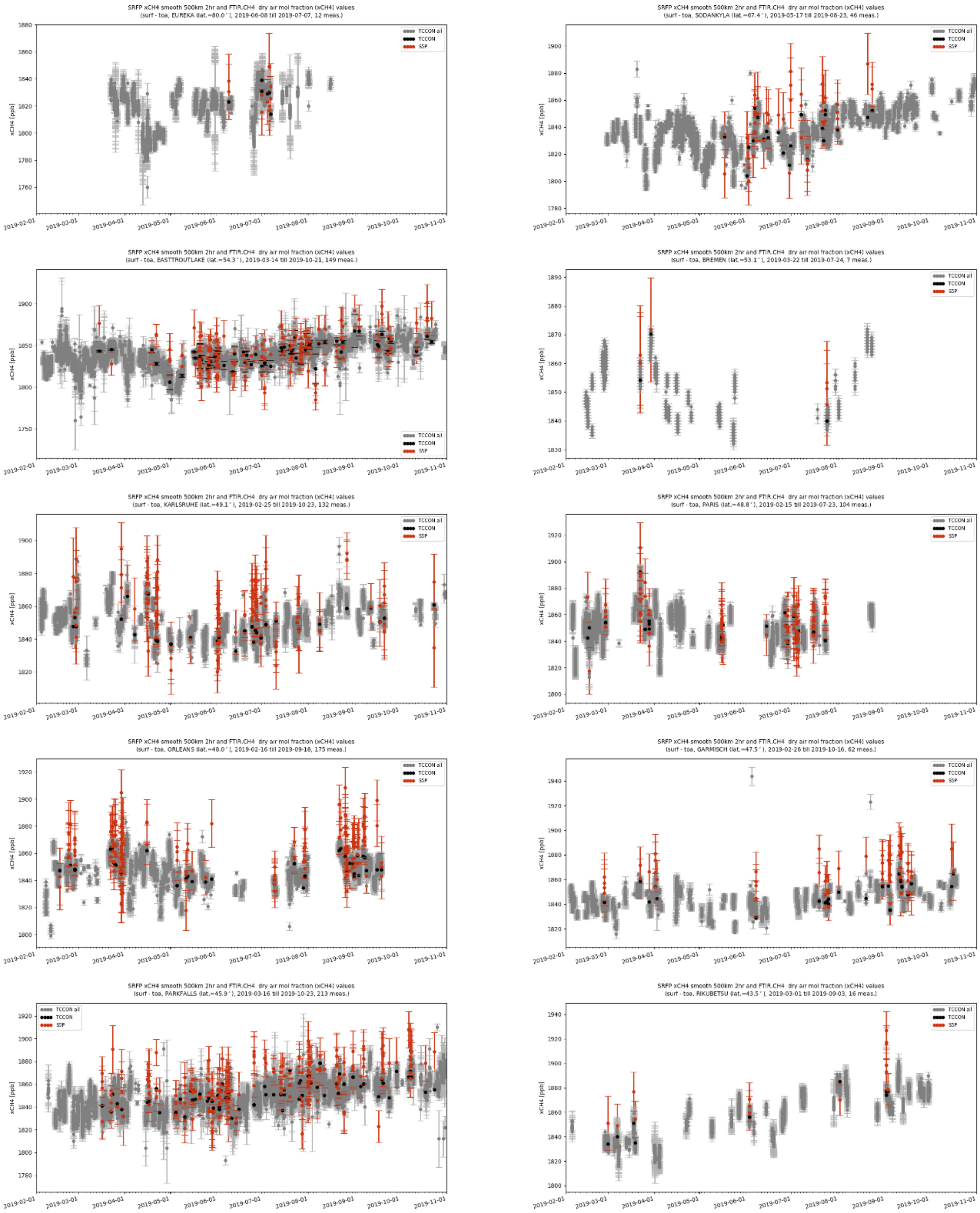
SRFP xCH4 smooth 500km 2hr and FTIR.CH4 dry air mol fraction (xCH4) values
(surf - toa, EUREKA (lat.=80.0°), 2019-06-08 till 2019-07-07, 12 meas.)
SRFP xCH4 smooth 500km 2hr and FTIR.CH4 dry air mol fraction (xCH4) values
(surf - toa, SODANKYLA (lat.=67.4°), 2019-05-17 till 2019-08-23, 46 meas.)
SRFP xCH4 smooth 500km 2hr and FTIR.CH4 dry air mol fraction (xCH4) values
(surf - toa, EASTTROUTLAKE (lat.=54.3°), 2019-03-14 till 2019-10-21, 149 meas.)
SRFP xCH4 smooth 500km 2hr and FTIR.CH4 dry air mol fraction (xCH4) values
(surf - toa, BREMEN (lat.=53.1°), 2019-03-22 till 2019-07-24, 7 meas.)
SRFP xCH4 smooth 500km 2hr and FTIR.CH4 dry air mol fraction (xCH4) values
(surf - toa, KARLSRUHE (lat.=49.1°), 2019-02-25 till 2019-10-23, 132 meas.)
SRFP xCH4 smooth 500km 2hr and FTIR.CH4 dry air mol fraction (xCH4) values
(surf - toa, PARIS (lat.=48.8°), 2019-02-15 till 2019-07-23, 104 meas.)
SRFP xCH4 smooth 500km 2hr and FTIR.CH4 dry air mol fraction (xCH4) values
(surf - toa, ORLEANS (lat.=48.0°), 2019-02-16 till 2019-09-18, 175 meas.)
SRFP xCH4 smooth 500km 2hr and FTIR.CH4 dry air mol fraction (xCH4) values
(surf - toa, GARMISCH (lat.=47.5°), 2019-02-26 till 2019-10-16, 62 meas.)
SRFP xCH4 smooth 500km 2hr and FTIR.CH4 dry air mol fraction (xCH4) values
(surf - toa, PARKFALLS (lat.=45.9°), 2019-03-16 till 2019-10-23, 213 meas.)
SRFP xCH4 smooth 500km 2hr and FTIR.CH4 dry air mol fraction (xCH4) values
(surf - toa, RIKUBETSU (lat.=43.5°), 2019-03-01 till 2019-09-03, 16 meas.)
TCCON all
TCCON
S5P
xCH4 [ppb]

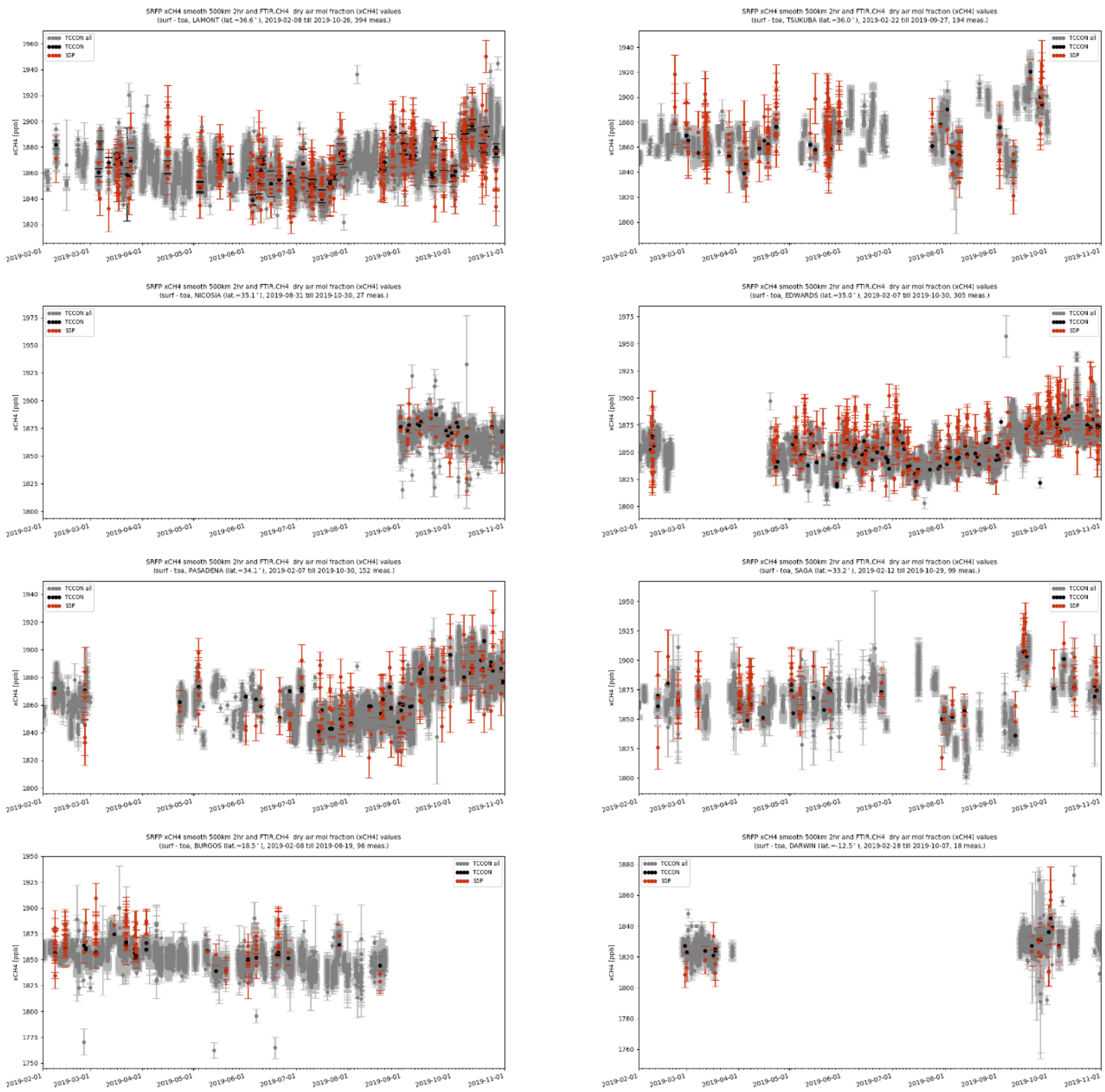

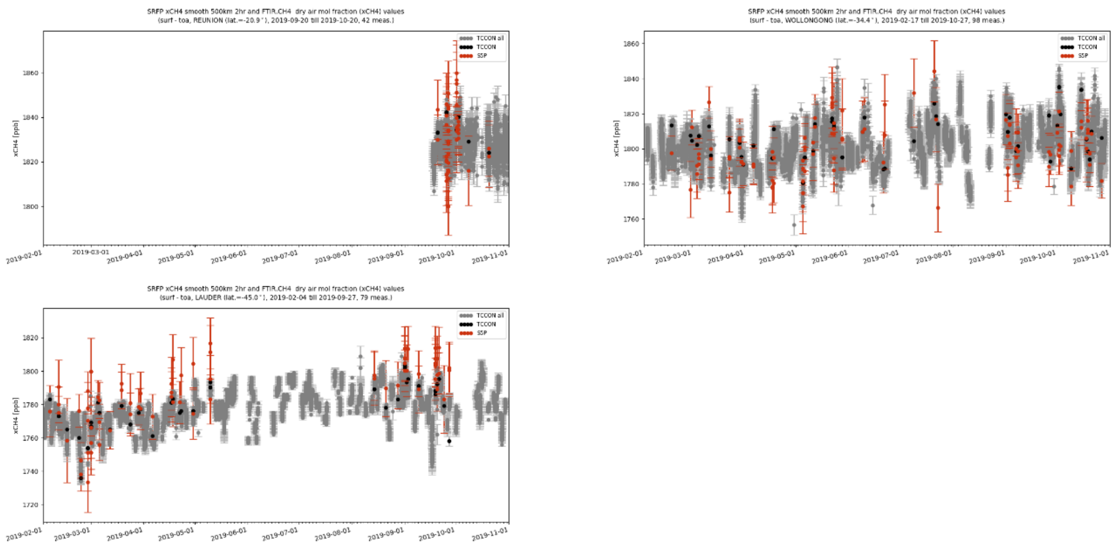

Figure 4-21: XCH_4 timeseries at all TCCON sites (red= CH4_GO2_SRFP data, black is collocated TCCON data and grey are the uncollocated TCCON data).

Figure 4-22 (left) shows monthly median timeseries for TCCON and SRFP XCH_4 for all data that fall within certain latitude bands, namely all sites North of 40°N latitude (top), all sites between 40°N and the equator (mid) and all sites in the Southern hemisphere (bottom). The plots also show the trend results of a trend+seasonality fit. As can be seen these numbers vary strongly, ranging from 18.2 ppb/year to 134.6 ppb/year. Needless to say that these figures do not represent any real long term trend in the data but are the direct result of the limited dataset which does not even cover a full season.
That said, we do observe a significant bias for the Northern latitude band (North of 40°N), with contributions from stations such as Rikubetsu, Parkfalls, Garmisch and Orleans, which all feature significant positive biases. Apart from this bias, SRFP and TCCON follow the same general pattern of XCH_4 variability.

When we opt not to smooth the SRFP and TCCON data, these biases are no longer present (see **Figure 4-22, right**). Apart from this bias shift, both comparison datasets are near identical.

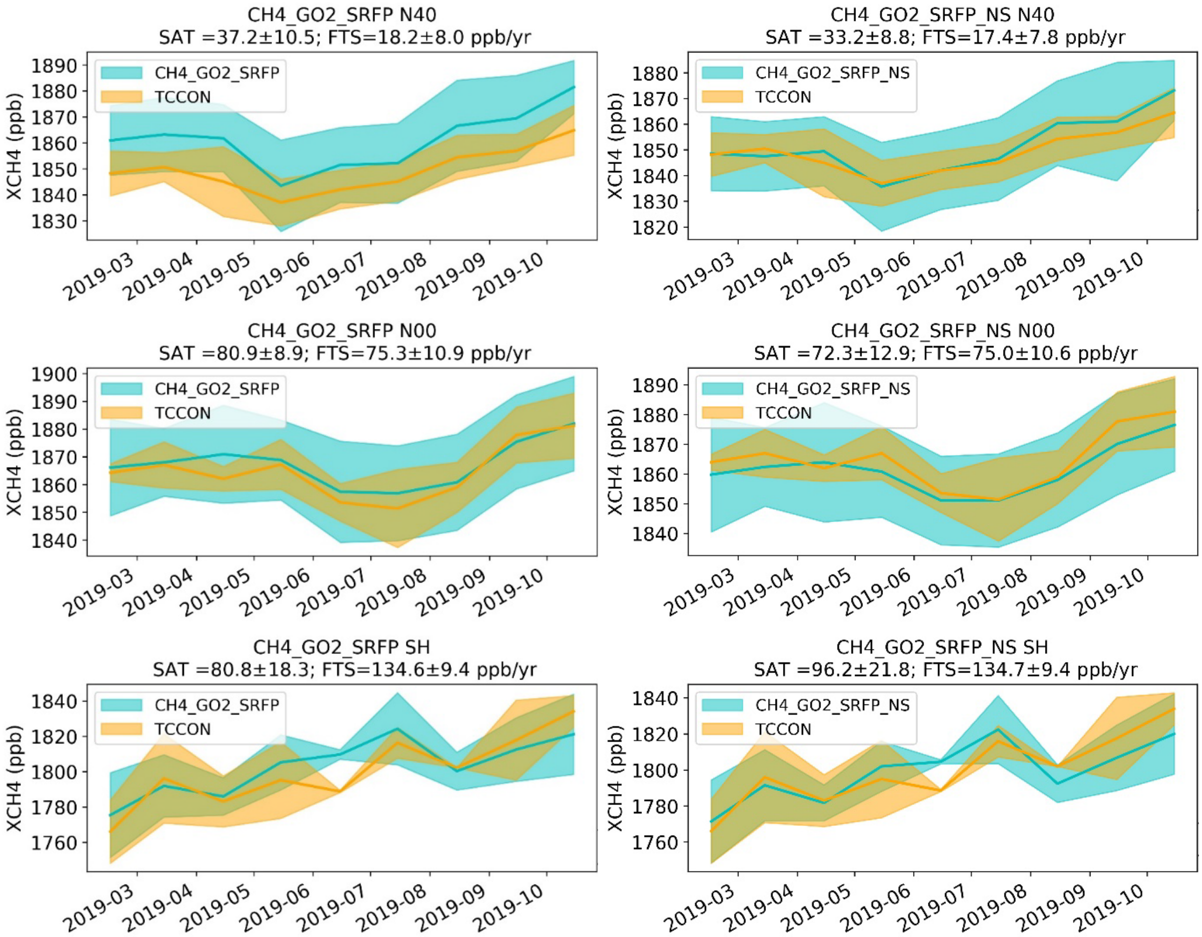

Figure 4-22: Monthly median collocated Sat and TCCON XCH_4 concentrations as a function of time. The shaded areas correspond with the scaled median absolute deviation. Smoothed SRFP XCH_4 comparisons on the left, Unsmoothed (tagged as CH4_GO2_SRFP_NS) on the right.

4.2.5.2 Summary

Listed in the table below (**Table 4-10**) are the Figure of Merit parameters as derived from the individual collocated data pairs at each station.

SRFP XCH_4's single measurement precision equals 14.9 ppb, reaching the Breakthrough target of <17 ppb. The error assessment is slightly underestimated with an uncertainty ratio of 0.87. The median bias however, as already discussed, is significant at 6.3 ppb with confidence bands between 4.1 and 11.5 ppb. When we look at the unsmoothed data the median bias sits at -3.1 [-6.9,-1.9] ppb, which is an equally statistically significant, although somewhat less outspoken, this time negative, bias.

Both the spatial and spatio-temporal relative accuracies reach the <10 ppb target

No meaningful estimate for the drift can be established nor do we see any obvious problems in this regard.

Table 4-10 presents an overview of the estimated data quality of CH4_GO2_SRFP, as obtained by the VALT team, from comparisons with TCCON ground-based reference observations. Values in square brackets [ ] correspond with the upper and lower 95% confidence bound on the parameter. The uncertainty ratio features 2 numbers as outlined in the validation method.

Product Quality Summary Table for Product: CH4_GO2_SRFP Level: 2, Version: v01.0.0, Time period covered: 2.2019 – 11.2019 Assessment: Validation Team (VALT)			
Parameter [unit]	**Achieved performance**	**Requirement**	**Comments**
Single measurement precision (1-sigma) in [ppm]	14.9 [14.0,16.6]	< 34 (T) < 17 (B) < 9 (G)	Computed as the median over all station scaled median absolute differences to TCCON
Uncertainty ratio [-]: Ratio reported uncertainty to standard deviation of satellite-TCCON difference	0.85, 0.87*	-	No requirement but value close to unity expected for a high quality data product with reliable reported uncertainty.
Median bias (global offset) [ppm]	6.3 [4.1,11.5]	-	No requirement but value close to zero expected for a high quality data product.
Accuracy: Relative systematic error [ppm]	Spatial: 6.4 [1.0,10.4] Spatio-temporal: 7.1 [4.3,8.8]	< 10	Spatial: Computed as standard deviation of the biases at the various TCCON sites. Spatio-temporal: As "Spatial" but also considering seasonal biases.
Stability: Drift [ppm/year]	-	< 3	Linear drift

4.2.6 Validation results for product CH4_GO2_SRPR

Below we show the validation results of the XCH_4 concentrations as derived by the CH4_GO2_SRPR algorithm using GOSAT-2 spectra. 'PR' stands for the proxy version of the algorithm developed at SRON, whereby the retrieved CH_4 concentration is scaled by the modelled CO_2/retrieved CO_2 ratio. Data was available from February 2019 up to and including November 2019. The SRPR algorithm provides *a priori* and column averaging kernel data on a 3 layer vertical profile.

As with SRFP, for similar reasons but probably exasperated by the very crude vertical resolution, smoothing has a profound impact on the overall bias (~10 ppb shift) and produces a slight 0.4 ppb improvement in the scatter. Again, given the very limited time period that is covered by this product, these validation results will be rather preliminary in nature, nor can we make useful statements about long term stability and even seasonality as it does not cover a full year of data.

4.2.6.1 Detailed results

The Taylor diagram below in **Figure 4-23** yields a concise overview of the capabilities of the CH4_GO2_SRPR algorithm. Most TCCON sites cluster between the 0.4 and 0.5 correlation line. The TCCON scatter is smaller than that of SRPR while the variability of the bias roughly ranges between 0.8 and 1, relative to the SRPR variability. These results are very similar to the ones obtained from its Full Physics counterpart and again the correlation values should improve as the time series gets expanded and with it the range of natural variability.

When looking at the mosaic plot (**Figure 4-24**), as with SRFP, the 40 to 50°N latitude band features some outspoken bias values. Somewhat lower biases seem to appear around the May-August period but that said it is hard to discern a pattern.

Table 4-11 lists all bias and scatter results derived from individual data pairs at all TCCON stations. The Proxy version of the algorithm produces more than 3 times as many collocated data pairs than its Full Physics counterpart, with on average ~340 data pairs per station, which corresponds with ~400 pairs per station per year. Stations such as Bremen which featured only 7 collocated data points in the Full Physics version, now show 46 collocated measurements. This comes at a slight cost as the single measurement precision is slightly worse: 15.8 ppb instead of 14.9 ppb. Which in turn negatively impacts the overall median correlation (0.43 instead of 0.55). The correlation using all data regardless of station equals 0.78 (again slightly lower than SRFP (0.80)).
The observed median bias ranges between -5.94 ppb (Reunion) and 20.19 ppb(Garmisch), while the scatter ranges between 10.91 ppb (Nicosia) and 22.54 ppb (Ny Alesund). As with the other SRON products, no long term drift numbers have been calculated.

The timeseries in **Figure 4-25** show individual satellite and ground-based TCCON measurements. While the scatter is even somewhat higher for SRPR XCH_4 with respect to both TCCON and SRFP, it is again relatively free of outliers. Looking at Tsukuba again, we clearly see that the algorithm manages to capture the natural variability of XCH_4.

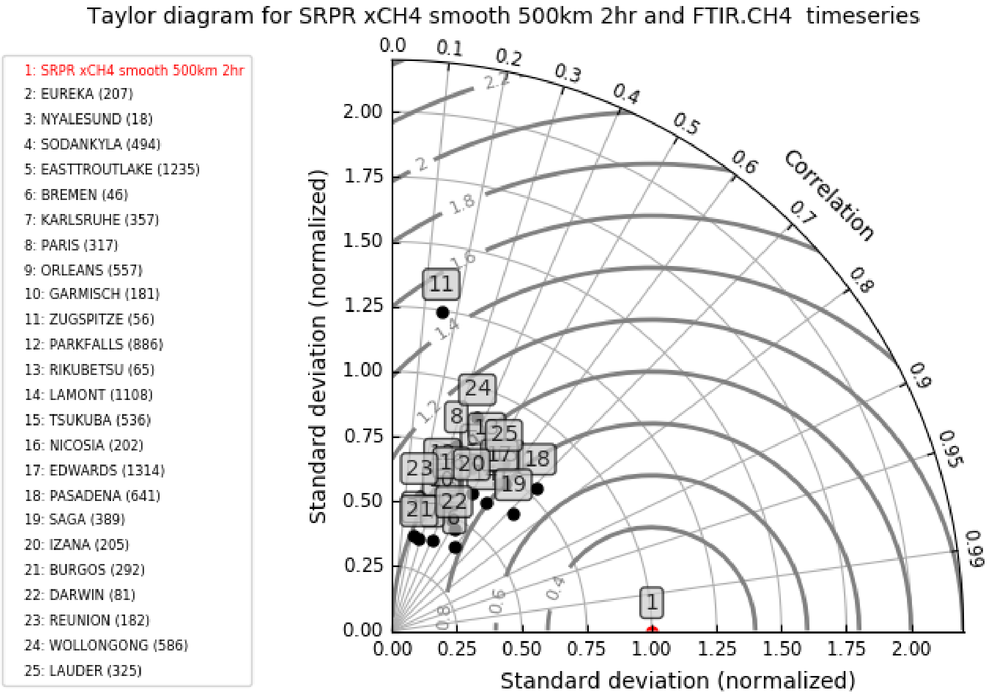

Figure 4-23: Tayor plot of XCH_4 TCCON values relative to CH4_GO2_SRPR. Straight lines correspond with the correlation, light grey lines yield the variability of the TCCON data relative to the satellite variability and the dark grey lines correspond with the variability of the Satellite -TCCON bias relative to the satellite variability.

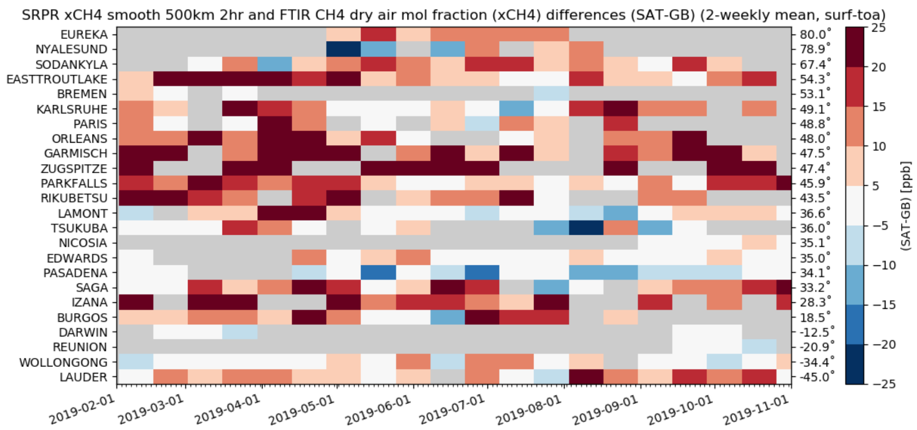

Figure 4-24. Mosaic plot of bi-weekly mean CH4_GO2_SRPR - TCCON XCH_4 biases as a function of time and TCCON station.

Table 4-11: Number of collocated data pairs (N), Correlation (R), Bias, Scatter, long term trend difference (ltt) and uncertainty thereon (ltt_err), seasonal amplitude difference (A) and uncertainty thereon (A_err) as well as the latitude of the TCCON station. The last row lists the median values over all stations. Product: CH4_GO2_SRPR.

STATION	N	R	Bias	Scat	ltt	ltt_err	A	A_err	lat
EUREKA	207	0.42	13.84	17.7	-	-	-	-	80
NYALESUND	18	0.22	6.02	22.54	-	-	-	-	78.9
SODANKYLA	494	0.38	9.53	19.75	-	-	-	-	67.4
EASTTROUTLAKE	1235	0.44	11.37	19.13	-	-	-	-	54.3
BREMEN	46	0.59	2.07	17.76	-	-	-	-	53.1
KARLSRUHE	357	0.41	7.58	17.47	-	-	-	-	49.1
PARIS	317	0.33	2.58	15.6	-	-	-	-	48.8
ORLEANS	557	0.47	12.76	15.51	-	-	-	-	48
GARMISCH	181	0.37	20.19	18.28	-	-	-	-	47.5
PARKFALLS	886	0.32	8.01	19.34	-	-	-	-	45.9
RIKUBETSU	65	0.48	17.1	12.62	-	-	-	-	43.5
LAMONT	1108	0.59	2.69	16.75	-	-	-	-	36.6
TSUKUBA	536	0.61	0.16	18.31	-	-	-	-	36
NICOSIA	202	0.39	3.95	10.91	-	-	-	-	35.1
EDWARDS	1314	0.59	1.65	15.22	-	-	-	-	35
PASADENA	641	0.71	-5.52	14.32	-	-	-	-	34.1
SAGA	389	0.72	11.59	14.57	-	-	-	-	33.2
BURGOS	292	0.28	7.35	15.95	-	-	-	-	18.5
DARWIN	81	0.52	0.62	12.1	-	-	-	-	-12.5
REUNION	182	0.2	-5.94	12.27	-	-	-	-	-20.9
WOLLONGONG	586	0.37	1.35	14.12	-	-	-	-	-34.4
LAUDER	325	0.56	9.32	11.38	-	-	-	-	-45
MEDIAN	**341**	**0.43**	**6.69**	**15.78**	**-**	**-**	**-**	**-**	**40.05**

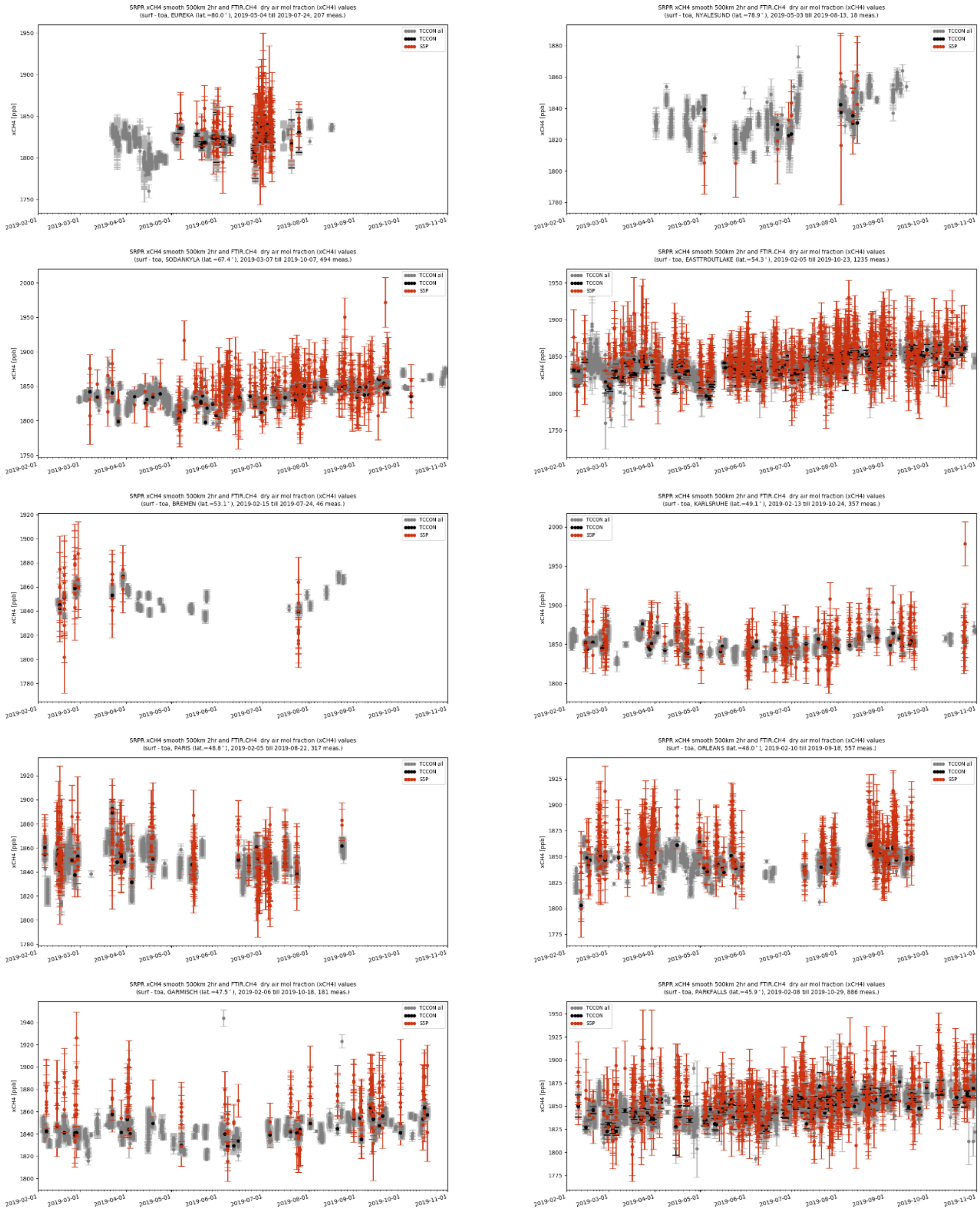

SRPR xCH4 smooth 500km 2hr and FTIR.CH4 dry air mol fraction (xCH4) values
(surf - toa, EUREKA (lat.=80.0 °), 2019-05-04 till 2019-07-24, 207 meas.)
SRPR xCH4 smooth 500km 2hr and FTIR.CH4 dry air mol fraction (xCH4) values
(surf - toa, NYALESUND (lat.=78.9 °), 2019-05-03 till 2019-08-13, 18 meas.)
SRPR xCH4 smooth 500km 2hr and FTIR.CH4 dry air mol fraction (xCH4) values
(surf - toa, SODANKYLA (lat.=67.4 °), 2019-03-07 till 2019-10-07, 494 meas.)
SRPR xCH4 smooth 500km 2hr and FTIR.CH4 dry air mol fraction (xCH4) values
(surf - toa, EASTTROUTLAKE (lat.=54.3 °), 2019-02-05 till 2019-10-23, 1235 meas.)
SRPR xCH4 smooth 500km 2hr and FTIR.CH4 dry air mol fraction (xCH4) values
(surf - toa, BREMEN (lat.=53.1 °), 2019-02-15 till 2019-07-24, 46 meas.)
SRPR xCH4 smooth 500km 2hr and FTIR.CH4 dry air mol fraction (xCH4) values
(surf - toa, KARLSRUHE (lat.=49.1 °), 2019-02-13 till 2019-10-24, 357 meas.)
SRPR xCH4 smooth 500km 2hr and FTIR.CH4 dry air mol fraction (xCH4) values
(surf - toa, PARIS (lat.=48.8 °), 2019-02-05 till 2019-08-22, 317 meas.)
SRPR xCH4 smooth 500km 2hr and FTIR.CH4 dry air mol fraction (xCH4) values
(surf - toa, ORLEANS (lat.=48.0 °), 2019-02-10 till 2019-09-18, 557 meas.)
SRPR xCH4 smooth 500km 2hr and FTIR.CH4 dry air mol fraction (xCH4) values
(surf - toa, GARMISCH (lat.=47.5 °), 2019-02-06 till 2019-10-18, 181 meas.)
SRPR xCH4 smooth 500km 2hr and FTIR.CH4 dry air mol fraction (xCH4) values
(surf - toa, PARKFALLS (lat.=45.9 °), 2019-02-08 till 2019-10-29, 886 meas.)
TCCON all
TCCON
SSP
xCH4 [ppb]

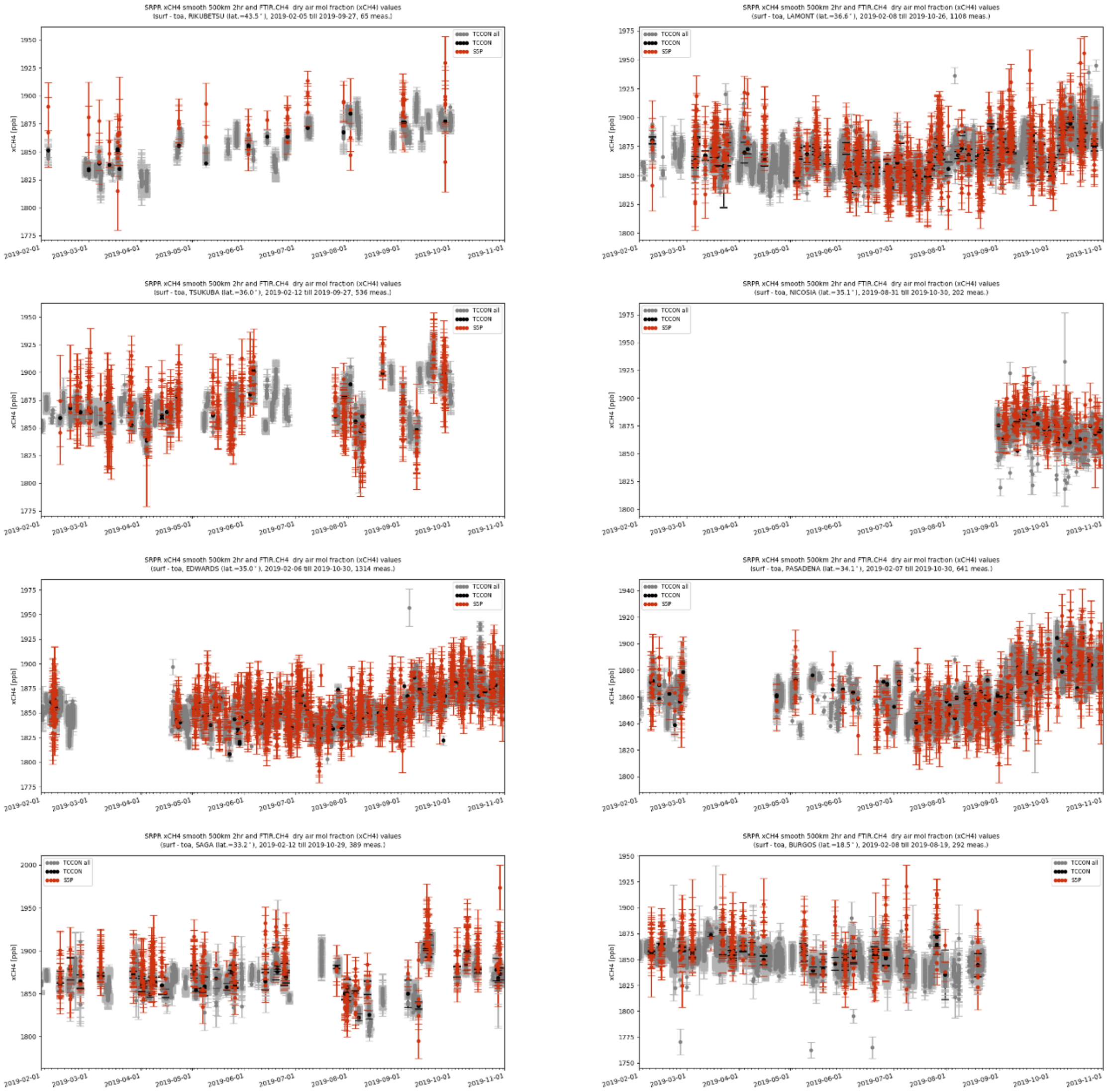
SRPR xCH4 smooth 500km 2hr and FTIR.CH4 dry air mol fraction (xCH4) values
(surf - toa, RIKUBETSU (lat.=43.5°), 2019-02-05 till 2019-09-27, 65 meas.)
SRPR xCH4 smooth 500km 2hr and FTIR.CH4 dry air mol fraction (xCH4) values
(surf - toa, LAMONT (lat.=36.6°), 2019-02-08 till 2019-10-26, 1108 meas.)
SRPR xCH4 smooth 500km 2hr and FTIR.CH4 dry air mol fraction (xCH4) values
(surf - toa, TSUKUBA (lat.=36.0°), 2019-02-12 till 2019-09-27, 536 meas.)
SRPR xCH4 smooth 500km 2hr and FTIR.CH4 dry air mol fraction (xCH4) values
(surf - toa, NICOSIA (lat.=35.1°), 2019-08-31 till 2019-10-30, 202 meas.)
SRPR xCH4 smooth 500km 2hr and FTIR.CH4 dry air mol fraction (xCH4) values
(surf - toa, EDWARDS (lat.=35.0°), 2019-02-06 till 2019-10-30, 1314 meas.)
SRPR xCH4 smooth 500km 2hr and FTIR.CH4 dry air mol fraction (xCH4) values
(surf - toa, PASADENA (lat.=34.1°), 2019-02-07 till 2019-10-30, 641 meas.)
SRPR xCH4 smooth 500km 2hr and FTIR.CH4 dry air mol fraction (xCH4) values
(surf - toa, SAGA (lat.=33.2°), 2019-02-12 till 2019-10-29, 389 meas.)
SRPR xCH4 smooth 500km 2hr and FTIR.CH4 dry air mol fraction (xCH4) values
(surf - toa, BURGOS (lat.=18.5°), 2019-02-08 till 2019-08-19, 292 meas.)
TCCON all
TCCON
SSP

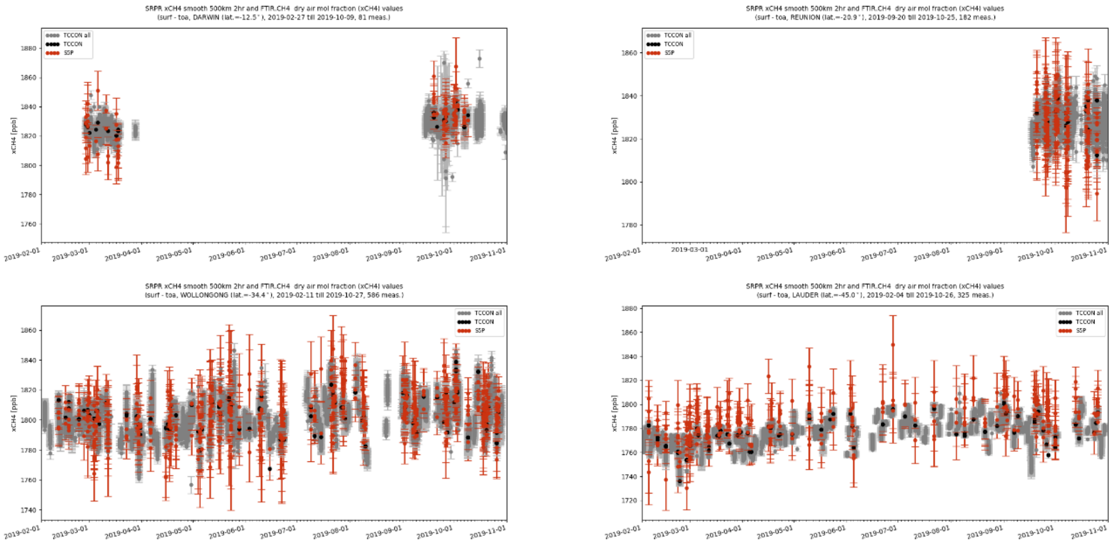

Figure 4-25: Timeseries of XCH_4 TCCON (collocated=black, all=grey) and CH4_GO2_SRPR (red) data at selected TCCON sites.

Figure 4-26 shows monthly median timeseries for TCCON and SRPR XCH_4 for all data that fall within certain latitude bands, namely all sites North of 40°N latitude (top), all sites between 40°N and the equator (mid) and all sites in the Southern hemisphere (bottom). Due to the short time window, the fitted long term trend values range from 3.4 to 131.8 ppb/year and should be ignored. As with SRFP, the top figure (latitude band North of 40°N) features a pronounced bias, but the overal evolution of the seasonal cycle is adequately captured.

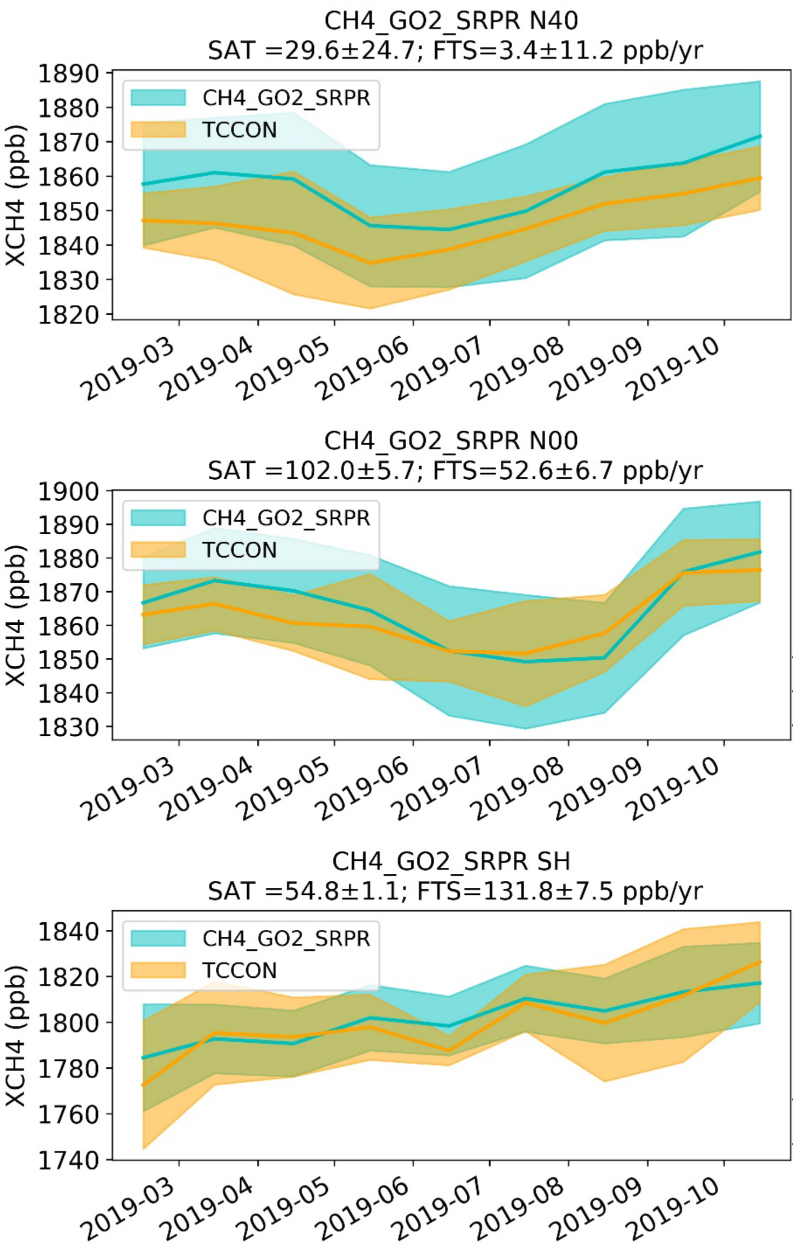

Figure 4-26: Monthly median collocated Sat and TCCON XCH_4 concentrations as a function of time. The shaded areas correspond with the scaled median absolute deviation.

4.2.6.2 Summary

Listed in the table below (**Table 4-12**) are the Figure of Merit parameters as derived from the individual collocated data pairs at each station.

SRPR XCH_4's single measurement precision equals 15.8 ppb, reaching the Breakthrough target of <17 ppb. The error assessment is slightly underestimated with an uncertainty ratio of 0.95. The median bias is, like its SRFP counterpart, significant at 6.7 ppb with confidence bands between 3.8 and 11.3 ppb. Both the spatial and spatio-temporal relative accuracies reach the <10 ppb target

No meaningful estimate for the drift can be established, nor did we find obvious issues in that regard.

When we compare the quality of SRPR with that of SRFP for XCH_4, we indeed observe small differences which amount to slightly more data at the cost of slightly higher scatter values for the Proxy version. However, the FoM themselves are very close to one another with significant overlap between the respective confidence bands. It would therefore be ill advised to claim superiority of one version over the other.

Table 4-12 presents an overview of the estimated data quality of CH4_GO2_SRPR, as obtained by the VALT team, from comparisons with TCCON ground-based reference observations. Values in square brackets [ ] correspond with the upper and lower 95% confidence bound on the parameter. The uncertainty ratio features 2 numbers as outlined in the validation method.

Product Quality Summary Table for Product: CH4_GO2_SRPR Level: 2, Version: v01.0.0, Time period covered: 2.2019 – 11.2019 Assessment: Validation Team (VALT)			
Parameter [unit]	**Achieved performance**	**Requirement**	**Comments**
Single measurement precision (1-sigma) in [ppm]	15.8 [13.8,17.2]	< 34 (T) < 17 (B) < 9 (G)	Computed as the median over all station scaled median absolute differences to TCCON
Uncertainty ratio [-]: Ratio reported uncertainty to standard deviation of satellite-TCCON difference	0.93,0.95*	-	No requirement but value close to unity expected for a high quality data product with reliable reported uncertainty.
Median bias (global offset) [ppm]	6.7 [3.8,11.3]	-	No requirement but value close to zero expected for a high quality data product.
Accuracy: Relative systematic error [ppm]	Spatial: 7.1 [4.1,11.3] Spatio-temporal: 9.1 [6.8,12.0]	< 10	Spatial: Computed as standard deviation of the biases at the various TCCON sites. Spatio-temporal: As "Spatial" but also considering seasonal biases.
Stability: Drift [ppm/year]	-	< 3	Linear drift

5 Validation and intercomparisons results from data provider

5.1 Validation and intercomparison results for product CO2_OC2_FOCA

5.1.1 Comparison with CAMS model results

This section bases on section 8.1 of FOCAL's **/ATBDv1 FOCAL, 2019/** which, in turn, summarizes results of a comparison of FOCAL v06 with the CAMS model done by **/Reuter et al., 2017b/**.

Here we compare one year (2015) of post-filtered and bias corrected FOCAL v09 XCO_2 results with corresponding values of the CAMS v15r4 model accounting for FOCAL's column averaging kernels (e.g., **/Rodgers, 2000/**). **Figure 5.1-1** shows 5°×5°monthly gridded values for six months (Feb., Apr., Jun., Aug., Oct., and Dec. 2015) of FOCAL data and **Figure 5.1-2** shows corresponding values of CAMS v15r4 data. The main spatial and temporal patterns are similar for FOCAL and CAMS with largest and smallest values in the northern hemisphere in April and August, respectively. Differences become larger at smaller scales, e.g., FOCAL sees larger values in natural and anthropogenic source regions of Sub-Saharan Africa and East Asia, e.g., in April but also above the Sahara, e.g., in August. However, it shall be noted that often only few data points are in the corresponding grid boxes.

In grid boxes with more than 100 soundings, the standard error of the mean becomes negligible (~0.1ppm). Therefore, the difference between FOCAL and CAMS in such grid boxes can be interpreted as systematic temporal and regional mismatch or bias. The heatmap shown in **Figure 5.1-3** (left) bases on these grid boxes. The standard deviation of this systematic mismatch (including also representation errors) amounts to 1.0 ppm and the correlation between FOCAL and CAMS is 0.88.

The standard deviation of the single sounding mismatch after subtracting the systematic mismatch amounts to 1.2 ppm which is consistent with the average reported uncertainty of 1.2 ppm.

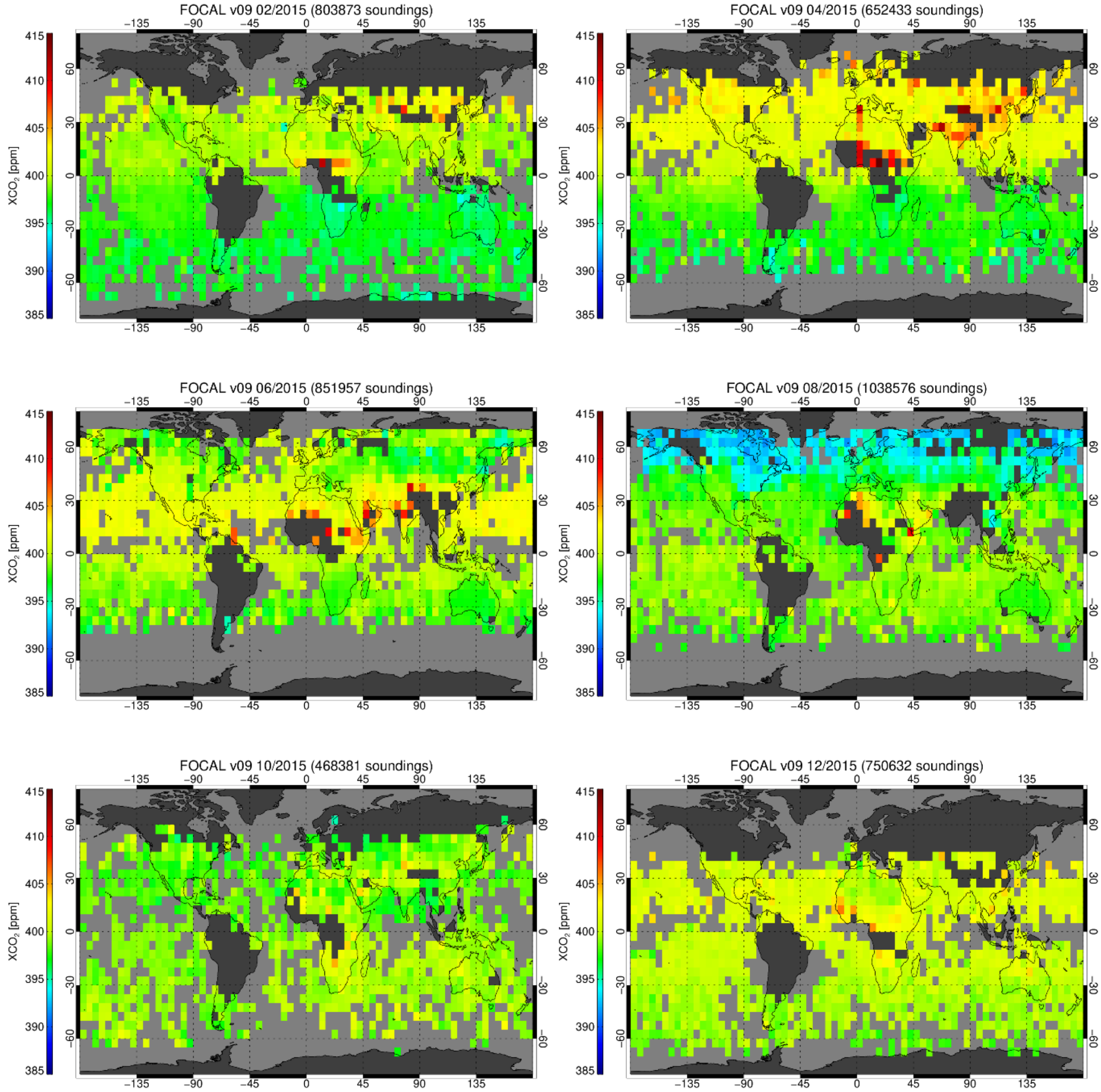

Figure 5.1-1: FOCAL v09 monthly mean XCO_2 gridded to 5°×5°. From top/left to bottom/right: Feb., Apr., Jun., Aug., Oct., and Dec. 2015.

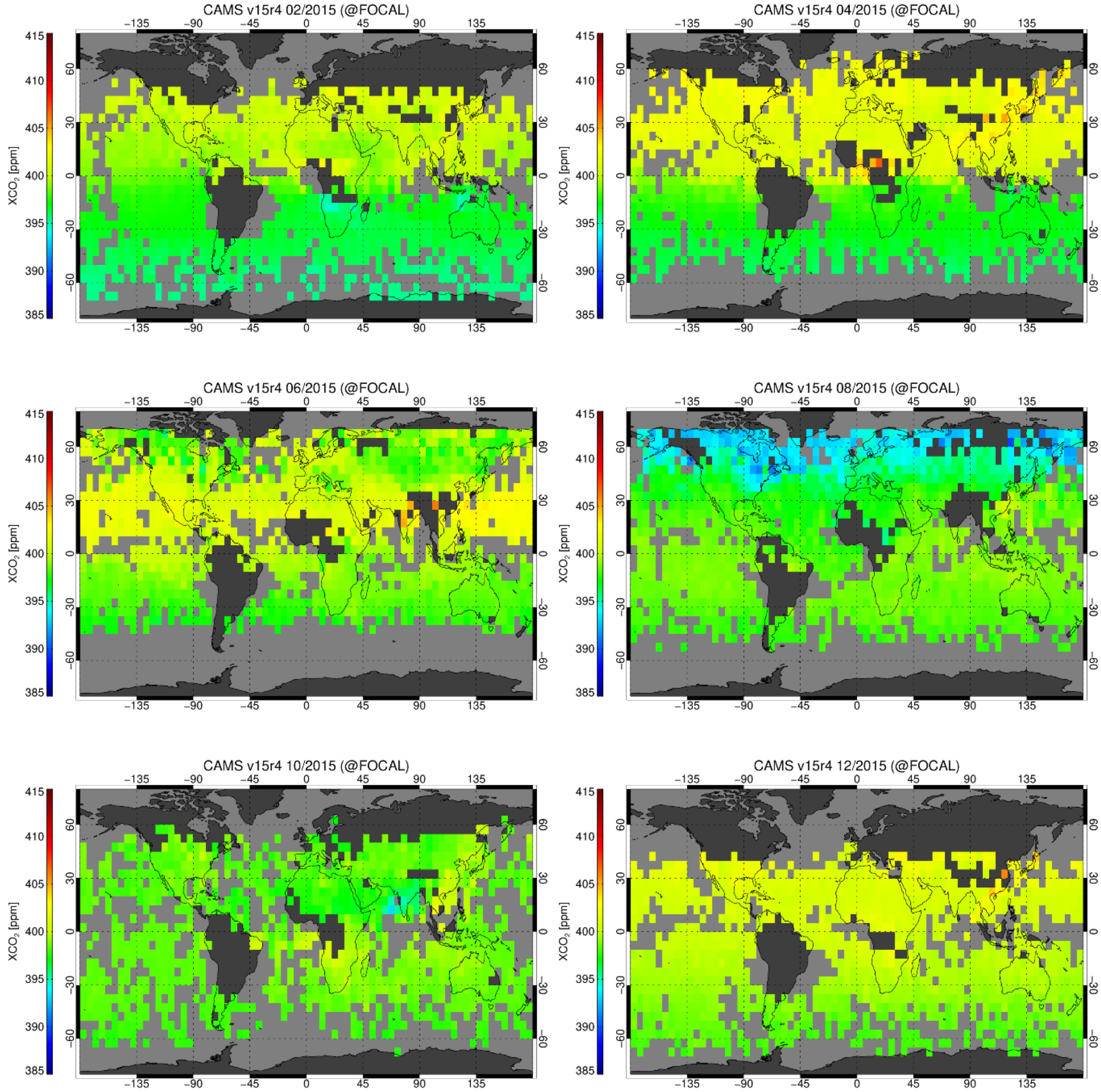

Figure 5.1-2: CAMS v15r4 monthly mean XCO_2 sampled as FOCAL and gridded to 5°×5°. From top/left to bottom/right: Feb., Apr., Jun., Aug., Oct., and Dec. 2015.

5.1.2 Comparison with NASA's operational OCO-2 L2 product

In this section we compare the same year of post-filtered and bias corrected FOCAL v09 XCO_2 results with NASA's operational OCO-2 L2 product v10.2. Our comparison method is similar to what has been done in **Section 5.1.1**. However, as FOCAL and the NASA product feature different samplings, we first gridded the NASA product and compared FOCAL with corresponding grid box averages. In order to improve the comparability, both data products have been adjusted for a common a priori **/Rodgers, 2000/** namely SECM2020 **/Reuter et al., 2012/**.

Comparing **Figure 5.1-1** with **Figure 5.1-4** shows similar large scale temporal and spatial patterns and also the relative enhancement in the anthropogenic source regions of East Asia in April are similar. The most obvious difference is that the NASA product has about three times more soundings. The primary reason for this is the inherently poor throughput (~11%) of the MODIS based cloud screening of FOCAL's preprocessor **/Reuter et al., 2017b/**. Additionally, one can observe a larger variability in the gridded FOCAL product which can only partly be explained by the sparser filling of the grid boxes.

Similarly, as done for the model comparison, we concentrate only on grid boxes with more than 100 FOCAL and NASA soundings so that the standard error of the mean becomes negligible (~0.1ppm). Therefore, the difference between FOCAL and NASA in such grid boxes can be interpreted as systematic temporal and regional mismatch or bias. The heatmap shown in **Figure 5.1-3** (right) bases on these grid boxes. The standard deviation of this systematic mismatch (including also representation errors) amounts to 1.0ppm and the correlation between FOCAL and NASA is 0.89.

FOCAL scatters within the grid boxes with a standard deviation of 1.3ppm which is similar to the average reported uncertainty of 1.2ppm.

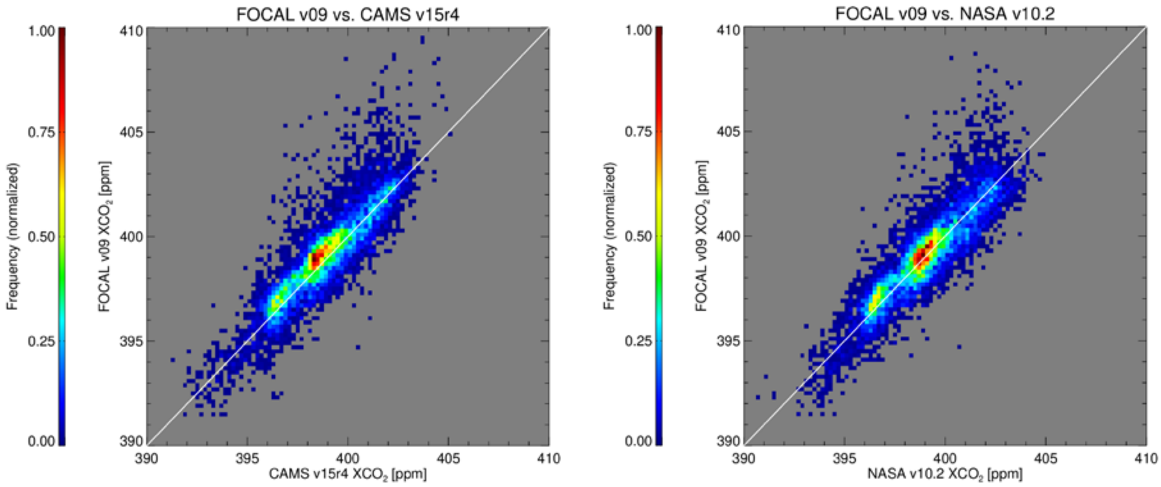

Figure 5.1-3: Heat maps of FOCAL v09 vs. CAMS v15r4 XCO_2 data (left) and FOCAL v09 vs. NASA v10.2 XCO_2 data (right) on the basis monthly 5°×5° grid boxes including more than 100 data points.

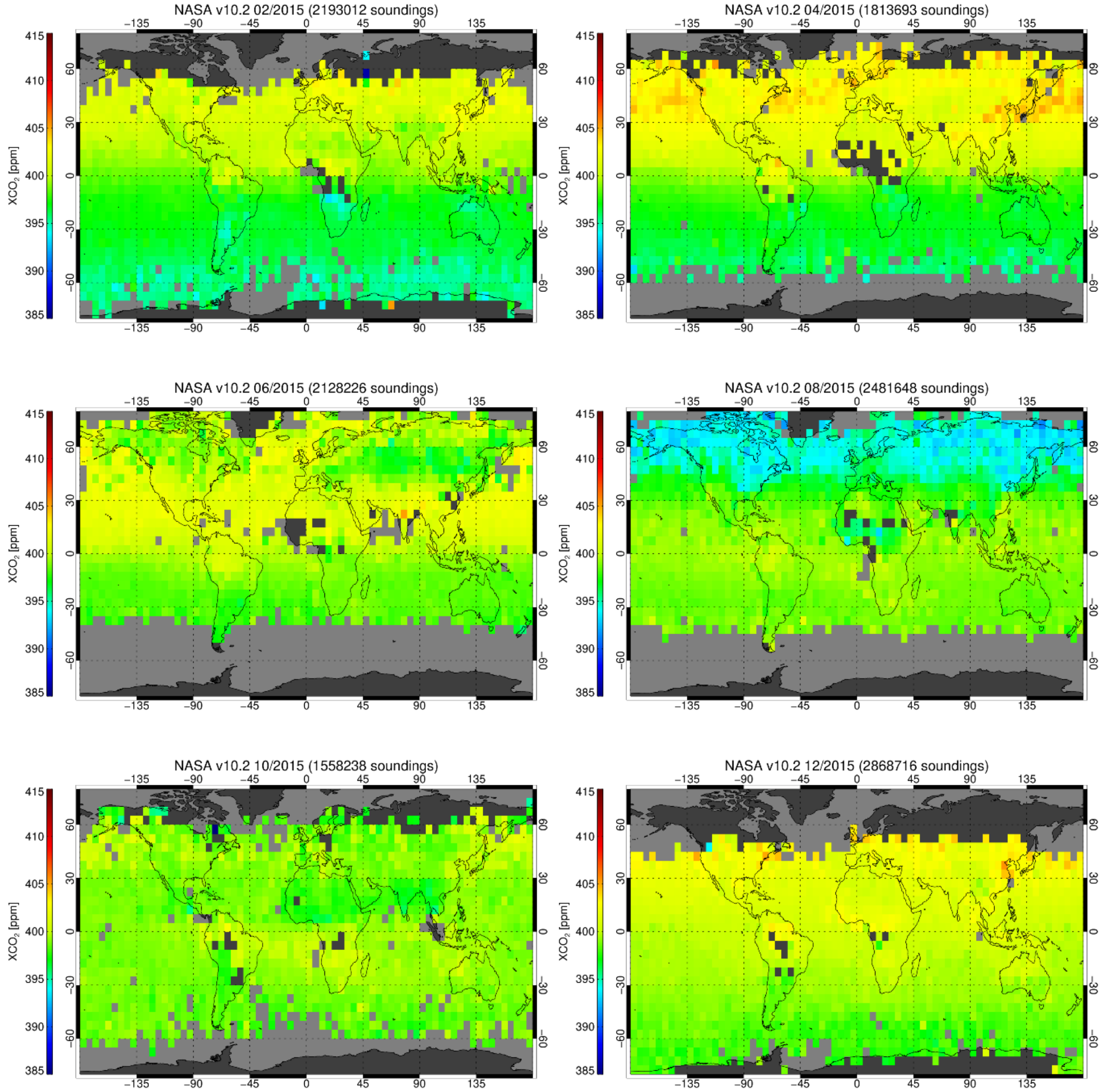

Figure 5.1-4: As **Figure 5.1-1** but for NASA's operational OCO-2 v10.2 L2 product.

5.1.3 Validation with TCCON

The validation results shown in this section are valid for FOCAL v09. The applied methods are similar to those described in BESD's Comprehensive Error Characterisation Report **/CECRv3, 2017/** and the Product Validation and Intercomparison Report **/PVIR v5, 2017/** of ESA's GHG CCI project and partly also in the publication of **/Reuter et al., 2011/**. For all comparisons, averaging kernels have been applied as described in the C3S GHG Product User Guide and Specification **/PUGS, 2019/**.

XCO_2

FOCAL's XCO_2 has been validated with TCCON GGG2014 measurements. The co-location criteria are defined by a maximum time difference of two hours, a maximum spatial distance of 500km, and a maximum surface elevation difference of 250m. **Figure 5.1-5** shows all co-located FOCAL and TCCON retrievals of the years 2015-2019 for TCCON sites with more than 250 co-locations and covering a time period of at least two years. One can see that FOCAL captures the year-to-year increase and the seasonal features. For each station, the performance statistics number of co- locations, station bias, seasonal bias, linear drift, and single measurement precision were calculated.

We define the station bias as average difference to TCCON. Seasonal bias, linear drift, and single sounding precision have been derived by fitting the following trend model:

$$\Delta \boldsymbol{X} = \boldsymbol{a_0} + \boldsymbol{a_1 t} + \boldsymbol{a_2} \sin(2\boldsymbol{\pi t} + \boldsymbol{a_3}) + \boldsymbol{\varepsilon} \quad (1)$$

Here, ΔX represents the difference satellite minus TCCON , and a_{0-3} the free fit parameters. Specifically, a_1 represents the linear drift and a_2 the amplitude of the seasonal bias. The single sounding precision is computed by the standard deviation of the residua ε.

Based on the per station statistics, the following summarizing statistics have been calculated: Total number of co-locations used for validation, average single measurement precision, station-to-station bias (standard deviation of the station biases), average seasonal bias (standard deviation of the seasonal bias term), and average linear drift. As the linear drift can be assumed to be globally constant, the station-to-station standard deviation of the linear drift is a measure for its uncertainty. Per station statistics and overall performance estimates are listed in **Table 5.1-1**.

In total, more than 700000 co-located FOCAL measurements have been used for the validation exercise. The overall single measurement precision is 1.48ppm and station-to-station biases amount to 0.57ppm.

In the context of station-to-station biases, it shall be noted that **/Wunch et al., 2010, 2011/** specifies the accuracy (1σ) of TCCON to be about 0.4ppm. This means it cannot be expected to find regional biases considerably less than 0.4ppm using TCCON as reference.

Seasonal cycle biases amount to 0.37ppm on average and no significant (temporally linear) drift can be found (0.03±0.26ppm/a).

Additionally, a measure for the year-to-year stability has been computed as follows. For each TCCON site, the residual difference (satellite - TCCON) which is not explained by station bias, seasonal bias, and/or linear drift has been derived by subtracting the fit of the bias model ΔX from the satellite minus TCCON difference. These time series were smoothed by a running average of 365 days. Only days where more than 10 co-locations contributed to the running average of at least 5 TCCON sites have been further considered. At these days, the station-to-station average has been calculated. The corresponding expected uncertainty has been computed from the standard error of the mean (derived from the station-to-station standard deviation and the number of stations) and by error propagation of the reported single sounding uncertainties. For FOCAL, the average is always between about -0.2 ppm and 0.2ppm (**Figure 5.1-6**) with an uncertainty of typically about 0.15 ppm. Most of the time, the average is not significantly different from zero, i.e., its one sigma uncertainty is larger than its absolute value. Due to the relatively large uncertainty, we decided to compute not the maximum minus minimum as a measure for the year-to-year stability because this quantity can be expected to increase with length of the time series simply due to statistics. Therefore, we estimate the year-to-year stability by randomly selecting pairs of dates with a time difference of at least 365 days. For each selection we computed the difference modified by a random component corresponding to the estimated uncertainty. From 1000 of such pairs we compute the standard deviation as estimate for the year-to-year stability. We repeat this experiment 1000 times and compute the average (0.18 ppm) and standard deviation (0.01 ppm).

From this, we conclude that the year-to-year stability is 0.18 ppm/a (**Figure 5.1-6**).

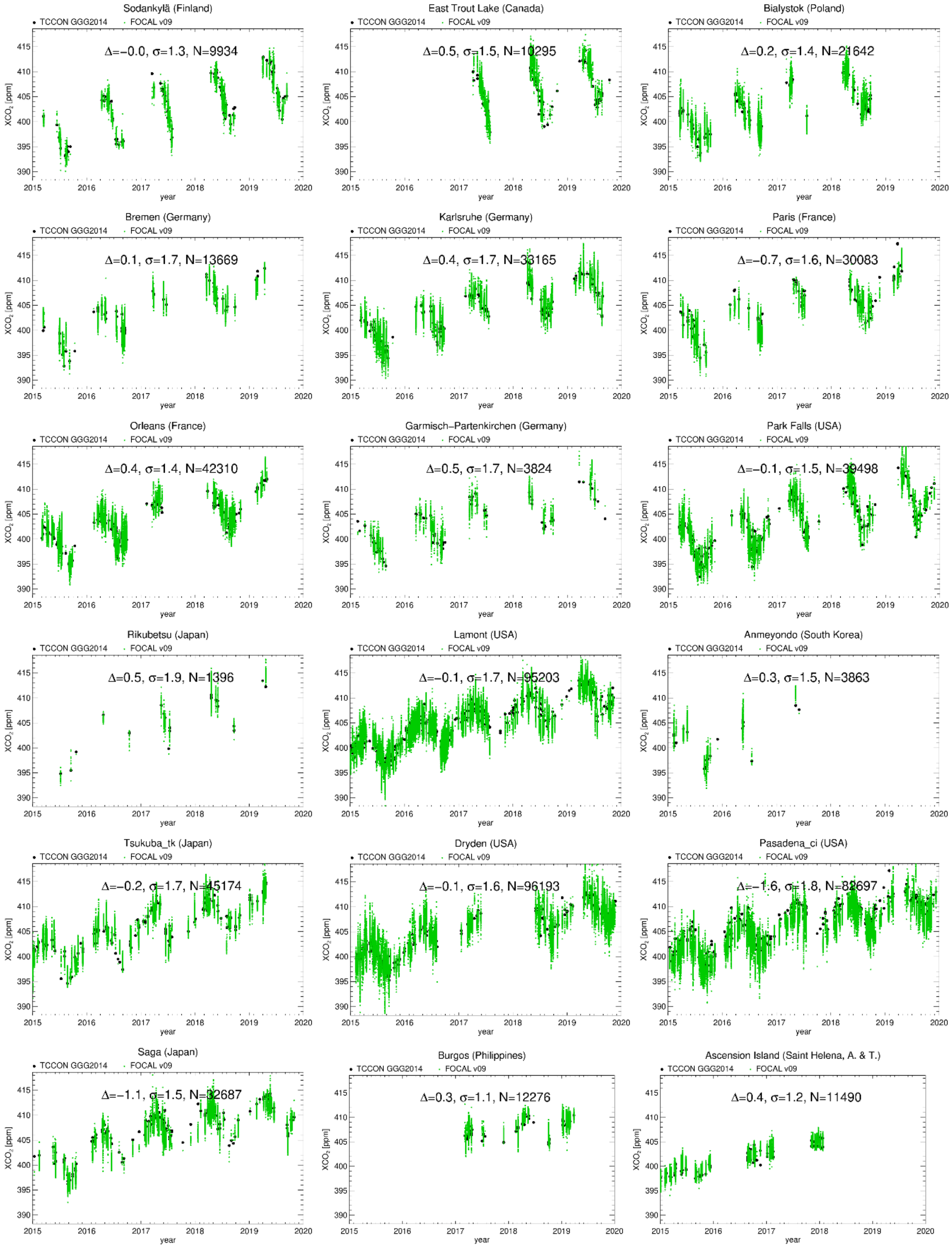
Sodankylä (Finland)
Δ=−0.0, σ=1.3, N=9934
East Trout Lake (Canada)
Δ=0.5, σ=1.5, N=10295
Bialystok (Poland)
Δ=0.2, σ=1.4, N=21642
Bremen (Germany)
Δ=0.1, σ=1.7, N=13669
Karlsruhe (Germany)
Δ=0.4, σ=1.7, N=33165
Paris (France)
Δ=−0.7, σ=1.6, N=30083
Orleans (France)
Δ=0.4, σ=1.4, N=42310
Garmisch−Partenkirchen (Germany)
Δ=0.5, σ=1.7, N=3824
Park Falls (USA)
Δ=−0.1, σ=1.5, N=39498
Rikubetsu (Japan)
Δ=0.5, σ=1.9, N=1396
Lamont (USA)
Δ=−0.1, σ=1.7, N=95203
Anmeyondo (South Korea)
Δ=0.3, σ=1.5, N=3863
Tsukuba_tk (Japan)
Δ=−0.2, σ=1.7, N=45174
Dryden (USA)
Δ=−0.1, σ=1.6, N=96193
Pasadena_ci (USA)
Δ=−1.6, σ=1.8, N=82697
Saga (Japan)
Δ=−1.1, σ=1.5, N=32687
Burgos (Philippines)
Δ=0.3, σ=1.1, N=12276
Ascension Island (Saint Helena, A. & T.)
Δ=0.4, σ=1.2, N=11490
TCCON GGG2014
FOCAL v09
XCO2 [ppm]
year

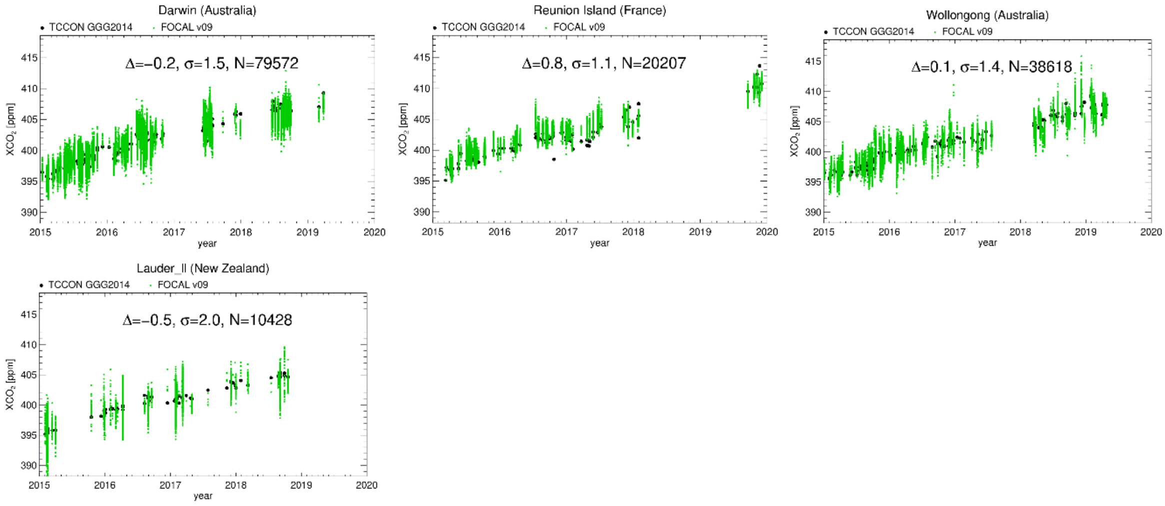

Figure 5.1-5: Validation of single soundings of FOCAL (**green**) with co-located TCCON measurements (**black**) at all TCCON sites with more than 250 co-locations and covering a time period of at least one year. Numbers in the figures: Δ = station bias, i.e., average of the difference; σ = single measurement precision, i.e., standard deviation of the difference; N = number of co-locations. From top/left to bottom/right the TCCON sites have been sorted by latitude.

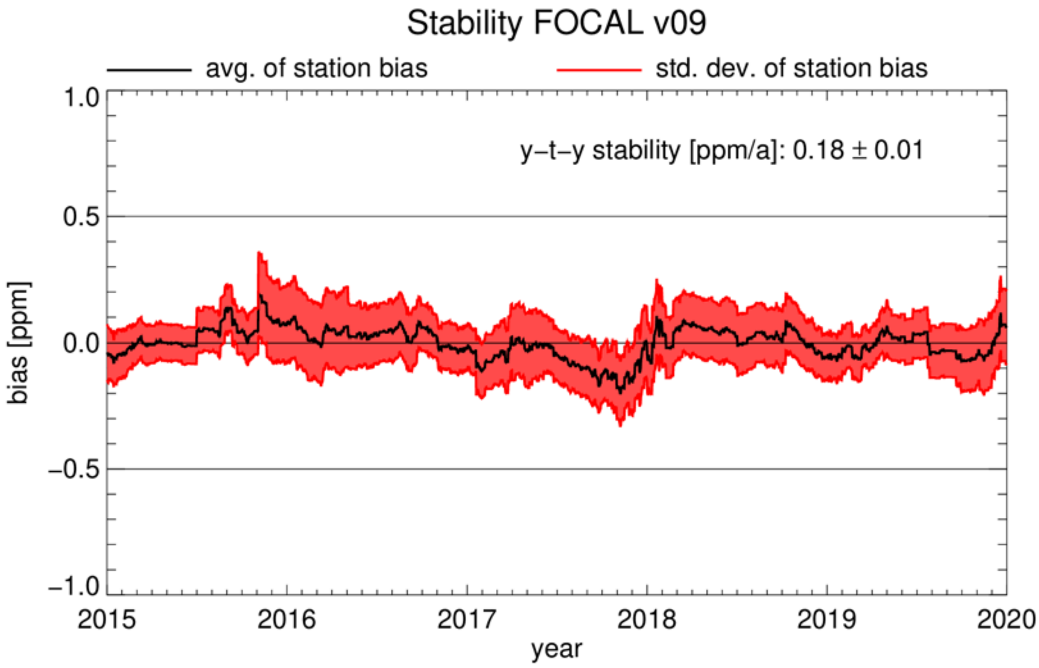

Figure 5.1-6: Stability analyses for FOCAL. The black curve shows the average station bias and the red curves its uncertainty represented by the station-to-station standard deviation and error propagation from single sounding measurement noise.

Table 5.1-1: Validation statistics for all TCCON sites with more than 250 co-locations and covering a time period of at least two years with number of co-locations (#col), number of days with co-locations (#day), single measurement precision (σ), station bias (Δ), seasonal bias (s) and linear drift (d). The last row contains the overall statistics. In this row σ represents the (quadratic) average single measurement precision, Δ the station-to-station bias (i.e., the standard deviation of the station biases), s the average seasonal bias, and d the average drift plus minus its standard deviation.

Station	#col	#day	σ [ppm]	Δ [ppm]	s [ppm]	d [ppm/a]
Sodankylä	9934	119	1.25	-0.03	0.28	-0.08
East Trout Lake	10295	79	1.43	0.48	0.43	0.22
Bialystok	21642	101	1.43	0.24	0.12	0.14
Bremen	13669	45	1.56	0.10	0.67	-0.20
Karlsruhe	33165	129	1.52	0.43	0.68	0.15
Paris	30083	77	1.57	-0.75	0.36	0.01
Orleans	42310	131	1.36	0.45	0.20	-0.07
Garmisch-P.	3824	70	1.62	0.54	0.57	0.27
Park Falls	39498	197	1.39	-0.07	0.53	0.15
Rikubetsu	1396	18	1.64	0.49	0.58	0.83
Lamont	95203	256	1.63	-0.11	0.25	-0.06
Anmeyondo	3863	18	1.44	0.31	0.28	-0.20
Tsukuba	45174	103	1.65	-0.22	0.37	-0.10
Dryden	96193	178	1.57	-0.12	0.34	-0.18
Pasadena	82697	255	1.74	-1.59	0.30	-0.08
Saga	32687	104	1.54	-1.13	0.10	0.12
Burgos	12276	33	1.01	0.35	0.32	0.15
Ascension Island	11490	61	1.13	0.36	0.22	0.16
Darwin	79572	146	1.37	-0.19	0.18	-0.37
Reunion Island	20207	78	1.01	0.77	0.27	-0.27
Wollongong	38618	123	1.38	0.15	0.22	-0.22
Lauder	10428	48	1.89	-0.46	0.76	0.30
Total	**600174**	**2369**	**1.48**	**0.57**	**0.37**	**0.03±0.26**

XCO_2 uncertainty

Especially for the application of flux inversion, reliable information on the uncertainty of each individual sounding is necessary. For this purpose, we analyzed the same validation dataset of co-located FOCAL and TCCON measurements also used in the last section.

For each co-location used for the validation, we have a residual ε of the bias model ΔX. From this, we computed our best estimate for the stochastic uncertainty (precision) as it does not include the analyzed systematic biases (trend, seasonal cycle, station-to-station).

For each ε, we have a corresponding uncertainty reported by FOCAL's optimal estimation retrieval. We pooled the entire data set of more than 700000 co-locations into 20 bins with increasing reported uncertainty in a way that each bin included the same number of co-locations. For each bin, we computed the (quadratic) average reported uncertainty and the standard deviation of the residual ε (actual precision).

Figure 5.1-7 shows that both quantities are connected by a fairly linear relationship. However, it shall be notated, that the reported uncertainty is mainly driven by the instrumental noise which is in turn driven by the radiance so that the darkest scenes usually have the largest reported uncertainties. This means, especially the bins including the largest (or smallest) reported uncertainties may be dominated by an individual validation site with especially dark (or bright) albedo, while the other bins usually consist of data from a lager mixture of TCCON sites.

The linear fit shown in **Figure 5.1-7** shows that FOCAL's reported uncertainties has a positive correlation with the actual precision but it shows also that FOCAL's reported uncertainty is somewhat to optimistic. However it shall be noted that the residual ε does not only include instrumental noise but also pseudo noise from representation errors.

In summary, we suggest that users who are interested in more realistic uncertainty estimates, shall apply the following error parameterization derived from the linear fit shown in **Figure 5.1-7**:

$$\boldsymbol{\sigma}_{\text{corrected}}^{\text{XCO}_2} = \boldsymbol{\sigma}_{\text{v09}}^{\text{XCO}_2} \cdot \mathbf{1.361 - 0.133ppm} \quad (2)$$

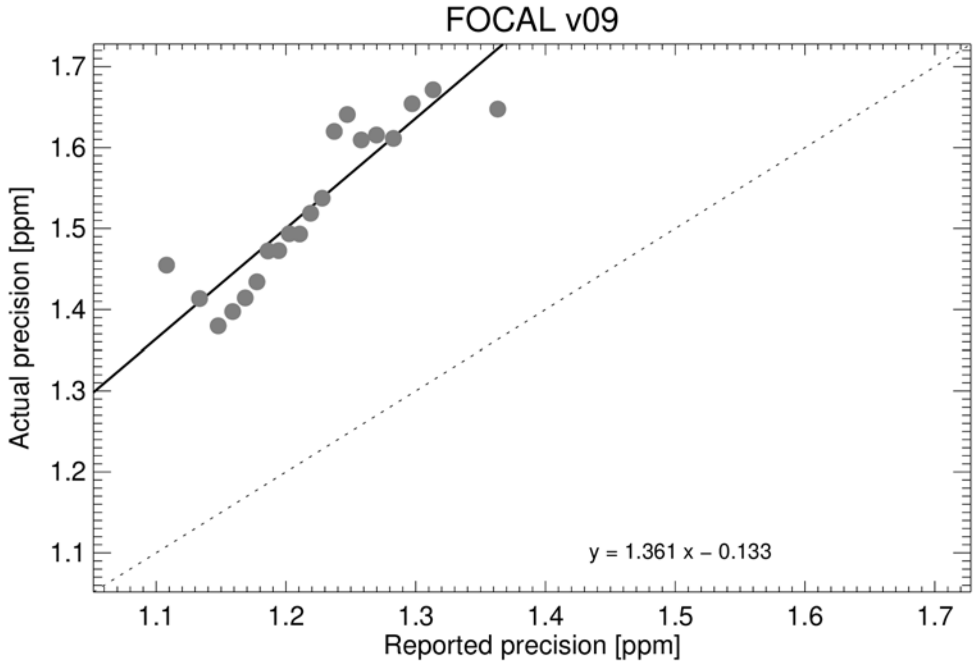

Figure 5.1-7: Reported uncertainty of FOCAL's optimal estimation retrieval vs. actual precision computed from the residual ε of the bias model.

5.1.4 Summary

Table 5.1-2 presents an overview of the estimated data quality as obtained from comparisons with TCCON ground-based reference observations.

Table 5.1-2: Summary validation of product CO2_OC2_FOCA.

Product Quality Summary Table for Product: CO2_OC2_FOCA Level: 2, Version: v09, Time period covered: 1.2015 – 12.2019 Assessment: Data Provider (DP)			
Parameter [unit]	**Achieved performance**	**Requirement**	**Comments**
Single measurement precision (1-sigma) in [ppm]	1.48	< 8 (T) < 3 (B) < 1 (G)	Computed as standard deviation of the difference to TCCON
Uncertainty ratio [-]: Ratio reported uncertainty to standard deviation of satellite-TCCON difference	0.83	-	No requirement but value close to unity expected for a high quality data product with reliable reported uncertainty.
Mean bias (global offset) [ppm]	-0.15	-	No requirement but value close to zero expected for a high quality data product.
Accuracy: Relative systematic error [ppm]	Spatial: 0.57 Spatio-temporal: 0.68	< 0.5	Spatial: Computed as standard deviation of the biases at the various TCCON sites. Spatio-temporal: As "Spatial" but also considering seasonal biases.
Stability: Drift [ppm/year]	0.03±0.26 (1-sigma)	< 0.5	Linear drift

5.2 Validation and intercomparison results for product CO2_TAN_OCFP

The UoL core CO_2 ECV product (CO2_TAN_OCFP v1) is retrieved from calibrated TanSat SWIR/NIR spectra using the UoL full-physics retrieval algorithm **/Boesch et al., 2011/**. The TanSat L1 spectra are retrieved for all TCCON overpasses for the time period March 2017 to May 2018 and are evaluated against rigorously validated ground based TCCON values.

5.2.1 Detailed results

To assess the quality of CO2_TAN_OCFP v1 observations against TCCON, OCFP (TanSat) soundings are matched to TCCON observations spatially and temporally. OCFP (TanSat) points are co-located with TCCON sites based on a quadrate latitude and longitude region around each TCCON site (in ±3º latitude/longitude box). Matching OCFP soundings with TCCON sites for time is a comparatively simple operation, selecting only those TCCON values whose observation time falls within ±1 hour of each TanSat sounding time. The average is taken of all TCCON points fitting these criteria for each OCFP sounding to provide the TCCON value against which to compare.

The co-location procedure matches 113,120 points for the CO2_TAN_OCFP v1 product. The comparions for each TCCON site is shown in **Figure 5.2-1** and the statics (mean bias, standard deviation and Pearson correlation coefficient R) for each site is given in **Table 5.2-1**. The bias per site varies between -1.40 ppm and 1.57 ppm with a standard deviation of the per-site bias of 0.84 ppm. It is important to highlight that the number of data points and the temporal coverage varies greatly between sites.

The overall correlation between the TanSat and TCCON retrievals is given in **Figure 5.2-2**. We find a small mean overall bias of 0.19 ppm and an all-site Pearson correlation coefficient of 0.82 which details a good match of OCFP and TCCON pairs. The all-site RMSE (mean of the standard deviation per site) of Δ (TCCON- OCFP) is 1.78 ppm.

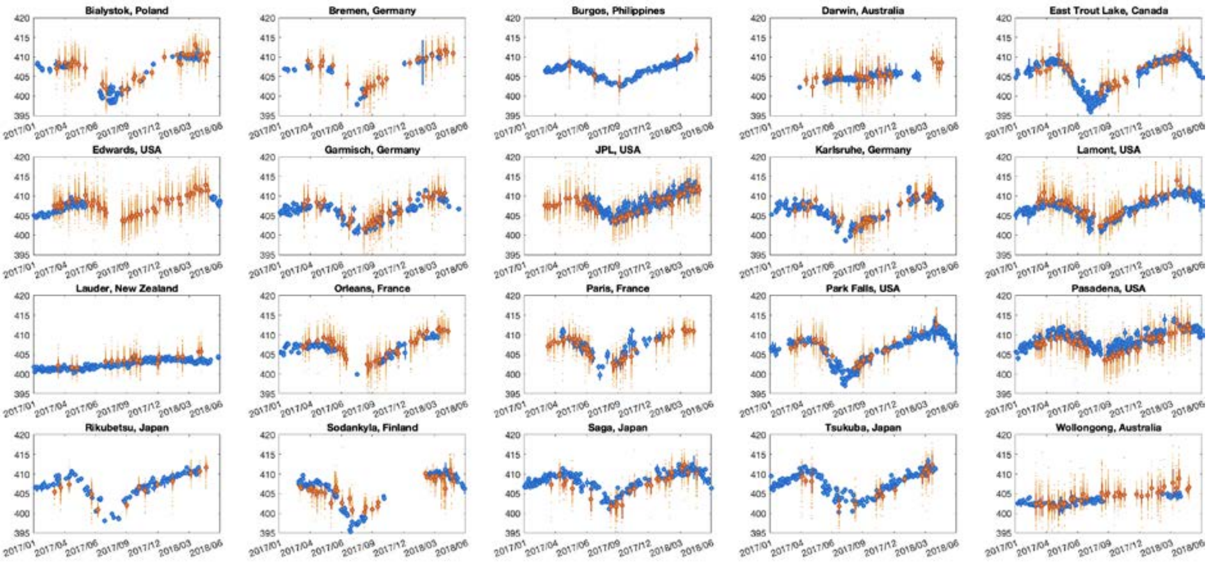

Figure 5.2-1: TanSat XCO_2 (product CO2_TAN_OCFP v1) observations plotted with their corresponding paired TCCON mean (blue) for the overpass. Overview statistics for each site reference to **Table 5.2-1**.

Table 5-2-1: Overview of the estimated data quality as obtained from comparisons with TCCON ground-based reference observations per site. The bottom row details statistics for all sites, with all co-located points used for calculations. XCO_2 units is in ppm. The overall mean Δ and σΔ is calculated by averaging of site values and R is calculated by all individual measurements.

Site	Mean Δ	σΔ	*R*	n obs.
Bialystok, Poland	-0.92	1.68	0.65	3,292
Bremen, Germany	0.25	1.20	0.25	1,610
Burgos, Philippines	-0.08	2.22	0.32	310
Darwin, Australia	-0.64	2.05	-0.33	5,534
East Trout Lake, Canada	-0.17	1.26	0.90	11,923
Edwards, USA	-1.40	1.96	0.55	2,763
Garmisch, Germany	-0.32	1.67	0.67	3,704
JPL, USA	1.17	2.07	0.81	15,209
Karlsruhe, Germany	-0.29	1.62	0.84	3,089
Lamont, USA	-0.35	1.35	0.86	18,274
Lauder, New Zealand	-1.31	1.88	0.72	2,999
Orléans, France	-0.66	1.46	0.18	2,243
Paris, France	-0.08	1.40	0.76	1,503
Park Falls, USA	-0.35	1.45	0.89	13,231
Pasadena, USA	1.57	2.47	0.65	12,807
Rikubetsu, Japan	0.54	1.27	0.84	1,473
Sodankylä Finland	-1.18	2.19	0.93	6,482
Saga, Japan	0.69	1.99	0.77	4,033
Tsukuba, Japan	0.94	2.46	0.79	866
Wollongong, Australia	-1.15	1.93	0.73	1,775
Overall	0.19	1.78	0.82	113,120

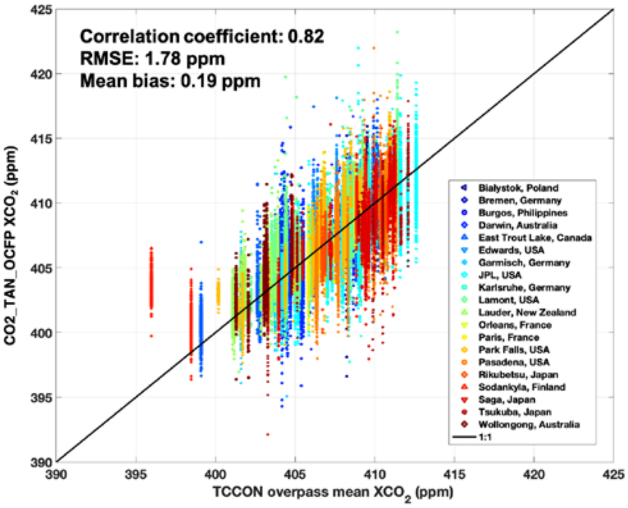

Figure 5.2-2: Correlation plot between all 113,120 co-located CO2_TAN_OCFP and TCCON XCO_2 pairs coloured by site.

The random error is assessed by comparing the overpass-mean reported uncertainty for an overapss over a TCCON site to the standard deviation of the TCCON–OCFP pairs for each overpass. **Figure 5.2-3** shows that the reported uncertainties are between 0.78 ppm (Lamont, U.S.A.) and 4.34 ppm (East Trout Lake, Canada). There is a relatively large spread of the data points with some clear outliers where the observed scatter is largely overestimated. We find that these overestimated errors are correlated with very low surface albedo of the CO_2 band and subsequently low information content for CO_2 so that the retrieved results remain close to the *a priori* values. The slope between the observed scatter between TanSat and TCCON retrievals and the reported uncertainties is 0.96.

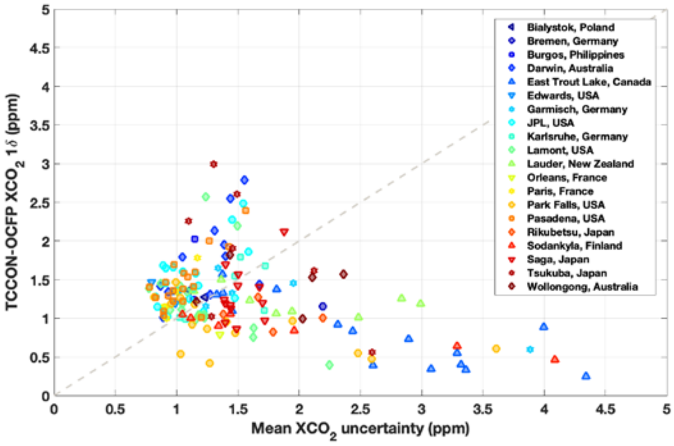

Figure 5.2-3: Correlation plot of the TCCON–OCFP Δ standard deviation per TCCON overpass and the reported overpass-mean a posteriori retrieval error for different TCCON sites.

5.2.2 Summary

The result of the validation of the CO2_TAN_OCFP v1.0 dataset is given in **Table 5.2-2** and compared to the requirement. The mean estimate of the single-measurement precision is 1.78 ppm which exceeds the goal requirement but is within the baseline requirement of 3 ppm. The reported uncertainties agree in average with the observed scatter of the data when compared to TCCON. The mean, global bias of the TanSat XCO_2 retrieval is 0.19 ppm with a relative accuracy of 0.84 ppm which is slightly larger than the requirement of 0.5 ppm. We have not assessed the spatio-temporal bias or the drift due to the short time period covered by the CO2_TAN_OCFP dataset.

Table 5.2-2: Summary validation of product CO2_TAN_OCFP by the data provider using TCCON ground-based reference data.

Product Quality Summary Table for Product: CO2_TAN_OCFP Level: 2, Version: v1, Time period covered: 3.2017 – 5.2018 Assessment: Data Provider (DP)			
Parameter [unit]	**Achieved performance**	**Requirement**	**Comments**
Single measurement precision (1-sigma) in [ppm]	1.78	< 8 (T) < 3 (B) < 1 (G)	Computed as standard deviation of the difference to TCCON
Uncertainty ratio [-]: Ratio reported uncertainty to standard deviation of satellite-TCCON difference	0.96	-	No requirement but value close to unity expected for a high quality data product with reliable reported uncertainty.
Mean bias (global offset) [ppm]	0.19	-	No requirement but value close to zero expected for a high quality data product.
Accuracy: Relative systematic error [ppm]	Spatial: 0.84 Spatio-temporal: Not evaluated	< 0.5	Spatial: Computed as standard deviation of the biases at the various TCCON sites. Spatio-temporal: As "Spatial" but also considering seasonal biases.
Stability: Drift [ppm/year]	Not evaluated	< 0.5	Linear drift

5.3 Validation and intercomparison results for product CO2_GO2_SRFP

The CO2_GO2_SRFP product is retrieved from GOSAT-2 TANSO-FTS SWIR spectra using the RemoTeC algorithm that has been jointly developed by SRON and KIT **/Butz et al., 2011; Schepers et al., 2012/**. The retrievals are performed globally for the time period between February and October 2019 and are evaluated against ground based TCCON observations.

5.3.1 Detailed results

To assess the quality of SRFP retrieval XCO_2 observations against TCCON values, SRFP soundings are matched to TCCON observations spatially and temporally. GOSAT-2 observations are co-located with TCCON sites based on a square latitude and longitude region around each TCCON site (in ±2.5º latitude/longitude box). For the temporal co-location we select only the TCCON measurements whose observation time falls within ±2 hour of each GOSAT-2 observation time. The TCCON observations that match these criteria are averaged for each individual GOSAT-2 observation.

The co-location procedure matches 1587 points for the CO2_GO2_SRFP product. The comparions for each TCCON site is shown in **Figure 5.3-1**. The statistics (mean bias, standard deviation and Pearson correlation coefficient R) for each site are given in **Table 5.3-1**. The bias per site varies between -0.92 ppm and 2.10 ppm. The standard deviation of the station-to station bias is 0.90 ppm, which mostly follows from the large bias found in the Lauder observations and the overall small number of compared values. Because of the limited time period, the number of data points and the temporal coverage varies greatly between sites.

The overall correlation between the GOSAT-2 and TCCON retrievals is given in **Figure 5.3-2**. We find a small mean overall bias of 0.01 ppm and an all-site Pearson correlation coefficient of 0.70 which, given the small number of co-locations, points to a good comparison of GOSAT-2 and TCCON pairs. The all-site RMSE (mean of the standard deviation per site) of ∆ (TCCON- GOSAT-2) is 2.04 ppm.

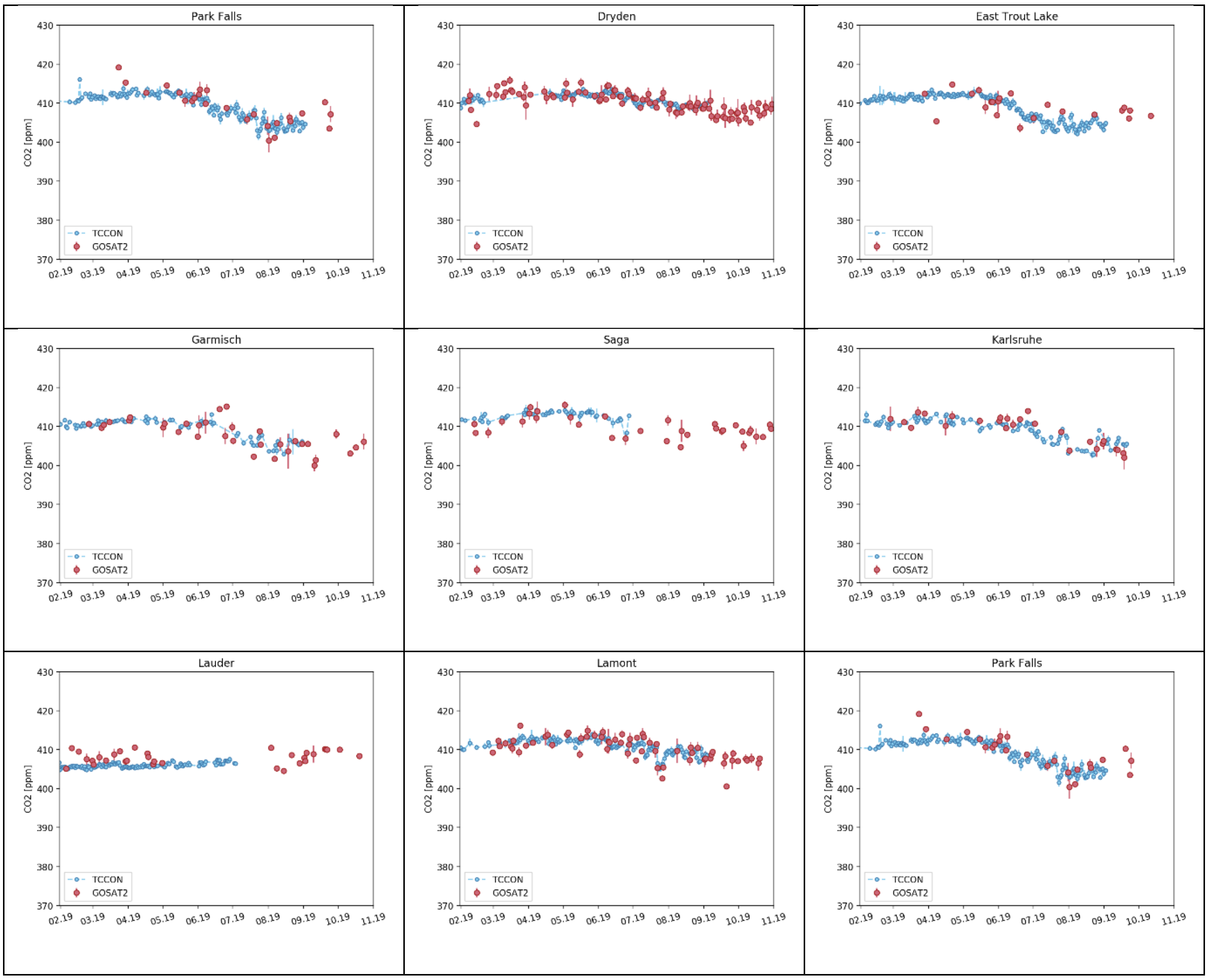

Figure 5-3-1: GOSAT-2 XCO_2 (CO2_GO2_SRFP, red) with co-located TCCON (blue) measurements at nine TCCON stations used for the validation for the period of February to October 2019.

Table 5.3-1: Overview of the estimated data quality as obtained from comparisons with TCCON observations per site. The bottom row details statistics for all sites, with all co-located points used for calculations. XCO_2 units are in ppm. The overall mean Δ and σΔ is calculated by averaging of site values and R is calculated by all individual measurements. The mean of site means $\bar{\mu}$ and spatial accuracy $\sigma_{\bar{\mu}}$ are calculated by taking the mean and standard deviation of the site means. The mean standard deviation $\bar{\sigma}$ and standard deviation of the standard deviations $\sigma_{\bar{\sigma}}$ are calculated by taking the mean and the standard deviation of the site standard deviations.

Site	Mean Δ	σΔ	*R*	n obs.
Pasadena, USA	-0.91	1.91	0.60	337
Dryden, USA	0.36	1.71	0.62	448
East Trout Lake, Canada	-0.77	2.66	0.43	62
Garmisch, Germany	-0.26	1.66	0.88	28
Saga, Japan	-0.73	1.96	0.70	98
Karlsruhe, Germany	0.80	2.48	0.68	115
Lauder, New Zealand	2.10	1.61	0.01	52
Lamont, USA	0.09	1.99	0.70	344
Park Falls, USA	0.55	2.41	0.88	103
All observations	0.01	2.10	0.70	1587
	$\bar{\mu}$	$\sigma_{\bar{\mu}}$	$\bar{\sigma}$	$\sigma_{\bar{\sigma}}$
Mean of sites	0.14	0.90	2.04	0.36

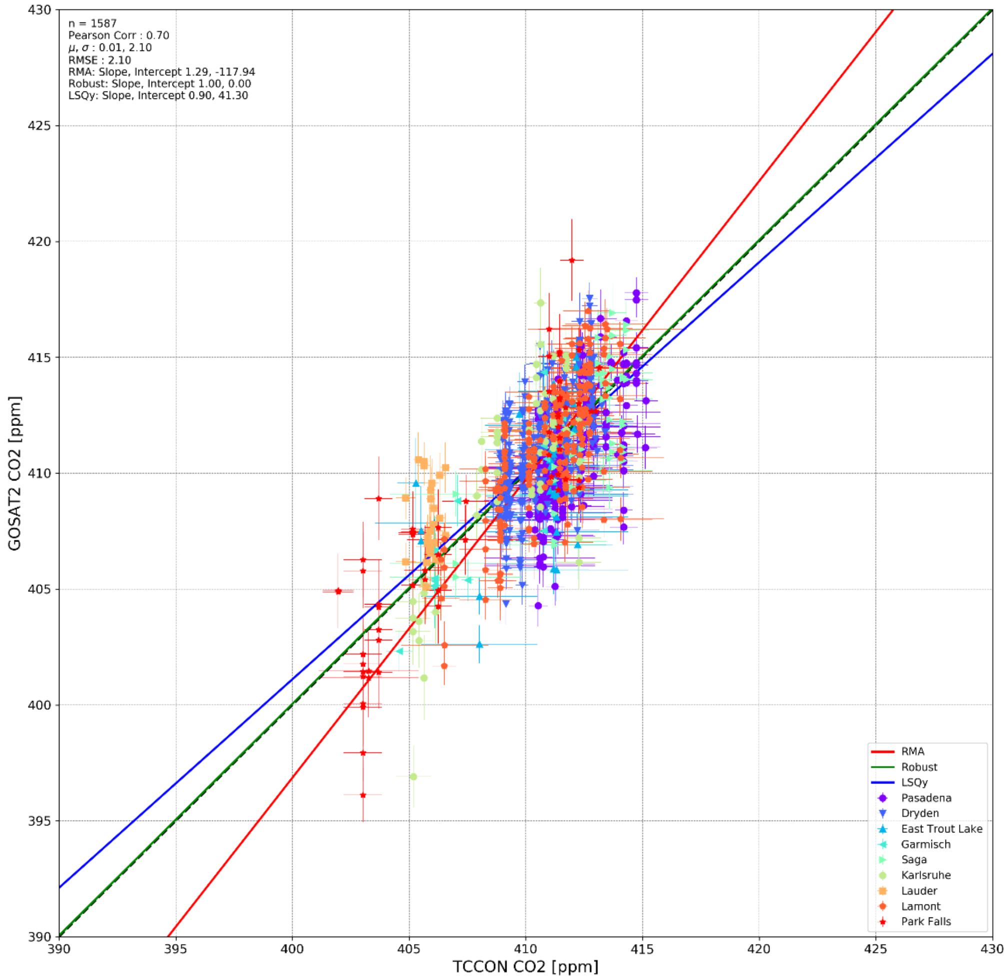

Figure 5-3-2: Correlation plot between all 1587 co-located CO2_GO2_SRFP and TCCON XCO_2 pairs coloured by site.

The error that comes out of the RemoTeC retrieval is just a purely statistical error on the radiance that has been propagated through the entire retrieval chain. In order to more accurately estimate the actual random error on the GOSAT-2 sounding, we applied the following procedure to obtain a scaling factor with which to scale our statistical error. We take the absolute difference of every co-located sounding and divide it by the retrieved statistical error corresponding to that sounding. We then average these values to obtain the average scaling factor by which to scale the retrieved statistical error to obtain a more correct estimate of the random error.

Based on the analysis, we obtain the following scaling factors for the SRFP XCO_2 product, 2.27 for the normal mode and 2.0 for the sunglint mode. Subsequently, we calculate the uncertainty ratio which is defined as the ratio of the mean value of the reported uncertainty

and the standard deviation of the difference to TCCON. We obtain uncertainty ratios of 0.44 for the normal mode and 0.50 for the sunglint mode.

5.3.2 Summary

The result of the validation of the CO2_GO2_SRFP dataset is given in **Table 5.3-2** and compared to the requirement. The mean estimate of the single-measurement precision is 2.10 ppm which exceeds the goal requirement but is within the breakthrough requirement of 3 ppm. The uncertainties provided by RemoTeC agree on average with the observed scatter of the data when compared to TCCON. The mean (global bias) of the GOSAT-2 XCO_2 retrieval is 0.01 ppm with a relative accuracy of 0.9 ppm which is larger than the requirement of 0.5 ppm. This can be attributed to the relatively small number of co-locations and short period of comparison. For comparison, we find a value of 0.7 ppm for GOSAT-1 over a multi-year period (2009-2019), while for the same 2019 period it is 1.0 ppm **/E3UBv1.1, 2020/**. We have not assessed the spatio-temporal bias or the drift due to the limited time period covered by the CO2_GO2_SRFP dataset.

Table 5.3-2: Summary validation of product CO2_GO2_SRFP by the data provider using TCCON ground-based reference data.

Product Quality Summary Table for Product: CO2_GO2_SRFP Level: 2, Version: v1, Time period covered: 2.2019 – 10.2019 Assessment: Data Provider (DP)			
Parameter [unit]	**Achieved performance**	**Requirement**	**Comments**
Single measurement precision (1-sigma) in [ppm]	2.10	< 8 (T) < 3 (B) < 1 (G)	Computed as standard deviation of the difference to TCCON
Uncertainty ratio [-]: Ratio reported uncertainty to standard deviation of satellite-TCCON difference	0.44 (0.50 sunglint)	-	No requirement but value close to unity expected for a high quality data product with reliable reported uncertainty.
Mean bias (global offset) [ppm]	0.01	-	No requirement but value close to zero expected for a high quality data product.
Accuracy: Relative systematic error [ppm]	Spatial: 0.90 Spatio-temporal: Not evaluated	< 0.5	Spatial: Computed as standard deviation of the biases at the various TCCON sites. Spatio-temporal: As "Spatial" but also considering seasonal biases.
Stability: Drift [ppm/year]	Not evaluated	< 0.5	Linear drift

5.4 Validation and intercomparison results for product CH4_S5P_WFMD

Validation results for XCH_4 retrieved from TROPOMI with the WFMDv1.2 algorithm **/Schneising et al., 2019/** are summarised in this section. The validation data set is the GGG2014 collection of the Total Carbon Column Observing Network (TCCON) (available from https://tccondata.org/). To ensure comparability, all TCCON sites use similar instrumentation (Bruker IFS 125HR) and a common retrieval algorithm. The TCCON data are tied to the WMO trace gas scale using airborne in situ measurements applying individual scaling factors for each species. The estimated TCCON accuracy (1σ) is about 3.5 ppb for XCH_4. From the validation with TCCON data at 24 TCCON sites, realistic error estimates of the satellite data are provided.

To compare the satellite data with TCCON quantitatively, it has to be taken into account that the sensitivities of the instruments differ from each other and that individual apriori profiles are used to determine the best estimate of the true atmospheric state, respectively. The first step is to correct for the apriori contribution to the smoothing equation by adjusting the measurements for a common apriori. Here we use the TCCON prior as the common apriori profile for all measurements:

$$\hat{c}_{adj} = \hat{c} + \frac{1}{m_0} \sum_l m_l \, (1 - A_l)(x^l_{a,T} - x^l_a)$$

In this equation, $\hat{c}$ represents the originally retrieved TROPOMI column-averaged dry air mole fraction, l is the index of the vertical layer, A_l the corresponding column averaging kernel of the TROPOMI algorithm, $\boldsymbol{x}_a$ and $\boldsymbol{x}_{a,T}$ the TROPOMI and TCCON apriori dry air mole fraction profiles. m_l is the mass of dry air determined from the dry air pressure difference between the upper and lower boundary of layer l and $m_0 = \sum_l m_l$ is the total mass of dry air. To minimise the smoothing error introduced by the averaging kernels we do not compare $\hat{c}_{adj}$ directly with the retrieved TCCON mole fractions $\hat{c}_T$ but rather with the adjusted expression

$$\hat{c}_{T,adj} = c_{a,T} + \left(\frac{\hat{c}_T}{c_{a,T}} - 1\right) \frac{1}{m_0} \sum_l m_l A_l x^l_{a,T}$$

Thereby, $c_{a,T}$ represents the TCCON apriori column-averaged dry air mole fraction associated with the apriori profile $\boldsymbol{x}_{a,T}$.

5.4.1 Detailed results

For the comparison a set of collocation criteria has been specified. The representativity is maximised by as strict as possible criteria while concurrently ensuring sufficient data for a sound and stable comparison. This trade-off is resolved by the following selection. The spatial collocation criterion requires the satellite measurements to lie within a radius of 100 km around the TCCON site and that the altitude difference is smaller than 250 m. The temporal collocation criterion is set to ±2 hours. For each satellite measurement within the collocation radius, all TCCON data meeting the temporal collocation criterion are averaged to obtain a unique satellite-TCCON data pair. This approach is consistent with the well-established methods used in previous GHG-CCI PVIRs.

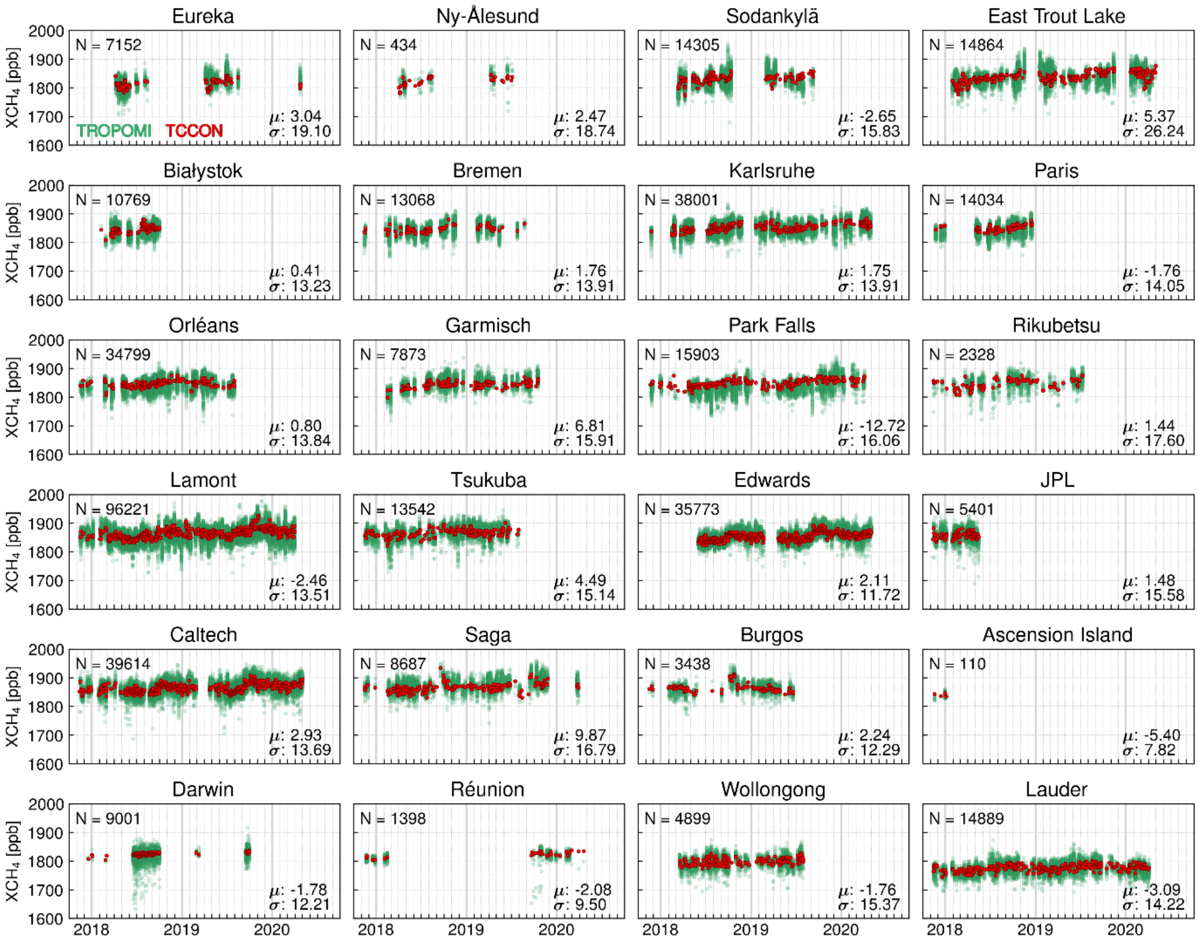

Figure 5.4-1: Comparison of the TROPOMI/WFMD v1.2 XCH_4 time series (green) with ground-based measurements from the TCCON (red). For each site, $\boldsymbol{N}$ is the number of collocations, $\boldsymbol{\mu}$ corresponds to the mean bias and $\boldsymbol{\sigma}$ to the scatter of the satellite data relative to TCCON in ppb.

The validation results are summarised in **Figure 5.4-1** including the mean bias μ and the scatter σ relative to TCCON for each site. As a consequence of the altitude representativity criterion, there are not enough collocations for a robust comparison at the mountain sites Zugspitze and Izaña. The parameter σ is estimated from Huber's Proposal-2 M-estimator, which is a well-established estimator of location and scale being robust against outliers of a normal distribution. This is an appropriate choice and preferred over the standard deviation, because one is interested in the actual single measurement precision without distortion of the results by a few outliers, which are rather attributed to systematic errors, e.g. due to residual clouds. As a consequence, outliers are fully included in the computation of the systematic error but get lower weight in the robust determination of the random error, which is interpreted as a measure of the repeatability of measurements.

It is also checked whether the respective site biases are sensitive to the selection of the spatial collocation radius, which is an indication of sources within the satellite collocation area with only marginal influence on the TCCON measurements itself. A considerable sensitivity was found for XCH_4 at Edwards. The collocation region intersects oil production areas in California's Central Valley (in contrast to Caltech and JPL, see **/Schneising et al., 2019/**) as well as the South Coast Air Basin (SoCAB), which has a well-known methane enhancement. As such nearby sources limit the representativity of affected satellite measurements, the collocation radius is reduced to 50 km for Edwards.

The results for the individual sites are condensed to the following parameters for the overall quality assessment of the satellite data: the global offset is defined as the mean of the local biases at the individual sites, the random error is the global scatter of the differences to TCCON after subtraction of the respective regional biases, and the spatial systematic error is the standard deviation of the local offsets relative to TCCON at the individual sites as a measure of the station-to-station biases. For XCH_4 the global offset amounts to 0.55 ppb, the random error is 14.28 ppb (16.02 ppb when using the standard deviation instead of Huber's Proposal-2 M-estimator), and the spatial systematic error is given by 4.36 ppb. The seasonal systematic error is defined as the standard deviation of the four overall seasonal offsets (using all sites combined after subtraction of the respective local offsets) relative to TCCON and amounts to 1.07 ppb. The spatio-temporal systematic error (defined as the the root-sum-square of the spatial and seasonal systematic errors) amounts to 4.50 ppb, which is on the order of the estimated (station-to-station) accuracy of the TCCON of about 3.5 ppb.

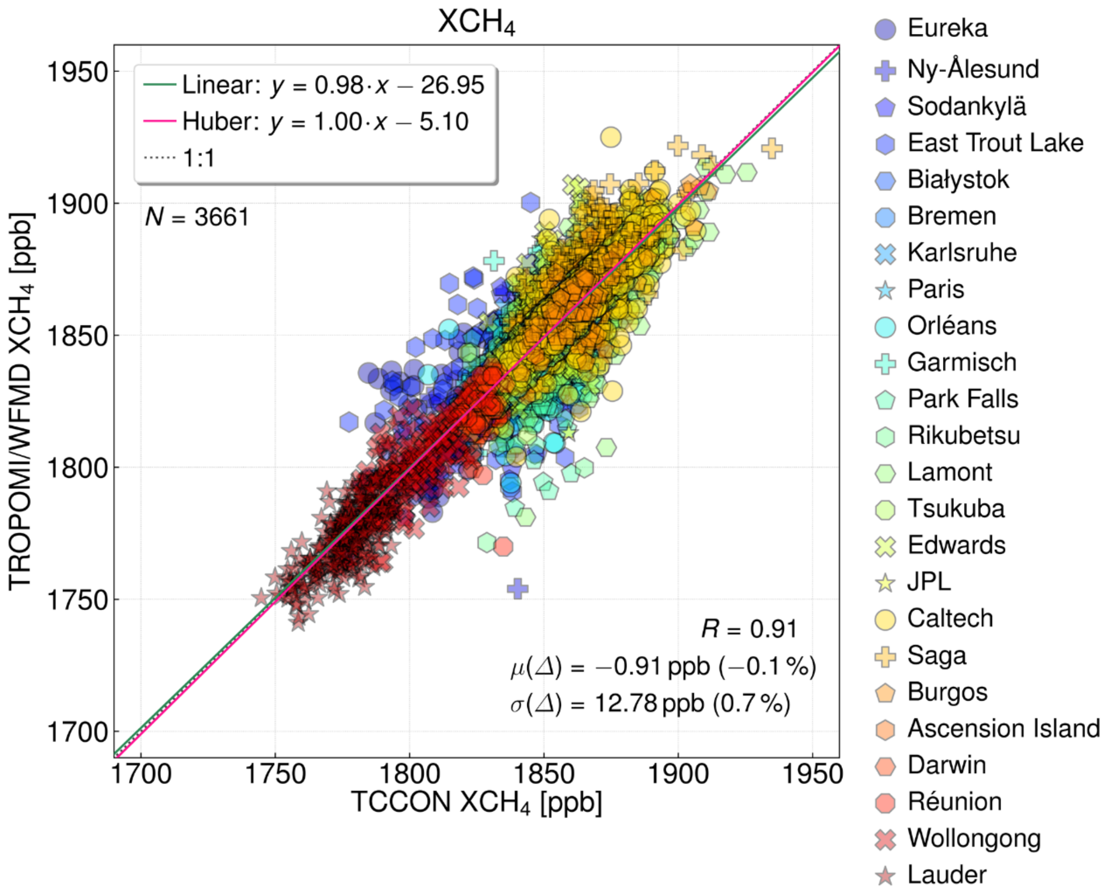

Figure 5.4-2: Comparison of the TROPOMI/WFMD data to the TCCON based on daily means. Specified are the linear regression results and the correlation of the data sets, as well as the mean and standard deviation of the difference. To analyse the impact of outliers, the regression is also performed for the Huber linear regression model, which is robust to outliers.

To further analyse how well the real temporal and spatial variations are captured by the TROPOMI data, **Figure 5.4-2** shows a comparison to TCCON based on daily means for days with more than three collocations. The obvious linear relationship with a high correlation of $R = 0.91$ underlines the typical good agreement of the satellite and validation data.

There are a few outliers where the satellite values are considerably lower than the TCCON values. These occasional instances are not site specific and can probably be ascribed to days with residual or partial cloud cover interfering with the satellite retrievals. Outliers with higher values compared to TCCON are dominated by collocations at high latitude sites during the first months of 2019 and may be attributable to Arctic polar vortex air potentially causing the following related issues: associated fronts of different air masses may complicate the identification of collocations near the vortex edge and/or the stratospheric part of the methane profiles may be largely affected by the polar vortex leading to a considerable deviation from the assumed apriori profile shapes. It is verified that the impact of outliers on the regression is marginal by repeating the fit with the Huber linear regression model, which is robust to outliers and provides similar results to the standard linear regression here.

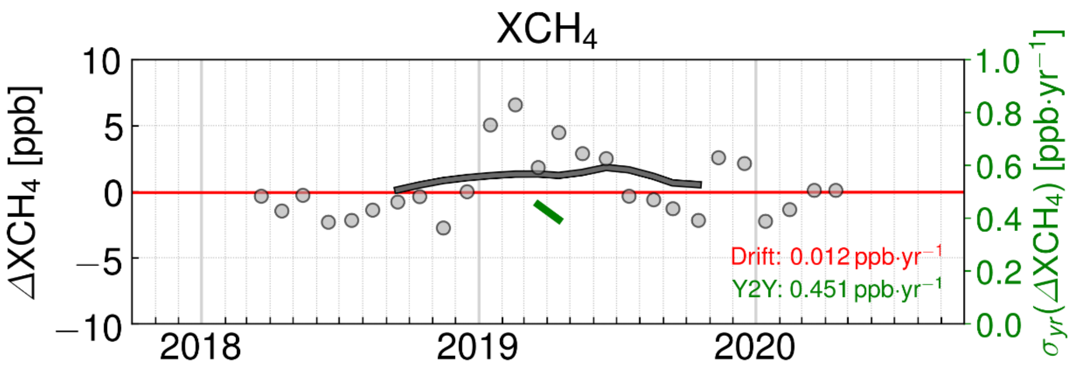

Figure 5.4-3: Long-term drift and year-to-year stability at TCCON sites.

To analyse the stability, we use comparisons with the TCCON since the start of the routine operations phase of Sentinel-5P to have sufficient data coverage. To assess the long-term drift stability, a robust Huber regression of the monthly mean differences relative to the reference (using all data combined after subtraction of the respective regional offsets) with time is used. The resulting stability estimate is 0.01 ppb/year (see red straight line in **Figure 5.4-3**).

The year-to-year stability allowing to detect potential jumps in the time series is defined in the following way: The one-year moving average of the differences relative to the reference (grey curve in **Figure 5.4-3**) is generated. For a given point in time t, let $\sigma_{yr}(t)$ be defined as the standard deviation of this deseasonalised difference within a one-year window around t (green curve in **Figure 5.4-3**). The year-to-year stability is then defined as the maximum of $\sigma_{yr}(t)$ over time, which amounts to 0.45 ppb/year here. Due to the moving average and the one-year moving standard deviation procedure, the green curve loses one year of data at the beginning and end of the time series. A longer time series of satellite data will allow a more sound and stable estimation of the year-to-year stability in the future.

The reported uncertainty of TROPOMI/WFMD v1.2 XCH_4 is estimated during the inversion procedure via error propagation from the uncorrelated spectral measurement errors given in the TROPOMI Level 1 files. The (unknown) pseudo-noise component determined by specific atmospheric parameters or instrumental features is not considered and thus the reported uncertainty σ is typically underestimating the actual uncertainty. To obtain a more realistic uncertainty estimate $\hat{\sigma}$, an error parameterisation based on a comparison of the reported uncertainty and measured scatter relative to the TCCON for different sites and seasons was introduced in the End-to-End ECV Uncertainty Budget (E3UB) and recommended to be applied in the Product User Guide (PUG) :

$$\hat{\sigma} = 1.37\sigma + 7.78\,ppb$$

After application of this uncertainty correction, the uncertainty ratio (reported uncertainty to measured scatter) improves from 0.32 to 0.98. This is close to 1 indicating a reliable estimation of the measurement uncertainties (when the correction is applied).

5.4.2 Summary

In summary, the natural XCH_4 variations are well captured by the satellite data. We find a single measurement precision of the TROPOMI data of about 0.8%, while the station-to-station accuracy of the satellite data (0.2%) is comparable to the TCCON.

The single measurement precision is below the breakthrough requirement and the uncertainty ratio is close to 1 after applying the uncertainty correction recommended in the Product User Guide. The accuracy also complies with the requirements and the mean bias is close to zero. The stability is well below the required value. **Table 5.4-1** presents an overview of the estimated data quality as obtained from comparisons with TCCON ground-based reference observations.

Table 5.4-1: Summary validation of product CH4_S5P_WFMD by the data provider using TCCON ground-based reference data.

Product Quality Summary Table for Product: CH4_S5P_WFMD Level: 2, Version: v1.2, Time period covered: 11.2017 – 04.2020 Assessment: Data Provider (DP)			
Parameter [unit]	**Achieved performance**	**Requirement**	**Comments**
Single measurement precision (1-sigma) in [ppb]	14.28	< 34 (T) < 17 (B) < 9 (G)	Computed as standard deviation of the difference to TCCON
Uncertainty ratio [-]: Ratio reported uncertainty to standard deviation of satellite-TCCON difference	0.98 After uncertainty correction recommended in the Product User Guide	-	No requirement but value close to unity expected for a high quality data product with reliable reported uncertainty.
Mean bias (global offset) [ppb]	0.55	-	No requirement but value close to zero expected for a high quality data product.
Accuracy: Relative systematic error [ppb]	Spatial: 4.36 Spatio-temporal: 4.50	< 10	Spatial: Computed as standard deviation of the biases at the various TCCON sites. Spatio-temporal: As "Spatial" but also considering seasonal biases.
Stability: Drift [ppb/year]	0.01	< 3	Linear drift

5.5 Validation and intercomparison results for product CH4_GO2_SRFP

The CH4_GO2_SRFP product is retrieved from GOSAT-2 TANSO-FTS SWIR spectra using the RemoTeC algorithm that has been jointly developed by SRON and KIT **/Butz et al., 2011; Schepers et al., 2012/**. The retrievals are performed globally for the time period between February and October 2019 and are evaluated against ground based TCCON observations.

5.5.1 Detailed results

To assess the quality of SRFP retrieval XCH_4 observations against ground based TCCON values, SRFP soundings are matched to TCCON observations spatially and temporally. GOSAT-2 observations are co-located with TCCON sites based on a square latitude and longitude region around each TCCON site (in ±2.5º latitude/longitude box). For the temporal co-location we select only the TCCON measurements whose observation time falls within ±2 hour of each GOSAT-2 observation time. The TCCON observations that match these criteria are averaged for each individual GOSAT-2 observation.

The co-location procedure matches 1587 points for the CH4_GO2_SRFP product. The comparions for each TCCON site is shown in **Figure 5.5-1**. The statistics (mean bias, standard deviation and Pearson correlation coefficient R) for each site are given in **Table 5.5-1**. The bias per site varies between -3.63 ppb at East Trout Lake to 4.18 ppb in Garmisch. The standard deviation of the station-to-station bias is 2.39 ppb, which mostly follows from the large bias found in the few Garmisch and East Trout Lake observations and the overall small number of compared values. Because of the short time period the number of data points and the temporal coverage varies greatly between sites.

The overall correlation between the GOSAT-2 and TCCON retrievals is given in **Figure 5.5-2**. We find a small mean overall bias of 0.09 ppb and an all-site Pearson correlation coefficient of 0.78 which, even for the small number of co-locations, points to a good comparison of GOSAT-2 and TCCON pairs. The all-site RMSE (mean of the standard deviation per site) of Δ (TCCON- GOSAT-2) is 13.03 ppb.

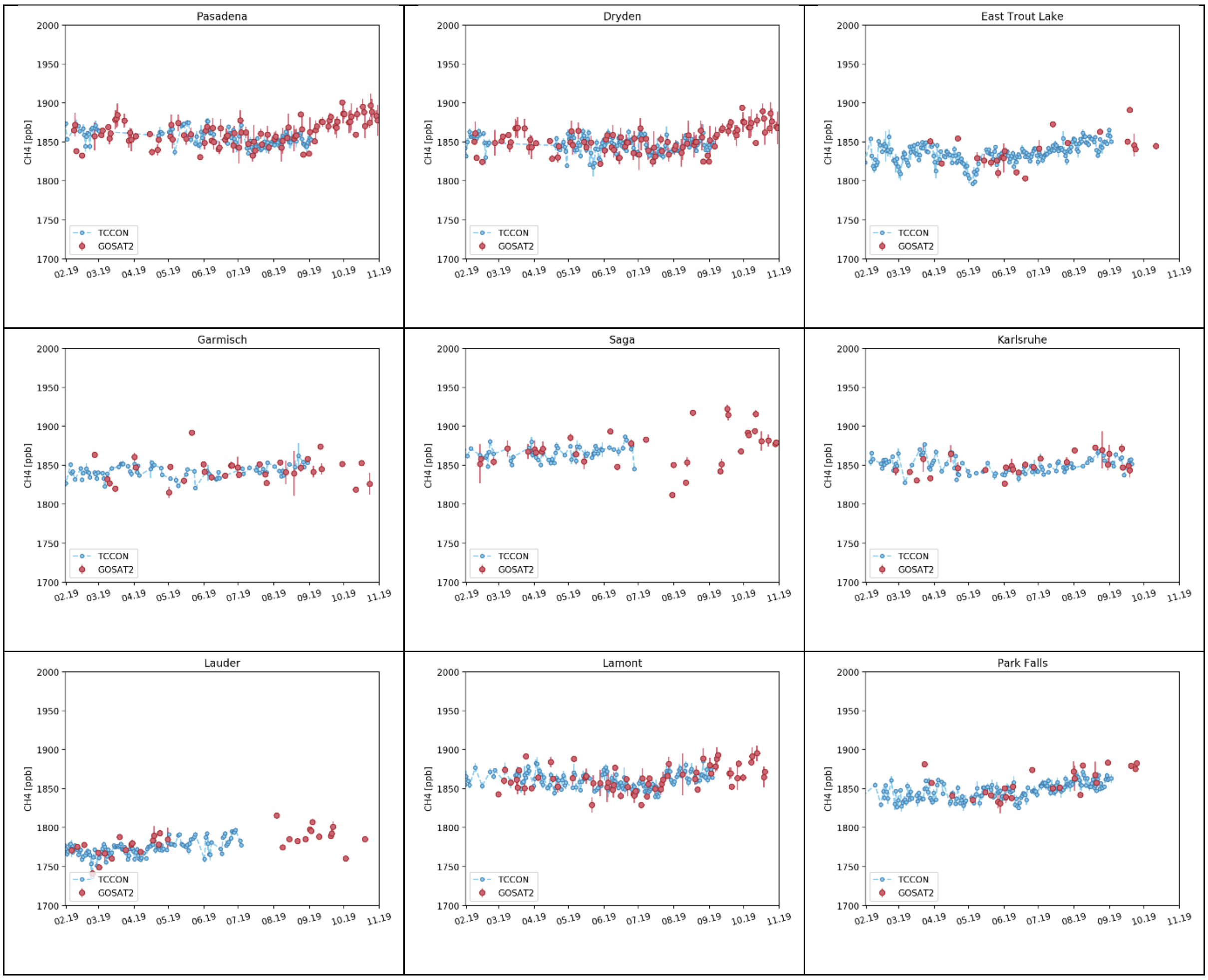

Figure 5.5-1: GOSAT-2 XCH_4 (CH4_GO2_SRFP, red) with co-located TCCON (blue) measurements at nine TCCON stations used for the validation for the period of February to October 2019.

Table 5.5-1: Overview of the estimated data quality as obtained from comparisons with TCCON ground-based reference observations per site. The bottom row details statistics for all sites, with all co-located points used for calculations. XCH_4 units are in ppb. The overall mean Δ and $\sigma\Delta$ is calculated by averaging of site values and R is calculated by all individual measurements. The mean of site means $\bar{\mu}$ and spatial accuracy $\sigma_{\bar{\mu}}$ are calculated by taking the mean and standard deviation of the site means. The mean standard deviation $\bar{\sigma}$ and standard deviation of the standard deviations $\sigma_{\bar{\sigma}}$ are calculated by taking the mean and the standard deviation of the site standard deviations.

Site	Mean Δ	$\sigma\Delta$	*R*	n obs.
Pasadena, USA	-2.03	15.70	0.47	337
Dryden, USA	0.22	15.36	0.40	448
East Trout Lake, Canada	-3.63	17.31	0.38	62
Garmisch, Germany	4.18	8.41	0.75	28
Saga, Japan	2.18	12.53	0.37	98
Karlsruhe, Germany	-1.31	11.17	0.58	115
Lauder, New Zealand	2.63	10.41	0.74	52
Lamont, USA	1.12	13.18	0.58	344
Park Falls, USA	2.43	13.24	0.64	103
All observations	0.09	14.36	0.78	1587
	$\bar{\mu}$	$\sigma_{\bar{\mu}}$	$\bar{\sigma}$	$\sigma_{\bar{\sigma}}$
Mean of sites	0.64	2.39	13.03	2.64

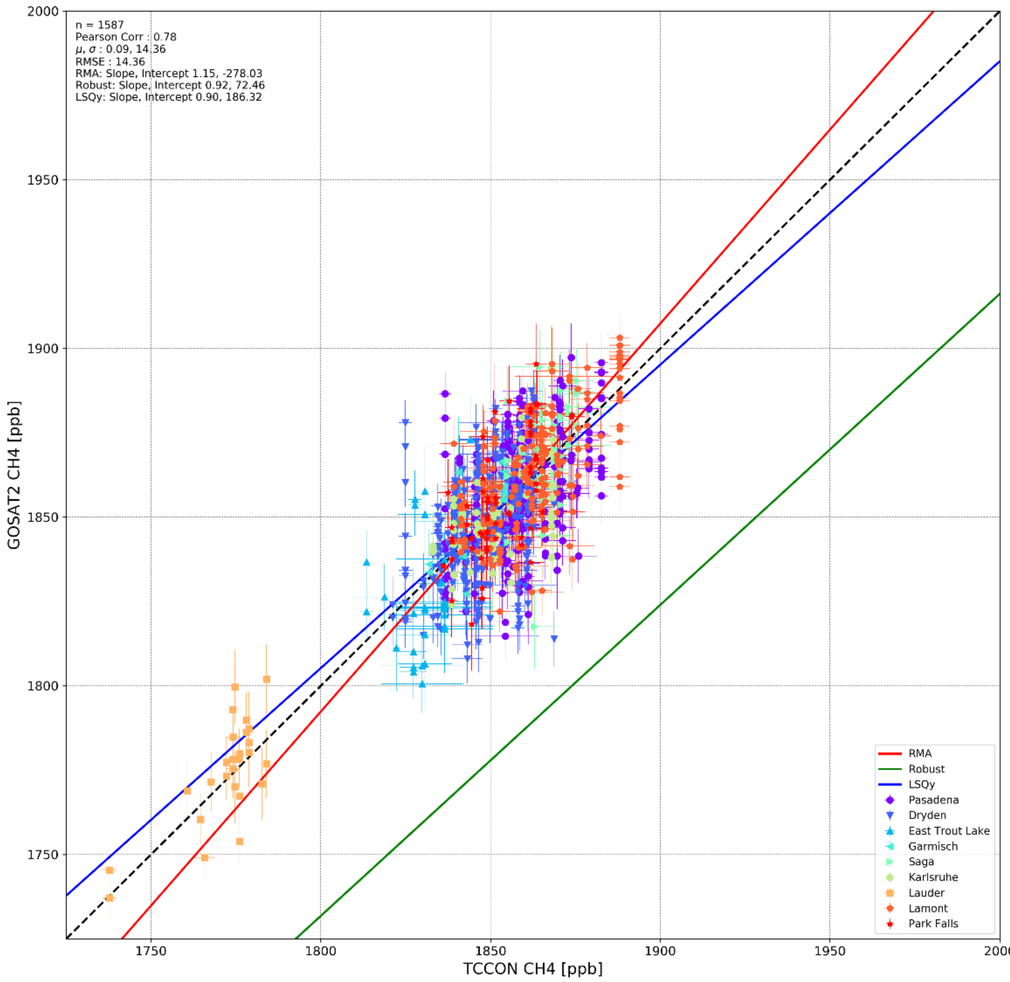

Figure 5.5-2: Correlation plot between all 1587 co-located CH4_GO2_SRFP and TCCON XCH_4 pairs coloured by site.

The error that comes out of the RemoTeC retrieval is just a purely statistical error on the radiance that has been propagated through the entire retrieval chain. In order to more accurately estimate the actual random error on the GOSAT-2 sounding, we applied the following procedure to obtain a scaling factor with which to scale our statistical error. We take the absolute difference of every co-located sounding and divide it by the retrieved statistical error corresponding to that sounding. We then average these values to obtain the average scaling factor by which to scale the retrieved statistical error to obtain a more correct estimate of the random error.

Based on the analysis, we obtain the following scaling factors for the SRFP XCH_4 product, 1.44 for the normal mode and 1.38 for the sunglint mode. Subsequently, we calculate the uncertainty ratio which is defined as the ratio of the mean value of the reported uncertainty

and the standard deviation of the difference to TCCON. We obtain uncertainty ratios of 0.69 for the normal mode and 0.72 for the sunglint mode.

5.5.2 Summary

The result of the validation of the CH4_GO2_SRFP dataset is given in **Table 5.5-2** and compared to the requirement. The mean estimate of the single-measurement precision is 14.36 ppb which exceeds the goal requirement but is within the breakthrough requirement of 17 ppb. The uncertainties provided by RemoTeC agree on average with the observed scatter of the data when compared to TCCON. The mean, global bias of the GOSAT-2 XCH_4 retrieval is 0.09 ppb with a relative accuracy of 2.39 ppb which is smaller than the requirement of 10 ppb. We have not assessed the spatio-temporal bias or the drift due to the limited time period covered by the CH4_GO2_SRFP dataset.

Table 5.5-2: Summary validation of product CH4_GO2_SRFP by the data provider using TCCON ground-based reference data.

Product Quality Summary Table for Product: CH4_GO2_SRFP Level: 2, Version: v1, Time period covered: 2.2019 – 10.2019 Assessment: Data Provider (DP)			
Parameter [unit]	**Achieved performance**	**Requirement**	**Comments**
Single measurement precision (1-sigma) in [ppb]	14.36	< 34 (T) < 17 (B) < 9 (G)	Computed as standard deviation of the difference to TCCON
Uncertainty ratio [-]: Ratio reported uncertainty to standard deviation of satellite-TCCON difference	0.69 (0.72 glint)	-	No requirement but value close to unity expected for a high quality data product with reliable reported uncertainty.
Mean bias (global offset) [ppb]	0.09	-	No requirement but value close to zero expected for a high quality data product.
Accuracy: Relative systematic error [ppb]	Spatial: 2.39 Spatio-temporal: Not evaluated	< 10	Spatial: Computed as standard deviation of the biases at the various TCCON sites. Spatio-temporal: As "Spatial" but also considering seasonal biases.
Stability: Drift [ppb/year]	Not evaluated (1-sigma)	< 3	Linear drift

5.6 Validation and intercomparison results for product CH4_GO2_SRPR

The CH4_GO2_SRPR product is retrieved from GOSAT-2 TANSO-FTS SWIR spectra using the RemoTeC algorithm that has been jointly developed by SRON and KIT **/Butz et al., 2011; Schepers et al., 2012/**. The retrievals are performed globally for the time period between February and October 2019 and are evaluated against ground based TCCON observations.

5.6.1 Detailed results

To assess the quality of SRPR retrieval XCH_4 observations against ground based TCCON values, SRPR soundings are matched to TCCON observations spatially and temporally. GOSAT-2 observations are co-located with TCCON sites based on a square latitude and longitude region around each TCCON site (in ±2.5º latitude/longitude box). For the temporal co-location we select only the TCCON measurements whose observation time falls within ±2 hour of each GOSAT-2 observation time. The TCCON observations that match these criteria are averaged for each individual GOSAT-2 observation.

The co-location procedure matches 2642 points for the CH4_GO2_SRPR product. The comparions for each TCCON site is shown in **Figure 5.6-1**. The statistics (mean bias, standard deviation and Pearson correlation coefficient R) for each site is given in **Table 5.6-1**. The bias per site varies between -5.61 ppb for Pasadena to 8.48 ppb in Saga. The standard deviation of the station-to-station bias is 4.24 ppb, which mostly follows from the opposite large bias found in the Pasadena and Saga observations and the overall small number of compared values. Because of the short time period the number of data points and the temporal coverage varies greatly between sites.

The overall correlation between the GOSAT-2 and TCCON retrievals is given in **Figure 5.6-2**. We find a small mean overall bias of 0.10 ppb and an all-site Pearson correlation coefficient of 0.76 which, even for the small number of co-locations, points to a good comparison of GOSAT-2 and TCCON pairs. The all-site RMSE (mean of the standard deviation per site) of Δ (TCCON- GOSAT-2) is 15.32 ppb.

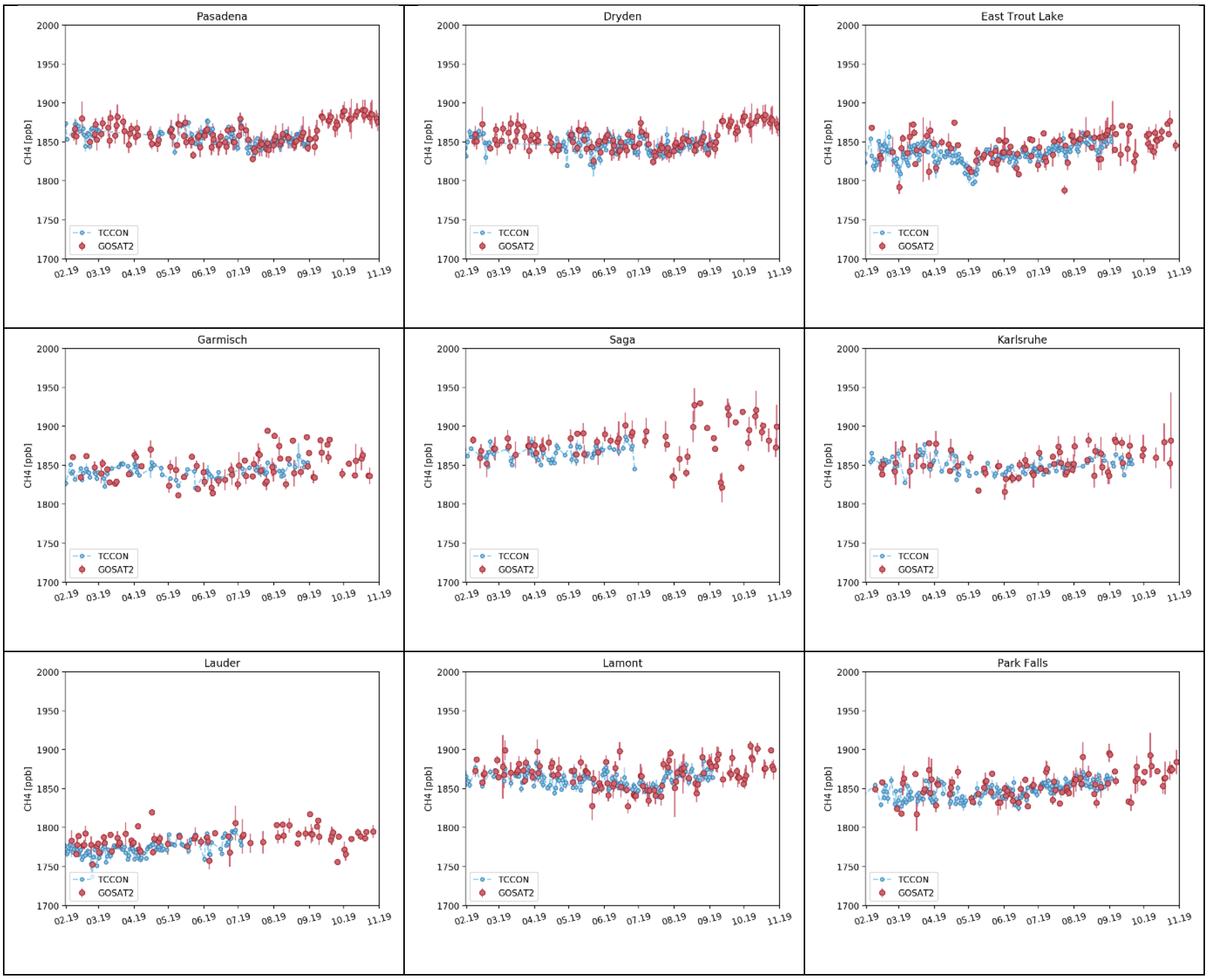

Figure 5.6-1: GOSAT-2 XCH_4 (CH4_GO2_SRPR, red) with co-located TCCON (blue) measurements at nine TCCON stations used for the validation for the period of February to October 2019.

Table 5.6-1: Overview of the estimated data quality as obtained from comparisons with TCCON ground-based reference observations per site. The bottom row details statistics for all sites, with all co-located points used for calculations. XCH_4 units are in ppb. The overall mean Δ and $\sigma\Delta$ is calculated by averaging of site values and R is calculated by all individual measurements. The mean of site means $\bar{\mu}$ and spatial accuracy $\sigma_{\bar{\mu}}$ are calculated by taking the mean and standard deviation of the site means. The mean standard deviation $\bar{\sigma}$ and standard deviation of the standard deviations $\sigma_{\bar{\sigma}}$ are calculated by taking the mean and the standard deviation of the site standard deviations.

Site	Mean Δ	$\sigma\Delta$	*R*	n obs.
Pasadena, USA	-5.61	13.12	0.53	545
Dryden, USA	-0.31	14.59	0.37	732
East Trout Lake, Canada	4.99	17.63	0.53	297
Garmisch, Germany	4.68	17.15	0.45	35
Saga, Japan	8.48	14.53	0.50	184
Karlsruhe, Germany	-2.51	17.12	0.41	115
Lauder, New Zealand	5.70	12.38	0.56	99
Lamont, USA	-0.22	14.70	0.65	400
Park Falls, USA	0.69	16.69	0.36	235
All observations	0.10	15.50	0.76	2642
	$\bar{\mu}$	$\sigma_{\bar{\mu}}$	$\bar{\sigma}$	$\sigma_{\bar{\sigma}}$
Mean of sites	1.76	4.24	15.32	1.79

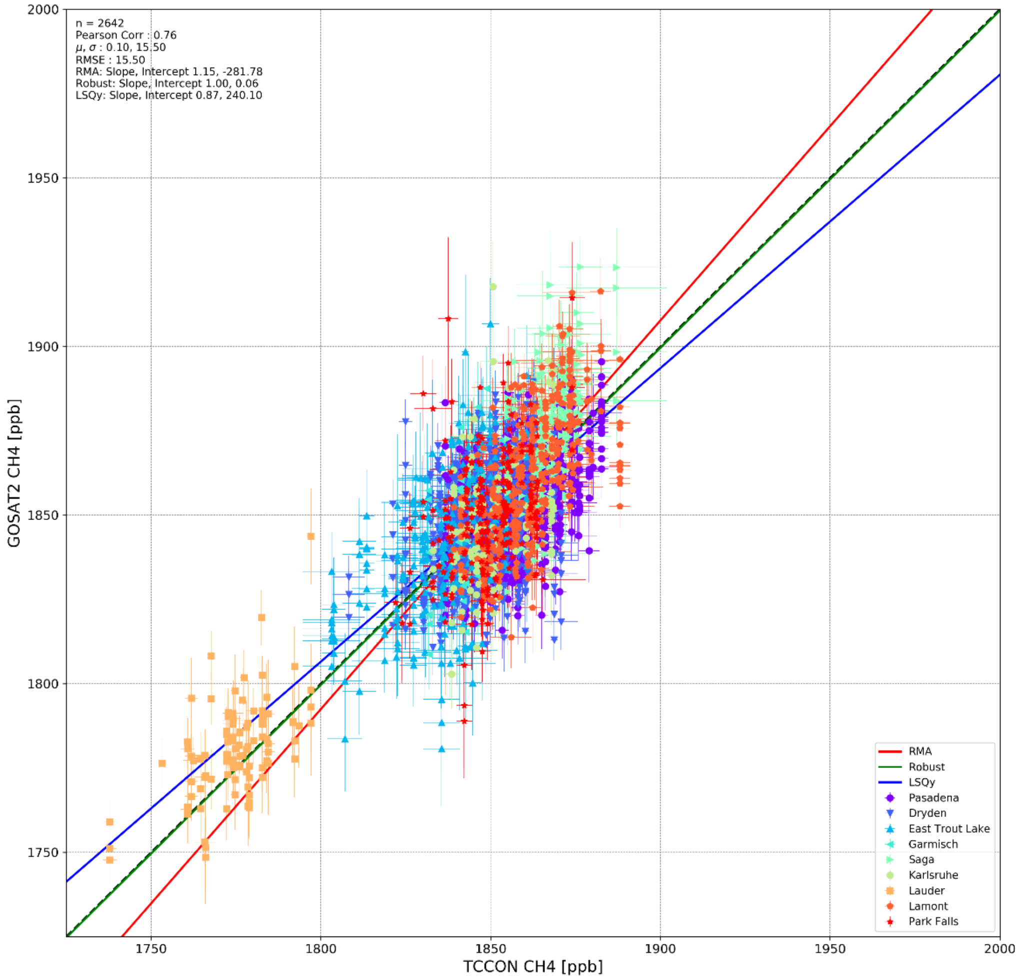

Figure 5.6-2: Correlation plot between all 2642 co-located CH4_GO2_SRPR and TCCON XCH_4 pairs coloured by site.

The error that comes out of the RemoTeC retrieval is just a purely statistical error on the radiance that has been propagated through the entire retrieval chain. In order to more accurately estimate the actual random error on the GOSAT-2 sounding, we applied the following procedure to obtain a scaling factor with which to scale our statistical error. We take the absolute difference of every co-located sounding and divide it by the retrieved statistical error corresponding to that sounding. We then average these values to obtain the average scaling factor by which to scale the retrieved statistical error to obtain a more correct estimate of the random error.

Based on the analysis, we obtain the following scaling factors for the SRPR XCH_4 product, 1.71 for the normal mode and 1.36 for the sunglint mode. Subsequently, we calculate the uncertainty ratio which is defined as the ratio of the mean value of the reported uncertainty

and the standard deviation of the difference to TCCON. We obtain uncertainty ratios of 0.58 for the normal mode and 0.74 for the sunglint mode.

5.6.2 Summary

The result of the validation of the CH4_GO2_SRPR dataset is given in **Table 5.6-2** and compared to the requirement. The mean estimate of the single-measurement precision is 15.50 ppb which exceeds the goal requirement but is within the breakthrough requirement of 17 ppb. The uncertainties provided by RemoTeC agree on average with the observed scatter of the data when compared to TCCON. The mean, global bias of the GOSAT-2 XCH_4 retrieval is 0.10 ppb with a relative accuracy of 4.24 ppb which is smaller than the requirement of 10 ppb. We have not assessed the spatio-temporal bias or the drift due to the limited time period covered by the CH4_GO2_SRPR dataset.

Table 5.6-2: Summary validation of product CH4_GO2_SRPR by the data provider using TCCON ground-based reference data.

Product Quality Summary Table for Product: CH4_GO2_SRPR Level: 2, Version: v1, Time period covered: 2.2019 – 10.2019 Assessment: Data Provider (DP)			
Parameter [unit]	**Achieved performance**	**Requirement**	**Comments**
Single measurement precision (1-sigma) in [ppb]	15.50	< 34 (T) < 17 (B) < 9 (G)	Computed as standard deviation of the difference to TCCON
Uncertainty ratio [-]: Ratio reported uncertainty to standard deviation of satellite-TCCON difference	0.58 (0.74 glint)	-	No requirement but value close to unity expected for a high quality data product with reliable reported uncertainty.
Mean bias (global offset) [ppb]	0.10	-	No requirement but value close to zero expected for a high quality data product.
Accuracy: Relative systematic error [ppb]	Spatial: 4.24 Spatio-temporal: Not evaluated	< 10	Spatial: Computed as standard deviation of the biases at the various TCCON sites. Spatio-temporal: As "Spatial" but also considering seasonal biases.
Stability: Drift [ppb/year]	Not evaluated (1-sigma)	< 3	Linear drift

6 References

/Aben et al., 2019/ Aben, I., L. Wu, O. Hasekamp, M. Buchwitz, M. Reuter, O. Schneising, H. Boesch, D. Yang, ESA Climate Change Initiative "Plus" (CCI+) System Specification Document (SSD) for the Essential Climate Variable (ECV) Greenhouse Gases (GHG): XCO_2 and/or XCH_4 from OCO-2, TanSat, Sentinel-5-Precursor and GOSAT-2, Version 1.0, 26-August-2019, pp. 33, 2019.

/Ackermann et al., 2010/ Ackerman, S.; Frey, R.; Strabala, K.; Liu, Y.; Gumley, L.; Baum, B.; Menzel, P. Discriminating Clear-Sky from Cloud with MODIS—Algorithm Theoretical Basis Document (MOD35); Version 6.1; Cooperative Institute for Meteorological Satellite Studies, University ofWisconsin—Madison: Madison, WI, USA, 2010.

/ATBDv1 FOCAL, 2019/ Reuter et al.: Algorithm Theoretical Basis Document Version 1 (ATBDv1) - Retrieval of XCO_2 from the OCO-2 satellite using the Fast Atmospheric Trace Gas Retrieval (FOCAL), ESA GHG-CCI project, 2019.

/Boesch et al., 2011/ Boesch, H., Baker, D., Connor, B., Crisp, D., and Miller, C.: Global characterization of CO_2 column retrievals from shortwave-infrared satellite observations of the Orbiting Carbon Observatory-2 mission, Remote Sens., 3, 270–304, doi:10.3390/rs3020270, 2011.

/Butz et al., 2009/ Butz, André, Otto P. Hasekamp, Christian Frankenberg, and Ilse Aben, "Retrievals of atmospheric CO_2 from simulated space-borne measurements of backscattered near-infrared sunlight: accounting for aerosol effects," Appl. Opt. 48, 3322-3336 (2009)

/Butz et al., 2010/ Butz, André, Otto P. Hasekamp, Christian Frankenberg, Jerome Vidot, and Ilse Aben, ",CH4 retrievals from space-based solar backscatter measurements: Performance evaluation against simulated aerosol and cirrus loaded scenes" , J. Geophys. Res., 115, 24,302, doi:10.1029/2010JD014514, 2010.

/Butz et al., 2011/ Butz, A., S. Guerlet, O. Hasekamp, et al., Toward accurate CO_2 and CH_4 observations from GOSAT, Geophys. Res. Lett., Geophys. Res. Lett., doi:10.1029/2011GL047888, 2011.

/CECRv3 BESD, 2017/ M. Reuter, O. Schneising, M. Buchwitz, J. Heymann: Comprehensive Error Characterisation Report: BESD full-physics retrieval algorithm for XCO_2 for the Essential Climate Variable (ECV) Greenhouse Gases (GHG), ESA GHG-CCI project, 2017.

/Eldering et al., 2015/ Eldering, A.; Pollock, R.; Lee, R.; Rosenberg, R.; Oyafuso, F.; Crisp, D.; Chapsky, L.; Granat, R. Orbiting Carbon Observatory-2 (OCO-2) - LEVEL 1B - Algorithm Theoretical Basis; Version 1.2 Rev 1; National Aeronautics and Space Administration, Jet Propulsion Laboratory, California Institute of Technology: Pasadena, CA, USA, 2015

/Frankenberg et al., 2005/ Frankenberg, C., Meirink, J.F., van Weele, M., Platt, U., Wagner, T. (2005), Assessing methane emissions from global space-borne obseravtions, Science, ., doi:10.1126/science.1106644

/Frankenberg et al., 2011/ Frankenberg, C., Aben, I., Bergamaschi, P., et al. (2011), Global column-averaged methane mixing ratios from 2003 to 2009 as derived from SCIAMACHY: Trends and variability, J. Geophys. Res., doi:10.1029/2010JD014849.

/GCOS-154/ Global Climate Observing System (GCOS), SYSTEMATIC OBSERVATION REQUIREMENTS FOR SATELLITE-BASED PRODUCTS FOR CLIMATE, Supplemental details to the satellite-based component of the "Implementation Plan for the Global Observing System for Climate in Support of the UNFCCC (2010 update)", Prepared by World Meteorological Organization (WMO), Intergovernmental Oceanographic Commission, United Nations Environment Programme (UNEP), International Council for Science, Doc.: GCOS 154, link: http://cci.esa.int/sites/default/files/gcos-154.pdf, 2011.

/GCOS-195/ Status of the Global Observing System for Climate. GCOS-195. Link: https://library.wmo.int/pmb_ged/gcos_195_en.pdf, 2015.

/GCOS-200/ The Global Observing System for Climate: Implementation Needs, GCOS 2016 Implementation Plan, World Meteorological Organization (WMO), GCOS-200 (GOOS-214), pp. 325, link: https://library.wmo.int/opac/doc_num.php?explnum_id=3417, 2016.

/HITRAN2016/ Gordon et al., The HITRAN2016 molecular spectroscopic database, J. Quant. Spectrosc. Radiat. Transfer, 203, 3-69, 2017.

/Kuruz, 1994/ Kurucz, H.L. The Solar Spectrum: Atlases and Line Identifications, Workshop on Laboratory and Astronomical High Resolution Spectra. Astronomical Society of the Pacific Conference Series. In Proceedings of the ASP Conference, Brussels, Belgium, 29 August–2 September 1994; pp. 17–31

/Langerock et al., 2015/ Langerock, B., De Mazière, M., Hendrick, F., Vigouroux, C., Desmet, F., Dils, B., and Niemeijer, S.: Description of algorithms for co-locating and comparing gridded model data with remote-sensing observations, Geosci. Model Dev., 8, 911–921, https://doi.org/10.5194/gmd-8-911-2015, 2015.

/Lunneborg, 2020/ Lunneborg, C. E. Data analysis by resampling: Concepts and applications. PacificGrove, CA: Duxbury, 2000

/O'Dell et al., 2012/ O'Dell, C.W.; Connor, B.; Bösch, H.; O'Brien, D.; Frankenberg, C.; Castano, R.; Christi, M.; Eldering, D.; Fisher, B.; Gunson, M.; et al. The ACOS CO_2 retrieval algorithm - Part 1: Description and validation against synthetic observations. Atmos. Meas. Tech. 2012, 5, 99–121

/Parker et al., 2011/ Parker, R., Boesch, H, Cogan, A., et al. (2011), Methane Observations from the Greenhouse gases Observing SATellite: Comparison to ground-based TCCON data and Model Calculations, Geophys. Res. Lett., doi:10.1029/2011GL047871.

/PUGS, 2019/ Buchwitz, M., Aben, I., J., Armante, R., Boesch, H., Crevoisier, C., Di Noia, A., Hasekamp, O. P., Reuter, M., Schneising-Weigel, O., Wu, L.., Product User Guide and Specification (PUGS) – Main document for Greenhouse Gas (GHG: CO_2 & CH_4) data set CDR 3 (2003-2018), C3S project C3S_312b_Lot2_DLR, v3.1, 97 pages, https://www.iup.uni-bremen.de/carbon_ghg/docs/C3S/CDR3_2003-2018/PUGS/C3S_D312b_Lot2.3.2.3-v1.0_PUGS-GHG_MAIN_v3.1.pdf, 2019.

/PVIR v5, 2017/ Product Validation and Intercomparison Report" (PVIR), ESA Climate Change Initiative (CCI) GHG-CCI project, Version 5, 9 Feb 2017, 2017.

/PVIR GHG-CCI+ v1.1, 2020/ ESA Climate Change Initiative "Plus" (CCI+) Product Validation and Intercomparison Report (PVIR) for the Essential Climate Variable (ECV) Greenhouse Gases (GHG): XCO2 and/or XCH4 from OCO-2, TanSat, Sentinel-5-Precursor and GOSAT-2,13 Mar 2020, version 1.1, pp. 74, 2020.

/Reuter et al., 2011/ Reuter, M., Bovensmann, H., Buchwitz, M., Burrows, J. P., Connor, B. J., Deutscher, N. M., Griffith, D.W. T., Heymann, J., Keppel-Aleks, G., Messerschmidt, J., and et al.: Retrieval of atmospheric CO_2 with enhanced accuracy and precision from SCIAMACHY: Validation with FTS measurements and comparison with model results., Journal of Geophysical Research, 116, doi:10.1029/2010JD015047, URL http://dx.doi.org/10.1029/2010JD015047, 2011.

/Reuter et al., 2012/ M. Reuter, M. Buchwitz, O. Schneising, F. Hase, J. Heymann, S. Guerlet, A.J. Cogan, H. Bovensmann, J.P. Burrows: A simple empirical model estimating atmospheric CO_2 background concentrations, Atmospheric Measurement Techniques, 5, 1349-1357, 2012.

/Reuter et al., 2013/ Reuter, M., H. Boesch, H. Bovensmann, A. Bril, M. Buchwitz, A. Butz, J. P. Burrows, C. W. O'Dell, S. Guerlet, O. Hasekamp, J. Heymann, N. Kikuchi, S. Oshchepkov, R. Parker, S. Pfeifer, O. Schneising, T. Yokota, and Y. Yoshida, A joint effort to deliver satellite retrieved atmospheric CO_2 concentrations for surface flux inversions: the ensemble median algorithm EMMA, Atmos. Chem. Phys., 13, 1771-1780, 2013.

/Reuter et al., 2017a/ M.Reuter, M.Buchwitz, O.Schneising, S.Noël, V.Rozanov, H.Bovensmann and J.P.Burrows: A Fast Atmospheric Trace Gas Retrieval for Hyperspectral Instruments Approximating Multiple Scattering - Part 1: Radiative Transfer and a Potential OCO-2 XCO_2 Retrieval Setup, Remote Sensing, 9(11), 1159; doi:10.3390/rs9111159, 2017.

/Reuter et al., 2017b/ M.Reuter, M.Buchwitz, O.Schneising, S.Noël, H.Bovensmann and J.P.Burrows: A Fast Atmospheric Trace Gas Retrieval for Hyperspectral Instruments Approximating Multiple Scattering - Part 2: Application to XCO_2 Retrievals from OCO-2, Remote Sensing, 9(11), 1102; doi:10.3390/rs9111102, 2017.

/Rodgers, 2000/ Rodgers, C. D.: Inverse Methods for Atmospheric Sounding: Theory and Practice, World Scientific Publishing, 2000.

/**Schepers et al., 2012/** Schepers, D., Guerlet, S., Butz, A., et al. (2012), Methane retrievals from Greenhouse Gases Observing Satellite (GOSAT) shortwave infrared measurements: Performance comparison of proxy and physics retrieval algorithms, *J. Geophys. Res*., 117, D10307, doi:10.1029/2012JD017549.

/Schneising et al., 2011/ Schneising, O., Buchwitz, M., Reuter, M., et al., Long-term analysis of carbon dioxide and methane column-averaged mole fractions retrieved from SCIAMACHY, Atmos. Chem. Phys., 11, 2881-2892, 2011.

/Schneising et al., 2012/ Schneising, O., Bergamaschi, P., Bovensmann, H., et al, Atmospheric greenhouse gases retrieved from SCIAMACHY: comparison to ground-based FTS measurements and model results, Atmos. Chem. Phys., 12, 1527-1540, 2012.

/Schneising et al., 2019/ Schneising, O., Buchwitz, M., Reuter, M., Bovensmann, H., Burrows, J. P., Borsdorff, T., Deutscher, N. M., Feist, D. G., Griffith, D. W. T., Hase, F., Hermans, C., Iraci, L. T., Kivi, R., Landgraf, J., Morino, I., Notholt, J., Petri, C., Pollard, D. F., Roche, S., Shiomi, K., Strong, K., Sussmann, R., Velazco, V. A., Warneke, T., and Wunch, D.: A scientific algorithm to simultaneously retrieve carbon monoxide and methane from TROPOMI onboard Sentinel-5 Precursor, Atmos. Meas. Tech., 12, 6771-6802, https://doi.org/10.5194/amt-12-6771-2019, 2019.

/Stammes, 2002/ Stammes, P. OMI Algorithm Theoretical Basis Document, Volume III, Clouds, Aerosols, and Surface UV Irradiance (ATBD-OMI-03); Royal Netherlands Meteorological Institute (KNMI): De Bilt, The Netherlands, 2002

/Thompson et al., 2012/ Thompson, D.R.; Chris Benner, D.; Brown, L.R.; Crisp, D.; Malathy Devi, V.; Jiang, Y.; Natraj, V.; Oyafuso, F.; Sung, K.; Wunch, D.; et al. Atmospheric validation of high accuracy CO_2 absorption coefficients for the OCO-2 mission. J. Quant. Spectrosc. Radiat. Transf. 2012, 113, 2265–2276

/URDv2.1/ User Requirements Document (URD), ESA Climate Change Initiative (CCI) GHG-CCI project, Version 2.1, 38 pages, 19-Oct-2016, http://cci.esa.int/sites/default/files/URDv2.1_GHG-CCI_Final.pdf, 2016.

/Wunch et al., 2010/ Wunch, D., Toon, G. C., Wennberg, P. O., Wofsy, S. C., Stephens, B. B., Fischer, M. L., Uchino, O., Abshire, J. B., Bernath, P., Biraud, S. C., Blavier, J.-F. L., Boone, C., Bowman, K. P., Browell, E. V., Campos, T., Connor, B. J., Daube, B. C., Deutscher, N. M., Diao, M., Elkins, J. W., Gerbig, C., Gottlieb, E., Griffith, D. W. T., Hurst, D. F., Jiménez, R., Keppel-Aleks, G., Kort, E. A., Macatangay, R., Machida, T., Matsueda, H., Moore, F., Morino, I., Park, S., Robinson, J., Roehl, C. M., Sawa, Y., Sherlock, V., Sweeney, C., Tanaka, T., and Zondlo, M. A.: Calibration of the Total Carbon Column Observing Network using aircraft profile data, Atmospheric Measurement Techniques, 3, 1351–1362, doi:10.5194/amt-3-1351-2010, URL http://www.atmos-meas-tech.net/3/1351/2010/, 2010.

/Wunch et al., 2011/ Wunch, D., Toon, G. C., Blavier, J.-F. L., Washenfelder, R. A., Notholt, J., Connor, B. J., Griffith, D. W. T., Sherlock, V., and Wennberg, P. O.: The Total Carbon Column Observing Network (TCCON), Philosophical Transactions of the Royal Society of London, Series A: Mathematical, Physical and Engineering Sciences, 369, 2087–2112, doi:10.1098/rsta.2010.0240, 2011.

7 List of Acronyms and Abbreviations

Abbreviation	Meaning
AAI	Absorbing Aerosol Index
ACA	Additional Constraints Algorithm
AOD	Aerosol Optical Depth
AOT	Aerosol Optical Thickness
ATBD	Algorithm Theoretical Basis Document
BIRA-IASB	Royal Belgian Institute for Space Aeronomy
CCI	Climate Change Initiative
CDR	Climate Data Record
CMUG	Climate Modelling User Group (of ESA's CCI)
COD	Cloud Optical Depth
CRG	Climate Research Group
D/B	Data base
DOAS	Differential Optical Absorption Spectroscopy
DPM	Detailed Processing Model
EC	European Commission
ECA	ECV Core Algorithm
ECMWF	European Centre for Medium Range Weather Forecasting
ECV	Essential Climate Variable
EO	Earth Observation
ESA	European Space Agency
ESM	Earth System Model
FCDR	Fundamental Climate Data Record
FOCAL	Fast atmOspheric traCe gAs retrievaL
FoM	Figure of Merit
FP	Full Physics
FTIR	Fourier Transform InfraRed

FTS	Fourier Transform Spectrometer
GCOS	Global Climate Observing System
GEO	Group on Earth Observation
GEOSS	Global Earth Observation System of Systems
GHG	GreenHouse Gas
GMES	Global Monitoring for Environment and Security
GOSAT	Greenhouse Gas Observing Satellite
IDL	Interactive Data Language
ITT	Invitation To Tender
IODD	Input Output Data Definition
IPCC	International Panel in Climate Change
IPR	Intellectual Property Right
IUP	Institute of Environmental Physics (IUP) of the University of Bremen, Germany
JCGM	Joint Committee for Guides in Metrology
LMD	Laboratoire de Météorologie Dynamique
LUT	Look-up table
MACC	Monitoring Atmospheric Composition and Climate, EU GMES project
MERIS	Medium Resolution Imaging Spectrometer
MIPAS	Michelson Interferometer for Passive Atmospheric Sounding
MODIS	Moderate Resolution Imaging Spectrometer
N/A	Not applicable
NDACC	Network for the Detection of Atmospheric Composition Change
NASA	National Aeronautics and Space Administration
NIES	National Institute for Environmental Studies
NOAA	National Oceanic and Atmospheric Administration
OCO	Orbiting Carbon Observatory
OD	Optical Depth
OE	Optimal Estimation

PBL	Planetary Boundary Layer
PMD	Polarization Measurement Device
PR	Proxy (retrieval method)
PVP	Product Validation Plan
PVR	Product Validation Report
RA	Relative Accuracy
RD	Reference Document
RMS	Root-Mean-Square
RTM	Radiative transfer model
S5P	Sentinel-5 Precursor
SoW	Statement of work
SQWG	SCIAMACHY Quality Working Group
SRA	Seasonal Relative Accuracy
SRD	Software Requirements Document
SRON	Netherlands Institute for Space Research
SUM	Software User Manual
SVR	Software Verification Report
TANSAT	CarbonSat
TANSO	Thermal And Near infrared Sensor for carbon Observation
TBC	To be confirmed
TCCON	Total Carbon Column Observing Network
TBD	To be defined / to be determined
TROPOMI	TROPOspheric Monitoring instrument
WFM-DOAS (or WFMD)	Weighting Function Modified DOAS
WG	Working Group

***** End of Document *****